JOURNAL OF CAMEL PRACTICE AND RESEARCH

CAMEL PUBLISHING HOUSE • BIKANER

In This Issue

Next 92 km

Save the Camels in Australia

JOURNAL OF CAMEL PRACTICE AND RESEARCH

CAMEL PUBLISHING HOUSE
Bikaner - 334001, INDIA

SUBSCRIPTION RATE – 2020

CONTENTS

Volume 26	December 2019	Number 3

SOUTH AUSTRALIA TO CULL 10,000 CAMELS-INHUMANE AND UNETHICAL

Thousands of camels in South Australia will be shot dead from helicopters as a result of extreme heat and drought. The marksmen who will shoot the animals come from Australia's department for environment and water. A five-day cull started on Wednesday, as Aboriginal communities in the region have reported large groups of camels damaging towns and buildings. Some complain that they are roaming the streets looking for water and we are worried about the safety of the young children and others say that we have been stuck in stinking hot and uncomfortable conditions, feeling unwell, because all the camels are coming in and knocking down fences, getting in around the houses and trying to get water through air-conditioners. The slaughter will take place in the area of Anangu Pitjantjatjara Yankunytjatjara (APY) - a sparsely-populated part of South Australia which is home to a number of indigenous groups. Some feral horses will also be killed. The camel cull is not directly linked to the fires crisis but owing to ongoing dry conditions and the large camel congregations threatening all of the main APY communities and infrastructure, immediate camel control was needed. Killing camels is a inhumane and unethical. Government of Australia should instead find some other measures to provide drinking water to these camels who are encroaching in human dwellings.

People's Republic of China organised 7th China Camel Industry Development Conference (2019) in Ejina Banner, Alxa League, Inner Mongolia, China from 25 to 27 November 2019. China is marching ahead in developing camel product industry in a big way.

The closing issue of year 2019 is rich in the manuscripts based on Bactrian and dromedary camels, both. Bactrian based manuscripts covered the topics, i.e. proteome profiles of hypothalamus, pituitary gland, adrenal glands and kidney, proteomic characterisation of serum during breeding cycle, isolation, culture and identification of skeletal muscle satellite cells, *Dipetalonema evansi* infection Itraconazole effect on the pharmacokinetics of midazolam. The manuscripts based on dromedary covered the topics, i.e. pharmacokinetics of cefquinome, pancreas of the camel foetus, beta casein gene polymorphism in Indian camel breeds, antibacterial functions of neutrophil and monocyte in newborn calves, assessment of genetic variability in Kappa casein gene, histology of atrioventricular node and atrioventricular bundle in foetus, molecular identification of 20 *Escherichia coli* isolates from 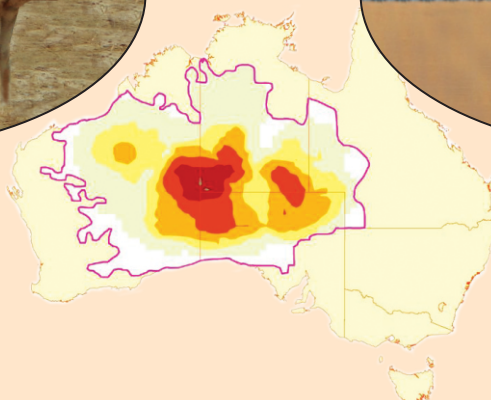dead neonatal camel calves, multiple splenic abscessation, ovarian neoplasms and Sertoli-Leydig cell tumour. This issue also contains review of a new important reference book "Handbook of Research on Health and Environmental Benefits of Camel Products" authored by Omar Amin Alhaj, Bernard Faye and Rajendra Prasad Agrawal which is published in the United States of America by IGI Global.

I wish a Merry Christmas and Happy New Year 2020 to all the members of the editorial board and esteemed authors. I am sure that Journal of Camel Practice and Research will continue to serve as an important resource of Camelid literature across the world.

(Dr. T.K. Gahlot)
Editor

PROTEOME PROFILES OF HYPOTHALAMUS, PITUITARY GLAND, ADRENAL GLANDS AND KIDNEY OF BACTRIAN CAMEL

Bin Yang[1], Tuya[2], Tuya Liu[3], Haobo Li[1], Erdendalai[4], Haifeng Huang[4], Surlig[5], Bayartai[5] and Demtu Er[1]

[1]College of Veterinary Medicine, Inner Mongolia Agricultural University, Huhhot 010018, China; Key Laboratory of Clinical Diagnosis and Treatment Technology in Animal Disease, Ministry of Agriculture, P.R. China, Huhhot 010018, China
[2]Detachment of Alxa league Agriculture and Animal Husbandry Comprehensive Administrative Law Enforcement, Bayanhot, 750306, Inner Mongolia Autonomous Region, P.R. China
[3]Veterinary Bureau of Alxa Left Banner, Bayanhot, 750300, Inner Mongolia Autonomous Region, P.R. China
[4]Animal Supervision Station of Agriculture and Animal Husbandry Integrated Service Centre, Barenbelle Town, Alxa Left Banner, 750308, Inner Mongolia Autonomous Region, P.R. China
[5]Agriculture and Animal Husbandry Integrated Service Centre of Yinggen Sumu, Alxa Left Banner, Inner Mongolia Autonomous Region, P.R. China

ABSTRACT

The hypothalamus-pituitary-adrenal (HPA) system is a neuroendocrine system that is closely linked to stress and the restoration of homeostasis. The kidney plays an important role in regulating water metabolism. We identified proteome profiles of hypothalamus, pituitary gland, adrenal gland and kidney of Bactrian camel using a shotgun proteomic approach. GO annotation and KEGG were predicted using bioinformatic tools. As a result, a total of 2016, 1412, 1333 and 2294 proteins were identified, respectively. We found that the four organs are equipped with a variety of functional proteins related to metabolic process, cellular process, biological regulation, catalytic activity, binding, cell, cell part and organelle. More than 300 pathways in each tissue were identified by KEGG analysis. Plenty of proteins related to adaptation to the desert environment were identified.

Key words: Bactrian camel, proteome, shotgun

Camel is an important livestock species uniquely adapted to hot arid environments. Camels have the incredible capability to withstand thirsty, thermal stress and other harsh environmental conditions (Hoter *et al,* 2019). The hypothalamic-pituitary-adrenal (HPA) axis is central to homeostasis, stress responses and energy metabolism (Miller, 2018). The camel's kidneys play a major role in the process of conserving water through increasing the osmolarity of urine (Gebreyohanes and Assen, 2017).

Vasopressin is synthesised mainly in the neuroendocrine neurons of the supraoptic, paraventricular and suprachiasmatic nuclei of the hypothalamus. Vasopressin participates in the regulation of the water-electrolyte balance through the regulation of water and electrolyte transport in the renal tubules (Szczepanska-Sadowska *et al,* 2018). The rennin-angiotensin-aldosterone system (RAAS) regulates water-electrolyte balance by regulating reabsorption and excretion of Na^+, K^+ and Cl^- in the kidney (Yamazaki *et al,* 2019). Renin is predominantly produced and secreted by the kidney (Peters, 2008). Aldosterone is synthesised in and secreted from the adrenal cortex (Bollag, 2014). We speculate that there are plenty of proteins related to regulation of the water-electrolyte balance in hypothalamus, pituitary gland, adrenal gland and kidney of Bactrian camel.

Several attempts have been carried out to understand the mystery of camel adaptation to the desert environment (Warda *et al,* 2014; Wu *et al,* 2014). However, there is no detailed report on the proteome of hypothalamus, pituitary gland, adrenal glands and kidney from Bactrian camel. To understand functions of neuroendocrine organs and kidney from Bactrian camel, it is important to define the molecular constituents of proteome profiles of these organs. The aim of the present study was to identify whole proteome profiles of hypothalamus, pituitary gland, adrenal glands and kidney of Bactrian camel using shotgun proteomic approach.

SEND REPRINT REQUEST TO DEMTU ER email: eedmt@imau.edu.cn

Materials and Methods

Transcriptome databases construction

Two adult bactrian camel at 10-years-old were used to harvest tissues. Hypothalamus, pituitary gland, adrenal gland and kidney from camels were collected and frozen in liquid nitrogen and stored at −80°C. Total RNA from 4 tissue samples were extracted according to the manufacturer's protocol. The total RNA quantity and purity were analysed. Sequencing libraries were constructed and sequenced on an Illumina Hiseq platform. After reads mapping to the reference genome, four-frame translation of our own hypothalamus, pituitary, adrenal and kidney transcriptome databases were constructed.

Shotgun

Sample pretreatment

Each sample was added SDT lysis buffer and homogenated . The sample was sonicated and incubated at 100°C for 10 min, then centrifuged at 12000g for 30 min. The supernatant was collected. Protein concentration was determined with BCA method.

FASP

The proteins were added with DTT and incubated at 100°C for 5 min. The sample was added with UA buffer and centrifuged at 14000g for 15 min. Then, IAA buffer was added and incubated for 30 min at room temperature in the dark. After centrifugation, UA buffer was added and centrifuged at 14000g for 15 min. NH_4HCO_3 was added and centrifuged at 14000g for 15 min. Trypsin buffer was added and and incubated at 37°C for 16-18 h.

LC-MS/MS

The LC-MS/MS analysis was performed on an Easy nLC system and Q-Exactive mass spectrometer system (Thermo Scientific). The sample was loaded onto a trap column (2cm×100µm, 5µm-C18, Thermo Scientific) and then separated onto a analytical column (75µm×100mm, 3µm-C18, Thermo Scientific) at a flow rate of 300 nL/min. Mass spectra were acquired with an Exactive mass spectrometer (Thermo Scientific). MaxQuant software was employed for protein quantitation. Only the protein identifications with false discovery rate (FDR) 1% or less were accepted in the final dataset.

Results and Discussion

A total of 2016 proteins in the hypothalamus, 1412 proteins in the pituitary gland, 1333 proteins in the adrenal gland and 2294 proteins in the kidney were identified using shotgun proteomic approach. These proteins were associated with metabolic process, cellular process, biological regulation, catalytic activity, binding, cell, cell part and organelle (Fig 1).

V-type H+-transporting ATPase subunit a, d, A, B, C, D, E, F, H, G, V-type H+-transporting ATPase 16kDa proteolipid subunit and F-type H+-transporting ATPase subunit alpha, beta, delta, gamma, b, d, f, g, O, 6, 8 were identified (Table 1). H+-ATPases have been reported to play an essential role in renal acid-base homeostasis (Blake-Palmer and Karet, 2009). The proteomic study showed that H+-ATPase subunit in camel brain guarantees a rapidly usable energy supply (Warda *et al*, 2014).

Ninty seven proteins related to tight junction, including claudin in the kidney were identified. Claudins in the kidney have a role in the bulk reabsorption of salt and water (Yu, 2015). 107 proteins related to glycolysis/gluconeogenesis in the kidney were identified (Fig 2). The mammalian kidney consumes a large amount of energy to support the reabsorptive work it needs to excrete metabolic wastes and to maintain homeostasis. Part of that energy is supplied via the metabolism of glucose (Chen *et al*, 2016). Aquaporin-1 (AQP1) in the kidney was identified. Aquaporin-1 is involved in water reabsorption in the kidney's proximal tubules (Dibas *et al*, 1998).

Table 1. The names of V-type and F-type H+-transporting ATPase subunit proteins identified in four tissues.

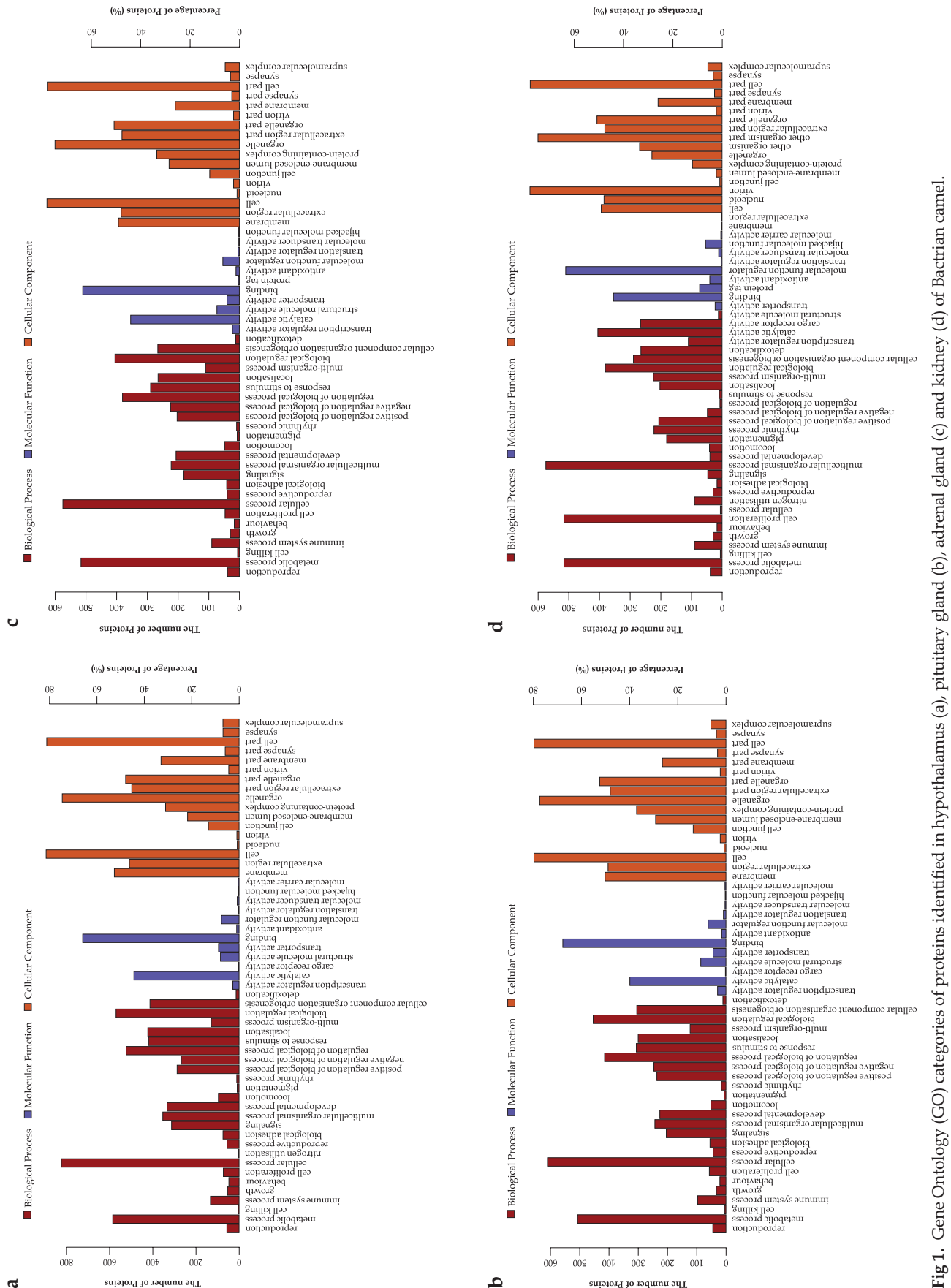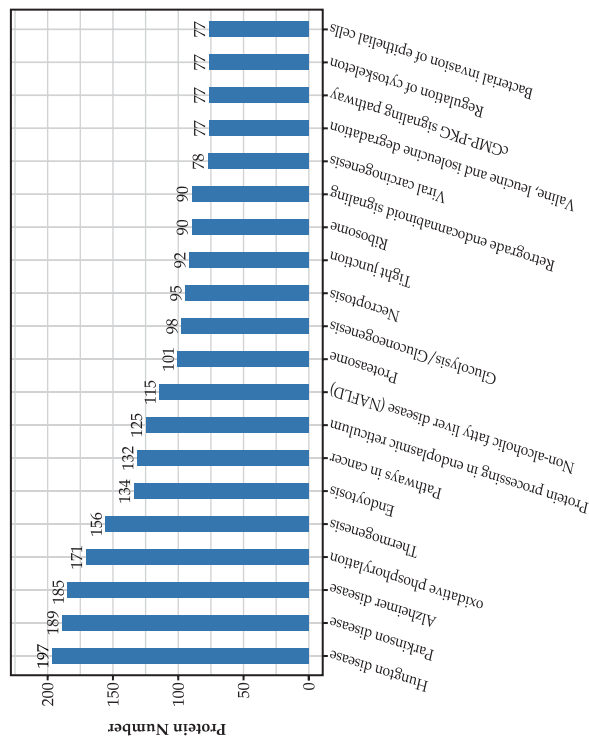| Tissues	Hypothalamus	Pituitary Gland	Adrenal Gland	Kidney
protein names	V-type H+-transporting ATPase subunit a, d, A, B, C, D, E, F, H, G; V-type H+-transporting ATPase 16kDa proteolipid subunit;	V-type H+-transporting ATPase subunit a, d, A, B, C, E, G;	V-type H+-transporting ATPase subunit a, d, A, B, E;	V-type H+-transporting ATPase subunit A, B, E,G;
	F-type H+-transporting ATPase subunit alpha, beta, delta, gamma, d, g, O, 6	F-type H+-transporting ATPase subunit alpha, beta, b,d, g, O	F-type H+-transporting ATPase subunit alpha, beta, gamma, b, d, O, 6,8	F-type H+-transporting ATPase subunit alpha, beta, delta, gamma, b,d, g, O, 6,8,f

Fig 1. Gene Ontology (GO) categories of proteins identified in hypothalamus (a), pituitary gland (b), adrenal gland (c) and kidney (d) of Bactrian camel.
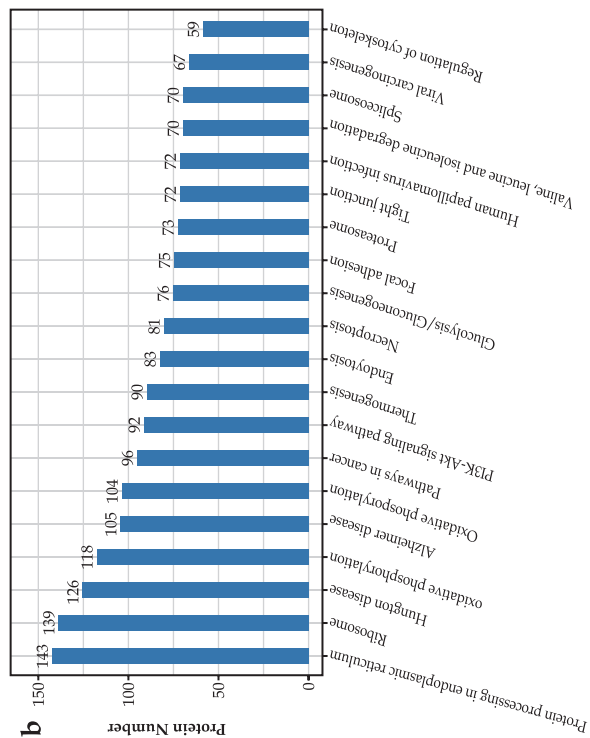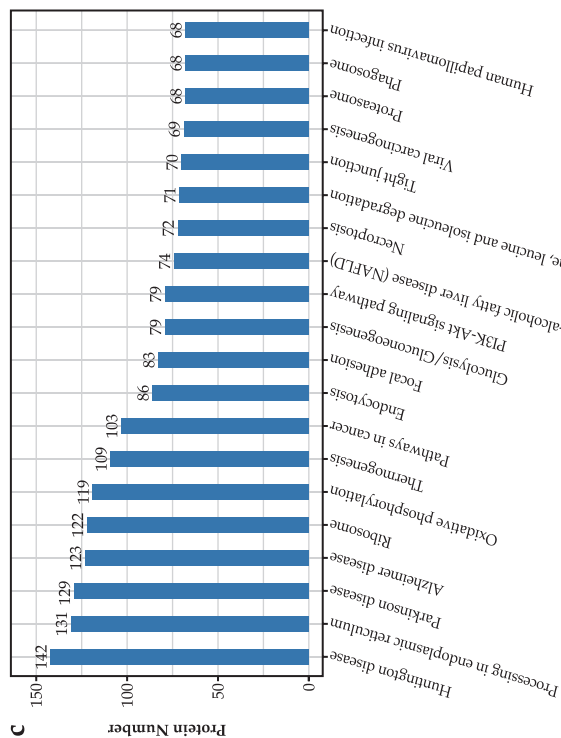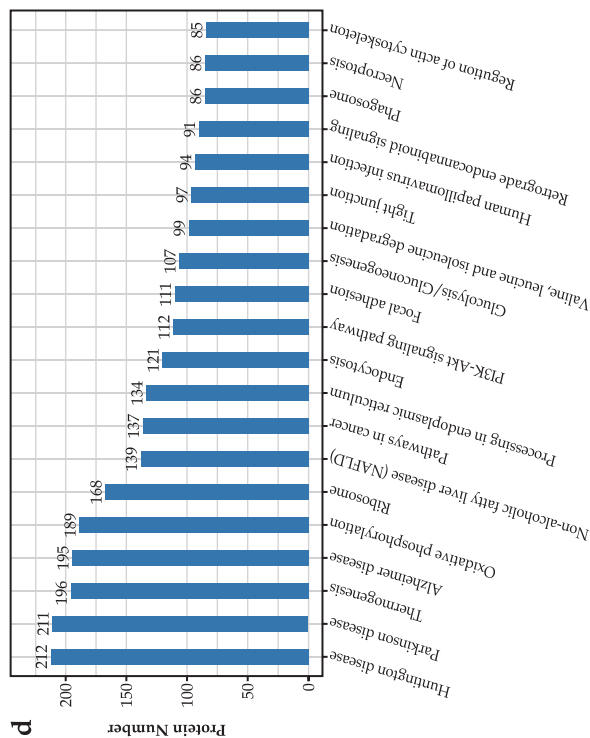
Fig 2. Pathway categories in hypothalamus (a), pituitary gland (b), adrenal gland (c) and kidney (d) of Bactrian camel according to Kyoto Encyclopedia of Genes and Genomes pathway taxonomy.

Table 2. The names of heat shock proteins identified in four tissues.

Tissues	Hypothalamus	Pituitary gland	Adrenal gland	Kidney
protein names	heat shock protein beta-1, heat shock 70kDa protein 1/2/6/8, heat shock 70kDa protein 4, heat shock 70kDa protein 5, heat shock protein 90kDa beta, heat shock protein 110kDa	heat shock protein beta-1, heat shock 70kDa protein 1/2/6/8, heat shock 70kDa protein 4, heat shock 70kDa protein 5, heat shock protein 90kDa beta	heat shock protein beta-1, heat shock 70kDa protein 1/2/6/8, heat shock 70kDa protein 4, heat shock 70kDa protein 5, heat shock protein 90kDa beta, heat shock protein 110kDa	heat shock protein beta-1, heat shock 70kDa protein 1/2/6/8, heat shock 70kDa protein 4, heat shock 70kDa protein 5, heat shock protein 90kDa beta

Proteins related to vasopressin-regulated water reabsorption in the hypothalamus, pituitary gland, adrenal gland and kidney of Bactrian camel identified were 43, 25, 33 and 33, respectively. Elven and 23 proteins related to renin secretion in the adrenal gland and kidney of Bactrian camel were identified. 5 proteins related to renin-angiotensin system in the kidney of Bactrian camel were identified. Twenty one proteins related to aldosterone synthesis and secretion in the adrenal gland of Bactrian camel were identified. Ten proteins related to aldosterone-regulated sodium reabsorption in the kidney of Bactrian camel were identified. Plenty of proteins related to regulation of the water-electrolyte balance in hypothalamus, pituitary gland, adrenal gland and kidney of Bactrian camel guarantee water-electrolyte homeostasis.

Proteins related to thermogenesis in the hypothalamus, pituitary gland, adrenal gland and kidney of Bactrian camel identified were 156, 90, 109 and 196, respectively (Fig 2). Plenty of proteins related to thermogenesis guarantee Bactrian camel to adapt to high and cold temperatures. Heat shock protein beta-1 (HSPB1), heat shock 70kDa protein 1/2/6/8 (HSPA1s), heat shock 70kDa protein 4 (HSPA4), heat shock 70kDa protein 5 (HSPA5), heat shock protein 90kDa alpha (HSP90A) and heat shock protein 110kDa (HSP110) were identified (Table 2). Camel HSPs have been reported to play a key role in its adaptation to heat stress (Hoter *et al*, 2019).

The current study can help us to understand the interplay between proteome-homeostasis in the Bactrian camel.

Acknowledgements

References

Blake-Palmer KG and Karet FE (2009). Cellular physiology of the renal H+ATPase. Current Opinion in Nephrology and Hypertension 18(5):433-438.

Bollag WB (2014). Regulation of aldosterone synthesis and secretion. Comprehensive Physiology 4(3):1017-1055.

Chen Y, Fry BC and Layton AT (2016). Modeling Glucose Metabolism in the Kidney. Bulletin of Mathematical Biology 78(6):1318-1336.

Dibas AI, Mia AJ and Yorio T (1998). Aquaporins (water channels): role in vasopressin-activated water transport. Proceedings of the Society for Experimental Biology and Medicine 219(3):183-199.

Gebreyohanes MG and Assen AM (2017). Adaptation Mechanisms of Camels (*Camelus dromedarius*) for Desert Environment: A Review. Journal of Veterinary Science and Technology 8:486.

Hoter A, Rizk S and Naim HY (2019). Cellular and Molecular Adaptation of Arabian Camel to Heat Stress. Frontiers in Genetics 10:588.

Miller WL (2018). The Hypothalamic-Pituitary-Adrenal Axis: A Brief History. Hormone Research in Paediatrics 89 (4):212-223.

Peters J (2008). Secretory and cytosolic (pro)renin in kidney, heart and adrenal gland. Journal of Molecular Medicine 86(6):711-714.
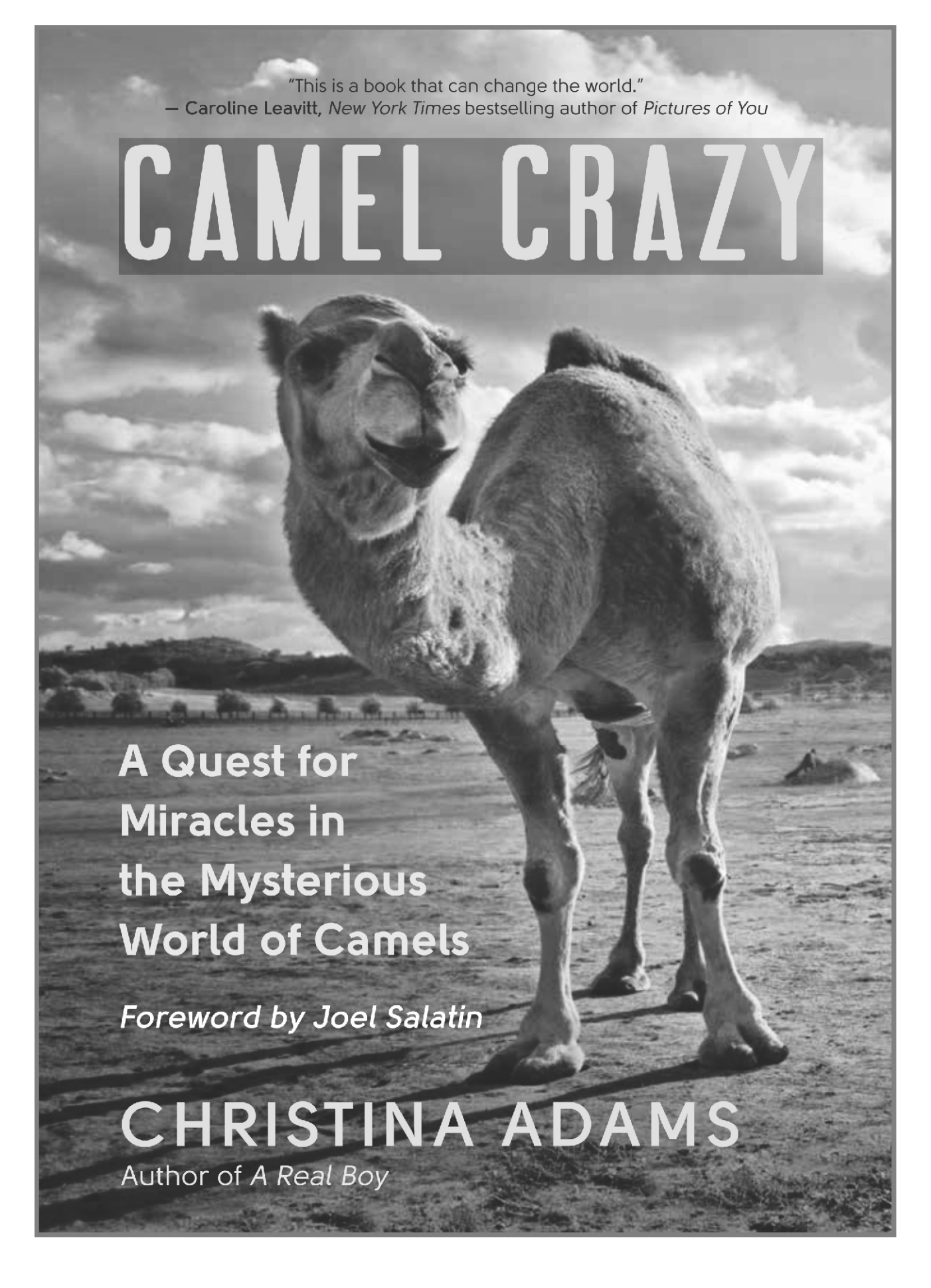
Szczepanska-Sadowska E, Czarzasta K and Cudnoch-Jedrzejewska A (2018). Dysregulation of the renin-angiotensin system and the vasopressinergic system interactions in cardiovascular disorders. Current Hypertension Reports 20(3):19.

Warda M, Prince A, Kim HK, Khafaga N, Scholkamy T, Linhardt RJ and Jin H (2014). Proteomics of old world camelid (*Camelus dromedarius*): Better understanding the interplay between homeostasis and desert environment. Journal of Advanced Research 5(2): 219-242.

Wu H, Guang X, Al-Fageeh MB, Cao J, Pan S, Zhou H, Zhang L, Abutarboush MH, Xing Y, Xie Z, Alshanqeeti AS, Zhang Y, Yao Q, Al-Shomrani BM, Zhang D, Li J, Manee MM, Yang Z, Yang L, Liu Y, Zhang J, Altammami MA, Wang S, Yu L, Zhang W, Liu S, Ba L, Liu C, Yang X, Meng F, Li L, Li E, Li X, Wu K, Zhang S, Wang J, Yin Y, Yang H and Al-Swailem AM (2014). Camelid genomes reveal evolution and adaptation to desert environments. Nature Communications 5:5188.

Yamazaki O, Ishizawa K, Hirohama D, Fujita T and Shibata S (2019). Electrolyte transport in the renal collecting duct and its regulation by the renin-angiotensin-aldosterone system. Clinical Science (Lond) 133(1):75-82.

Yu AS (2015). Claudins and the kidney. Journal of the American Society of Nephrology 26(1): 1-19.

CAMEL CRAZY

A Quest for Miracles in the Mysterious World of Camels

Foreword by Joel Salatin

CHRISTINA ADAMS

Author of *A Real Boy*

PROTEOMIC CHARACTERISATION OF SERUM DURING THE BREEDING CYCLE IN MALE BACTRIAN CAMELS

Le Hai[1], Rendalai Si[2], Fu-cheng Guo[1], Jing He[1], Li Yi[1], Liang Ming[1], Jun-wen Zhou[3], La Ba[3], Rigetu Zhao[3] and Rimutu Ji[1,2]

[1]Key Laboratory of Dairy Biotechnology and Bioengineering, Ministry of Education,
Inner Mongolia Agricultural University, Hohhot, Inner Mongolia, China
[2]Inner Mongolia Institute of Camel Research, Badanjiran, Inner Mongolia, China
[3]Alxa League Institute of Animal Husbandry, Alxa, Inner Mongolia, China

ABSTRACT

The duration of the breeding cycle in male Bactrian camels lasts 2–6 months, depending on geographical location, environmental conditions, nutritional parameters and health status. In China, the breeding cycle can span 4 months (December to March), except for this period libido is lost. Camels exhibit increased pacing and anxiety, and display morphological, behavioural and endocrinological peculiarities, including 16–25% weight loss due to suppressed appetite. Using label-free liquid chromatography-tandem mass spectrometry (LC-MS/MS) shotgun proteomics, we characterised the proteome at 4 key stages (pro-breeding, breeding, peak breeding and termination of breeding). We identified 210, 215, 220, 310 and 220 proteins in non-breeding (control) and breeding (stages 1 to 4) groups, respectively, of which 178 were common to all groups. Among these, 16, 20, 18 and 21 were differentially expressed ($p < 0.05$), with 4, 9, 11 and 11 up-regulated and 12, 11, 7 and 10 down-regulated in stages 1 to 4, respectively. Among differentially expressed proteins, 15 up-regulated and 8 down-regulated proteins were altered along with the breeding cycle. This is the first label-free proteomic characterisation of the Bactrian camel serum proteome. The findings provide new insight into temporal differences in serum protein composition in male Bactrian camel serum during the breeding cycle.

Key words: Bactrian camel, breeding cycle, protein serum proteome, shotgun proteomics

Camels are seasonal breeders, which exhibit maximum breeding activity during the cstrol cycle, peaks during the cooler winter and spring season, while breeding activity ceases almost entirely during the non-breeding cycle (summer and autumn seasons) (Zia-Ur-Rahman *et al,* 2007). The breeding cycle of male camels lasts between 2 and 6 months, from December to March in Tunisia (Fatnassi *et al,* 2014), November to February in the Gulf Area (Skidmore, 2000). Outside of the breeding cycle, male camels lose their libido and do not copulate with females, (El-Hassanein, 2003) even though they appear to be capable of mating with and fertilising females in breeding throughout the year (Al-Qarawi, 2005).

During the breeding season, male camels exhibit morphological, behavioural and endocrinological abnormalities, including increased pacing and anxiety, and aggression towards other males and people, to the extent that they cannot be handled safely (Cox *et al,* 2011). Upon entering the breeding season, male Bactrian camels lose their appetite and cease ruminating. The abdomen reduces in size, and consequently, body weight decreases by 16–25%, but despite this they grow in strength, and begin mating after gastric emptying.

Studies on sexual behaviour in captive camels are few in number, although, steroid hormones, electrolytes and trace elements, which contribute to controlling reproductive functions in males and females, have been investigated. These studies demonstrated that Na, K, Ca and Mg levels in genital organs are correlated with plasma testosterone (Al-Qarawi, 2000). Furthermore, steroid hormones, electrolytes and trace elements have distinct distributions during different physiological states (Zia-Ur-Rahman, 2007). Mass spectrometry-based proteomics approaches have recently been applied to camel research, specifically for identifying protein components of camel milk, tear fluids and meat, and for investigating the stability of camel milk proteins

after processing. However, information on Bactrian camel serum proteins remains limited. In the present study, we assessed the morphology of male Bactrian camels, analysed serum proteins during breeding and non breeding periods, and probed the mechanism of weight loss during the breeding cycle using proteomic approaches.

Materials and Methods

Animals and experimental design

The present study was carried out at the experimental station of the camel breeding base at Aalxa, Inner Mongolia, China. Three healthy male Bactrian camels were fed a diet consisting of straw, and grazed in the immediate area in individual territories.

The general and sexual behaviour of all animals were observed, and divided the breeding cycle into 4 stages according to the observation data. The trial lasted 12 weeks from December to March, to coincide with the breeding cycle of male Bactrian camels in China. The sexual behaviour of each male was observed and a sampling ethogram was complied. In addition, the frequency and occurrence of male behavioural events, including frothing of the mouth, sniffing, grinding of teeth, tail flapping, nervousness, poll gland secretion, and itching were recorded. General behaviour included frequency of feeding, rumination, standing, resting, and walking. In addition, body weight was recorded every 2 weeks.

Blood samples (30 ml) were extracted from the jugular vein using 10 ml procoagulation tubes and separated from blood by centrifugation at 3000g for 20 min at 4°C, and the supernatant was stored in a 1.5 ml centrifuge tube at -80°C until needed. Serum was separated by centrifugation at 3000g for 20 min at 4°C, and the supernatant (serum) was stored in a 1.5 ml centrifuge tube at -80°C until further analysis. Blood samples were taken once a week from the beginning (December) to the end (March) of the breeding, including from the non-breeding (control) group in June.

Ethics Statement

The experiments were performed in keeping with the ethical guidelines for animal studies of the Key Laboratory of Dairy Biotechnology and Bioengineering, and the study received the approval of the Animal Ethics Committee of Inner Mongolia Agricultural University.

Sample preparation

A ProteoMiner protein enrichment Kit (BioRad) was used following the manufacturer's protocol to remove the most abundant proteins. All samples were depleted and digested identically, and measured in triplicate. A 10 kDa ultrafiltration tube was employed to desalinate and concentrate low-abundance components, and the resulting sample was mixed with one volume of SDT buffer consisting of 4% sodium dodecyl sulphate (SDS), 100 mM dithiothreitol (DTT), and 150 mM TRIS-HCl pH 8.0, boiled for 15 min, centrifuged at 14,000g for 20 min, and the supernatant was collected and stored at -80°C until needed.

Serum proteins (200 µg) from 3 male Bactrian camels at the same stage were mixed with 30 µL SDT buffer. UA buffer (8 M urea, 150 mM TRIS-HCl pH 8.0) was used to remove detergent, DTT and other low-molecular-weight components by repeated ultrafiltration using 10 kDa Microcon units, and 100 µL 100 mM iodoacetamide (IAA) in UA buffer was added to reduce cysteine residues. Samples were incubated for 30 min in darkness, and filters were washed three times with 100 µL UA buffer, then twice with 100 µL 25mM NH_4HCO_3. Finally, protein suspensions were digested with 4 µg trypsin (Promega, Madison,United States) in 40 µL 25 mM NH_4HCO_3 buffer overnight at 37°C, and the resulting peptides were collected as filtrates. Empore standard density SPE C18 cartridges with an internal bed diameter of 7 mm and a volume of 3 ml (Sigma) were used to desalt peptide samples, which were subsequently concentrated by vacuum centrifugation and reconstituted with 40 µL 0.1% (v/v) formic acid. The peptide concentration was then estimated based on the tryptophan and tyrosine content in vertebrate proteins by measuring the absorbance at 280 nm using a UV/vis spectrophotometer with an extinctions coefficient of 1.1 for a 0.1% (g/L) solution.

Liquid chromatography (LC)-electrospray ionisation (ESI) tandem mass spectrometry (MS/MS) analysis

Empore standard density SPE C18 cartridges with an internal bed diameter of 7 mm and a volume of 3 ml (Sigma) were used to desalt peptide samples, which were subsequently concentrated by vacuum centrifugation and reconstituted with 40 µL 0.1% (v/v) formic acid. A Q Exactive mass spectrometer coupled with an Easy nLC instrument (Proxeon Biosystems, now Thermo Fisher Scientific) was employed for MS analysis. A 5 µg peptide sample was loaded onto a C18 reversed-phase column (Thermo

Scientific; 10 cm long, 75 μm internal diameter, 3 μm resin) equilibrated in buffer A (2% acetonitrile, 0.1% formic acid) and separated with a linear gradient of buffer B (80% acetonitrile, 0.1% formic acid) at a flow rate of 250 nL/min over 120 min controlled by an IntelliFlow apparatus. The data-dependent top 10 method was used for dynamic selection of the most abundant precursor ions from a survey scan (300–1800 m/z) for high-energy collision-induced (HCD) fragmentation from the MS data.

Determination of the target value was based on predictive automatic gain control (pAGC) with a dynamic exclusion duration of 25 s, and survey scans were acquired at a resolution of 70,000 at m/z 200 with a resolution for HCD spectra of 17,500 at m/z 200. The normalised collision energy was 30 eV, and the underfill ratio, which specifies the minimum percentage of the target value likely to be reached at maximum fill time, was defined as 0.1%. The instrument was run with peptide recognition mode enabled, and all MS experiments were performed in triplicate for each sample.

Sequence database searching and data analysis

MS data were analysed using MaxQuant software version 1.3.0.5. MS data were searched against the NCBI database (ftp://ftp.ncbi.nlm.nih.gov/genomes/all/GCF/000/311/805/GCF_000311805.1_CB1). An initial search was performed with a precursor mass window of 6 ppm, Trypsin/P cleavage, a maximum of two missed cleavage sites, and a mass tolerance of 20 ppm for fragment ions. Carbamidomethylation of cysteines was defined as a fixed modification, while protein N-terminal acetylation and methionine oxidation were defined as variable modifications for database searching. The cutoff for the global false discovery rate (FDR) for peptide and protein identification was 0.01. Label-free quantification was carried out in MaxQuant as previously described (Luber *et al*, 2010). Protein abundance was calculated based on the normalised spectral protein intensity (LFQ intensity).

Bioinformatics analysis

All bioinformatics analyses were performed with Perseus software within the MaxQuant computational platform. Potential functions of identified proteins were analysed using the UniProt (www.expasy.org) and Gene Ontology (GO; www.geneontology.org) databases. Identified proteins were imported into the online Search Tool for the Retrieval of Interacting Genes/Proteins (STRING) database (http://string-db.org) for known and predicted protein interactions (Franceschini, 2012). In order to minimise the rate of false positives, protein-protein interactions confirmed by experimental study were selected alongside pathways from curated databases and reported in abstracts of papers listed on PubMed. Interactions comprised both direct (physical) and indirect (functional) associations between proteins. Cluster 3.0 software was used to investigate the hierarchical clustering of identified proteins, and Java Treeview was used for visualisation.

Results and Discussion

Behavioural patterns

The patterns and extent of sexual behaviour of male Bactrian camels were evaluated for different breeding periods (Table 1). We observed that tail flapping occurred more frequently in animals that were more excited, whereas teeth grinding occurred constantly, regardless of the level of excitement. These results suggested that appetite decreased gradually during the breeding, leading to reduced feeding frequency and consumption of smaller amounts of food, and during peak breeding, camels stopped eating or drinking entirely for several days. According to appetite, body weight and sexual behavioural pattern, we divided the breeding cycle into 4 stages, namely pro-breeding, breeding, peak breeding, and termination of breeding (stages 1 to 4, respectively). The breeding cycle of each male Bactrian camel was divided into these 4 stages (Table 1).

The weight of male camels declined during the breeding period. In stage 1, body weight was not obviously changed, but sexual behaviour began to occur. In stages 2 and 3, appetite and body weight decreased rapidly, then appetite and body weight gradually increased in stage 4 (Fig 1).

Analysis of identified proteins

Proteins such as keratins, which can potentially be introduced during the blood sampling procedure, were excluded from the analysis. A total of 304 proteins were identified in camel serum during stages 1 to 4 and in the control group using the Label-free proteomic approach (Table S1, Supporting Information). Additional thresholds were also applied to characterise high-confidence targets in an attempt to discern the most biologically pertinent proteomic profiles during different stages of the breeding cycle. Only proteins detected at least twice in each group were included, and 207, 215, 218, 238 and 220

Table 1. Description of the behavioural patterns and appetite of male Bactrian camels during different stages of the breeding cycle.

Behavioural patterns	Description					
Frothing of the mouth	Salivary glands exhibit increased secretion of saliva, causing frothing of the mouth.					
Sniffing	Male camels approach females to sniff the perineal and vulva regions.					
Grinding of teeth	Male camels move the lower jaw sideways with a closed mouth.					
Tail flapping	Male camels stand with opened hind legs and hold the tail up for a few seconds, emitting small quantities of urine and beating the tail rhythmically to spread urine over the croup and surrounding areas.					
Nervousness	Increased pacing, anxiety, and sound generation, particularly when females are departing.					
Poll gland secretion	Occipital poll glands become enlarged and produce a tarry dark secretion.					
Itching	Male camels rub their neck and occipital area on walls and grass mounds, often rolling to spread scent.					
Date		02/12–19/12	20/12–02/01	03/01–17/01	18/08–02/02	03/02–24/02
Frothing of the mouth	1st camel	★★	★★★	★★★★	★★★	★★
	2nd camel	★	★★	★★★	★★★★	★★★
	3rd camel	★	★★	★★★	★★★★	★★★
Sniffing	1st camel	★★	★★★	★★★★	★★★	★★
	2nd camel	★	★	★★★	★★★★	★★
	3rd camel	★	★	★★★	★★★★	★★
Grinding of teeth	1st camel	★★	★★	★★★	★★	★★
	2nd camel	★	★★	★★★	★★★	★★
	3rd camel	★	★★	★★★	★★★	★★
Tail flapping	1st camel	★★	★★★	★★★★★	★★★	★★
	2nd camel	★	★★	★★★	★★★★★	★★
	3rd camel	★	★★	★★★	★★★★★	★★
Nervousness	1st camel	★★	★★★	★★★★★	★★★	★★
	2nd camel	★	★★	★★★	★★★★★	★★★
	3rd camel	★	★★	★★★	★★★★★	★★★
Itching	1st camel	★★	★★★	★★★★★	★★★	★★
	2nd camel	★	★★	★★★	★★★★	★★★
	3rd camel	★	★★	★★★	★★★★	★★★
Appetite	1st camel	★★★	★★	★	★★★	★★★
	2nd camel	★★★	★★★	★★	★	★★★
	3rd camel	★★★	★★★	★★	★	★★
	1st camel	pro-breeding	breeding	peak breeding	termination of breeding	termination of breeding
	2nd camel	Pro-breeding	Pro-breeding	breeding	peak breeding	termination of breeding
	3rd camel	Non-breeding	Pro-breeding	breeding	termination of breeding	termination of breeding

Asterisks represent the degree of behavioural expression (★ = normal, ★★ = infrequent, ★★★ = obvious and frequent, ★★★★ = very obvious and frequent, ★★★★★ = extremely obvious and frequent).

proteins were identified in the control group and in stages 1 to 4, respectively. Of these, 3, 5, 6 and 15 proteins were unique to each of the corresponding groups, respectively, and 178 proteins were present in all groups (Fig 2). These results provide useful information and highlight changes in serum proteins in male Bactrian camels during the breeding cycle.

Statistical analysis of identified proteins

We identified 16, 20, 18 and 21 differentially abundant proteins (p <0.05) in stages 1, 2, 3 and stage 4, respectively, compared with the control group (Tables S2– S5). Of these differential proteins, 4, 9, 11 and 11 were up-regulated and 12, 11, 7 and 10 were down-regulated in the 4 stages (compared with controls).

Among these proteins, 15 including tenascin (TN), S100A8 and alpha-1-antitrypsin (SERPINA1) displayed significant and regular changes in line with progression of the breeding cycle, but the magnitude of the changes differed. TN was the most highly up-regulated protein ($p < 10^{-7}$), and levels were increased in stages 1 to 3, then decreased in stage 4 (Fig 3). Antithrombin III (SERPINC1) and carboxypeptidase B2 (CPB2) were significantly up-regulated in stages 2 to 4, but there were no significant differences between the 4 stages. Tubulin beta (TUBB) and tubulin alpha (TUBA) were significantly up-regulated during stages 2 and 3, while lipopolysaccharide-binding protein (LBP) was significantly up-regulated during stages 3 and 4, and S100A8 was most abundant during stage 1 (Fig 3 and Fig S1).

Eight proteins were down-regulated compared with the control group during the 4 stages. Tensin (TNS) was the most down-regulated protein ($p < 10^{-6}$; Fig 3 and Table S2–5), and transferrin (TF), alpha-2-macroglobulin (A2M), SERPINA1, alpha-1B-glycoprotein (A1BG) and primary amine oxidase (AOC3) were decreased continually during all 4 stages (Fig 3). In addition, TNS, alpha-1-acid glycoprotein 1 (ORM1) and hemopexin (HPX) levels initially decreased then increased again as the breeding cycle progressed (Fig 3 and Fig S1).

Statistical analysis of each group identified 8, 5, 2 and 7 unique differential proteins in stages 1 to 4, respectively. These differential proteins were compared with the control group, and were also identified in other stages of the breeding cycle, but differences in abundance were only significant for their corresponding stages (Table. S2–5). Regarding the effects of weight loss during the breeding cycle, when body weight was at its lowest, this had a comprehensive systemic effect on the serum proteome profile. For instance, TN ($p < 10^{-11}$) and TUBB ($p < 10^{-7}$) were markedly up-regulated by 62-fold and 22-fold, respectively (Fig 4), whereas A2M and AOC3 (both $p < 10^{-5}$) were decreased by 0.039-fold and 0.072-fold (Fig 4).

Cluster Analysis

We selected 36 significantly differentially abundant proteins for further hierarchical clustering analysis, and the resulting heatmap showed that proteins in stage 2 and stage 4 groups clustered together, then further clustered with the remaining stage 3 proteins, while stage 1 proteins formed an independent cluster. Thus, changes in serum proteins during stages 2 and stage 4 were similar, and were

significantly differentially abundant during breeding, but not during peak breeding.

Characterisation of the serum proteome at different stages of the breeding cycle

We investigated the putative functions of the identified differentially abundant proteins during the different stages of the breeding cycle using gene ontology (GO) annotation, and categorised them into molecular function, cellular component, and biological process functional groups. GO slim analysis of each stage yielded a similar number of proteins associated with each biological process, with the largest number of proteins associated with biological regulation (≥30), cellular process (≥29), single organism process (≥73), and response to stimulus (≥29), (Fig S2). The most prevalent cellular component categories were extracellular region (≥30) and extracellular region part (≥26), (Fig S2). The most frequently encountered molecular functions were binding (≥31) and catalytic activity (≥6), (Fig S2).

GO annotation was applied to 141 proteins that differed significantly in terms of abundance between breeding (stages 1 to 4) cycle, including 136 differential proteins in biological process, 132 differential proteins in molecular function, and 137 differential proteins in cellular component. GO enrichment analysis identified 117 enriched terms for the 141 differential proteins, and the top 20 are shown in Fig 6. Three KEGG pathways were identified for the 141 differential proteins (Fig 7).

This study is the first non-gel-based mass spectrometry characterisation of the serum proteome during the breeding cycle in male Bactrian camels. To date, research on the camel serum proteome has been limited, and weight loss during the breeding cycle is poorly understood.

We monitored the sexual behaviour of camels because direct observation is currently regarded as the best method for obtaining detailed data on specific behaviours. Therefore, the observed sexual behavioural patterns of male Bactrian camels are descriptions based on observations rather than exact frequencies. However, during large-scale long-term continuous observation of animal behaviour, the number of reliable observations that can be made is limited, and this holds true for detailed analyses of behavioural changes associated with the breeding cycle. Furthermore, the accuracy of the data relies on the skill of the observer, and can be highly subjective and variable between observers (Cox *et al*, 2014). Although, automated video tracking systems can be
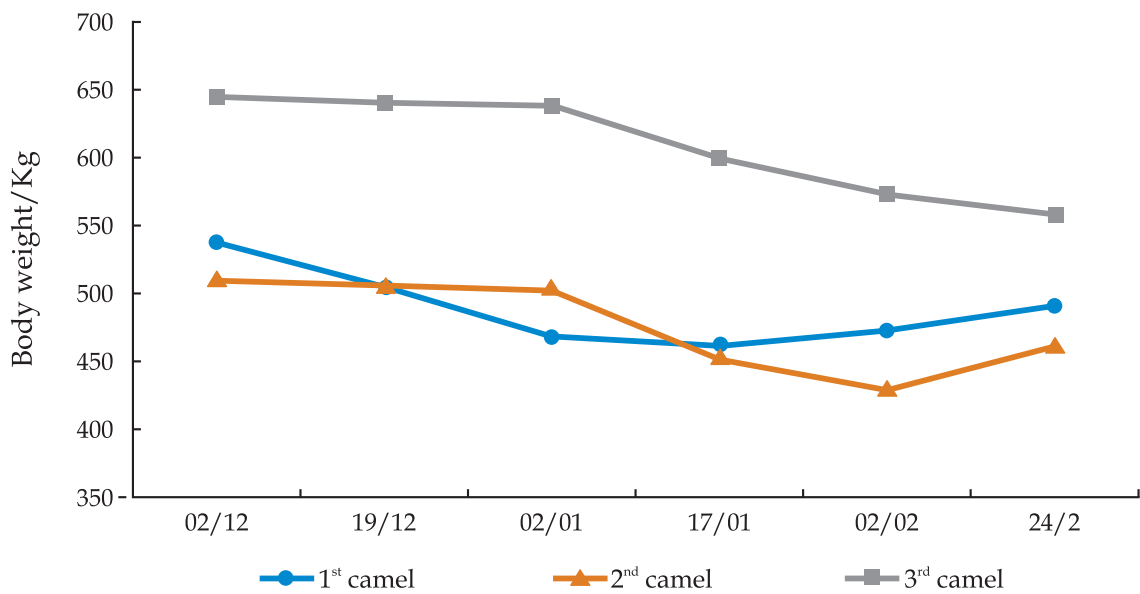
Fig 1. The body weight of the male Bactrian camel at the 4 stage.
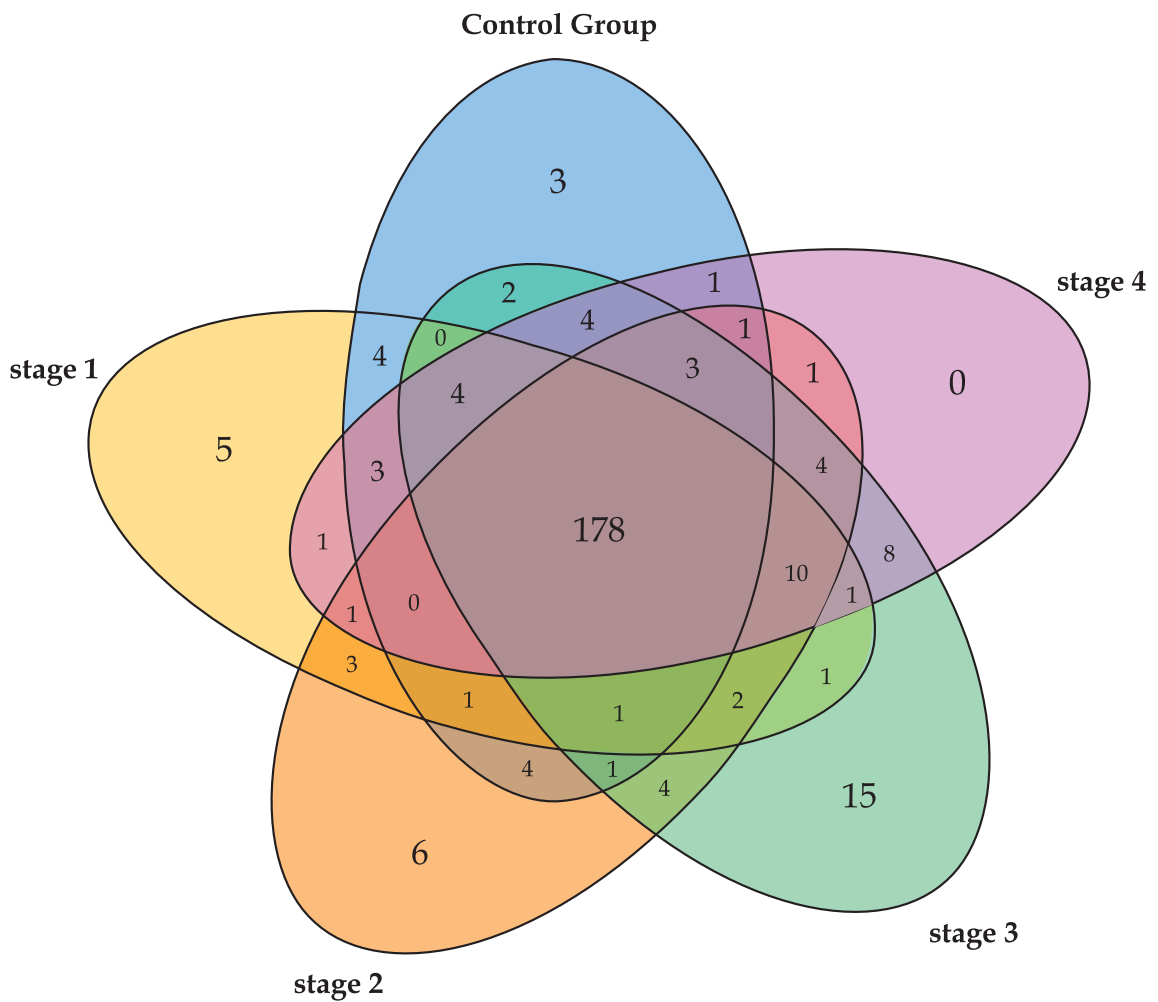
Fig 2. Unique and mutual proteins identified in the control group and stage from 1 to 4.
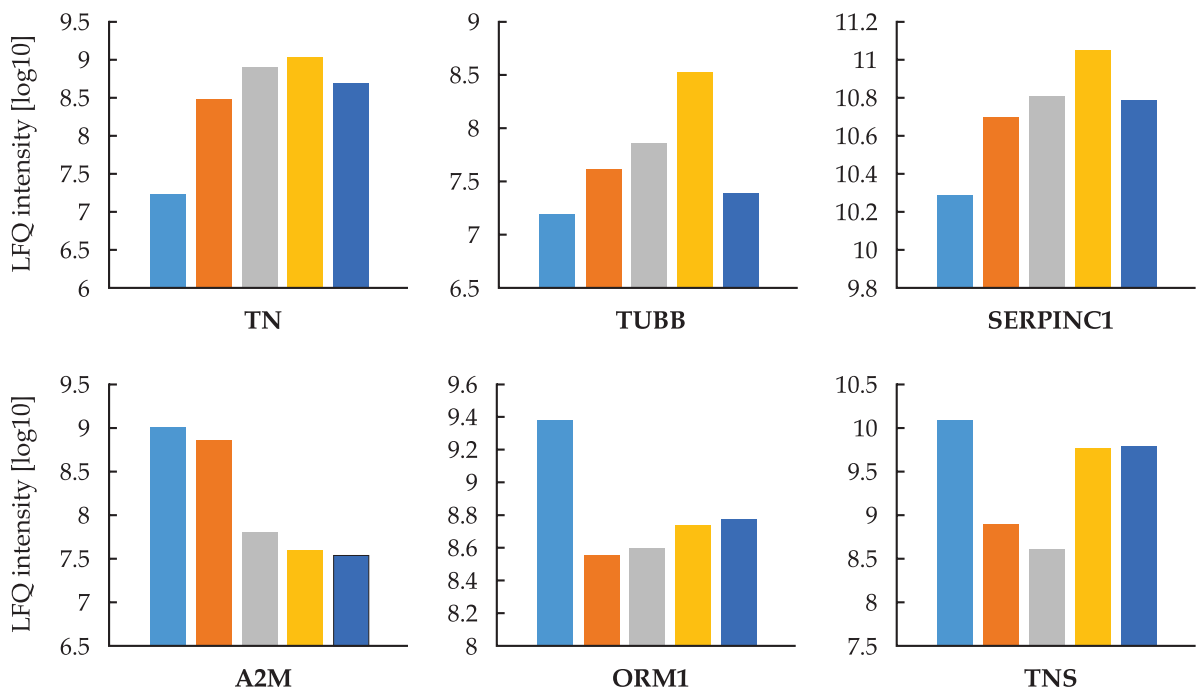
Fig 3. Changes in the proteins abundance are shown for each individual camel.
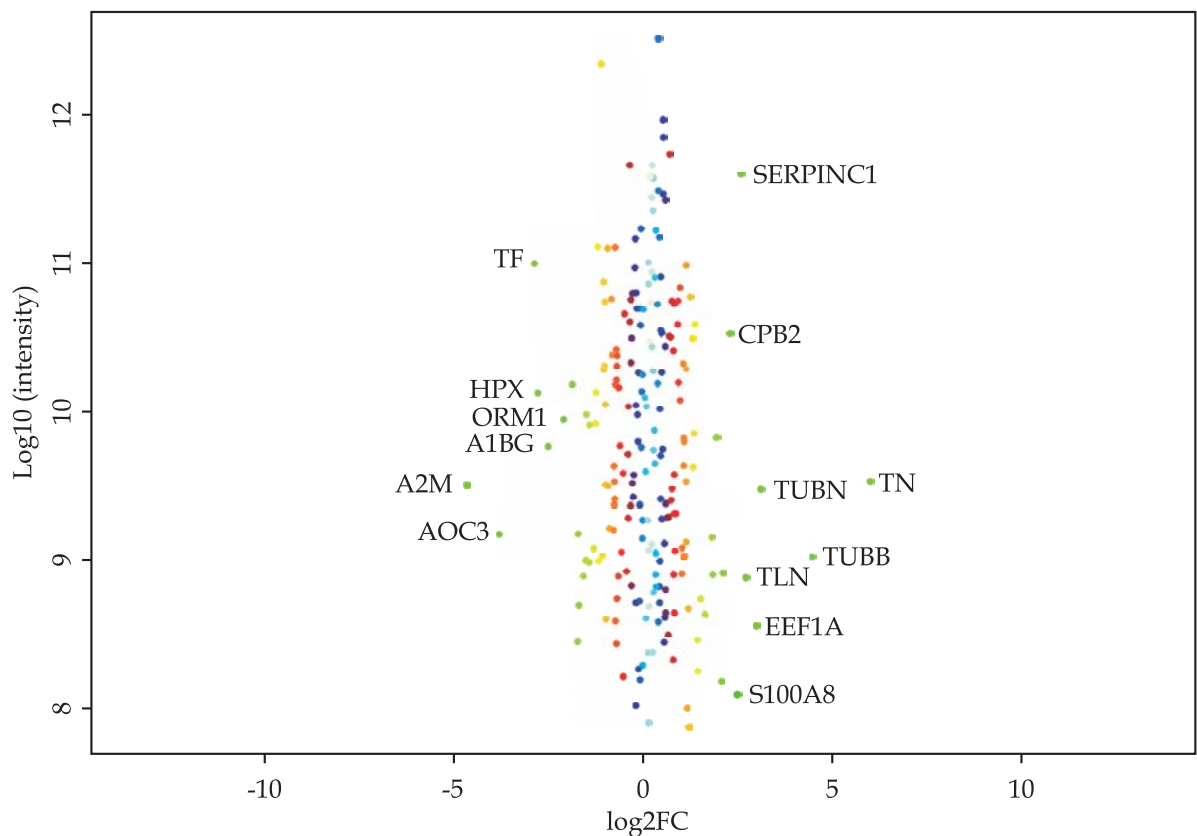
Fig 4. Volcano plot proteomes non-breeding (control group) and Heyday of the breeding (stage 3). With the x-axis depicting fold change [-log2] in protein levels and the y-axis the intensity [-log 10].
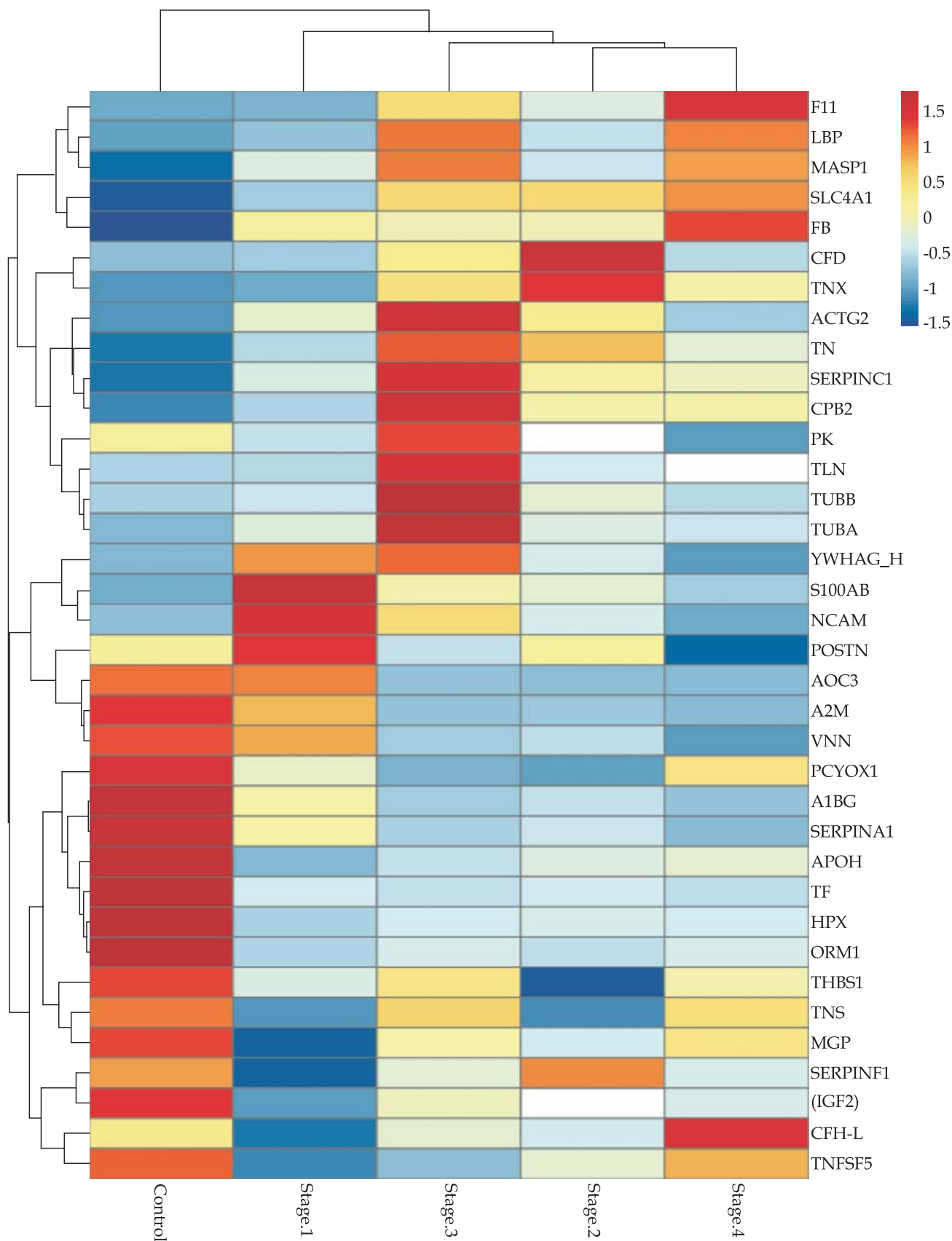
Fig 5. Hierarchical clustering of the differentially expressed proteins, clustering was based on the protein expression levels in non breeding (control group) and breeding cycle (stage 1 to 4). Bar colour represents a logarithmic scale from -1.5 to 1.5.
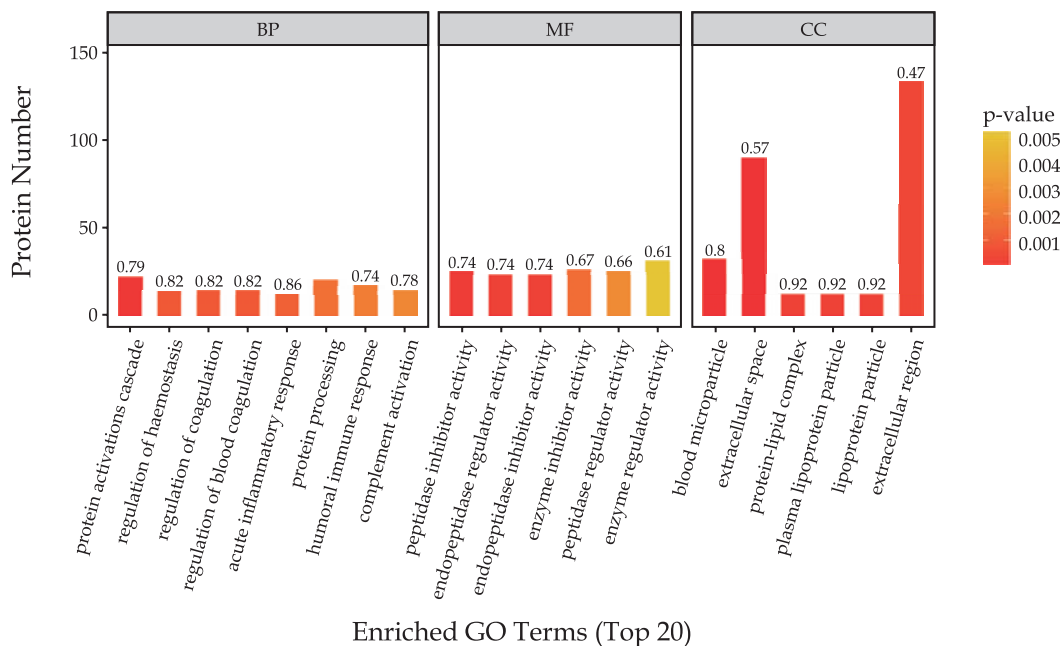
Fig 6. Gene Ontology (GO) slim terms and the numbers of proteins associated with each term. (i.e., differential proteins (N=141) in breeding cycle (stage 1 to 4)).
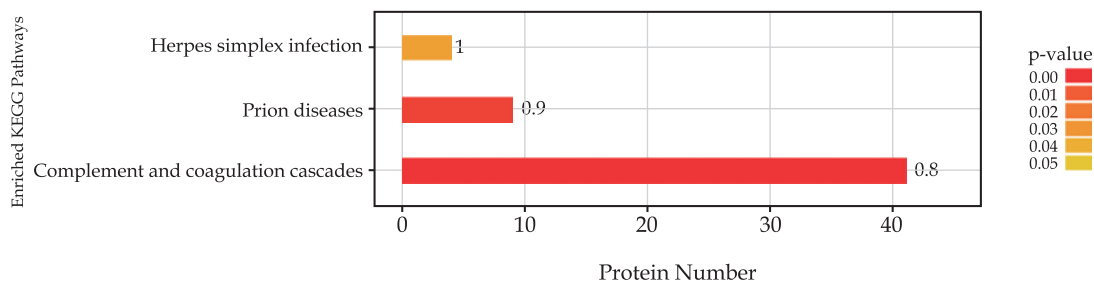
Fig 7. KEGG pathways Identified from the significantly different proteins from breeding cycle (stage 1 to 4).

applied in some studies on animal behaviour, their practical use currently remains limited to laboratory mice (Steele *et al,* 2007; Takahashi *et al,* 2010) and small insects (Cullen *et al,* 2012; Martin *et al,* 2004).

Changes in the release and/or concentration of certain proteins in the blood stream are considered indicative of inflammation, which is typically considered an acute phase reaction, even though it can occur in response to either acute or chronic inflammatory stress (Kushner, 1982). During inflammation, levels of at least 50 acute phase proteins (APP) are altered by more than 25% compared with their baseline concentrations under normal conditions (Gabay and Kushner, 1999; AmiGO2, 2014). These quantitative changes are mainly regulated by inflammatory mediators affecting both innate and adaptive immune systems, as well as neuroendocrine, vascular endothelial, haematopoietic, metabolic, and other defence and repair systems

(Gabay and Kushner, 1999). In the present study, LBP, HPX, ORM1, TF, SERPINA1 and F8 were altered at least 25% during the 4 stages, compared with the control group (S4), and were therefore, identified as APPs. The S100A8 protein is considered a clinical laboratory marker of inflammation (Foell *et al,* 2004). Antithrombin III (SERPINC1), a central component regulating haemostasis, is a potent anticoagulant that inhibits procoagulant processes (Opal *et al,* 2002), and influences the inflammatory process *via* its anti-inflammatory properties (Taylor *et al,* 1988), whether or not clotting is abnormal (Afshari *et al,* 2008). In the present work, a strong difference in the abundance of APPs between the control group and the 4 stages of the breeding cycle was observed (Fig 4). ORM1 is a typical inflammation-sensitive marker of inflammation that is up-regulated by 3–4-fold after an inflammatory stimulus (De *et al,* 1994; Hochepied *et al,* 2003). In cattle, Hp and SAA are

major APPs, while fibrinogen, alpha-AGP, Cp and alpha-antitrypsin are minor APPs. It is, therefore, speculated that male camels experience inflammation during the breeding cycle.

TN, identified as tenascin isoform X (also called tenascin X), was significantly up-regulated during the entire breeding cycle compared with the control group. TNX is an extracellular matrix (ECM) glycoprotein that is absent in adult tissues, only expressed during late stages of foetal development (Valcourt *et al*, 2015). The extracellular matrix (ECM), not only provides the basic scaffold in organs and tissues but is also important for regulating tissue to provide an optimal environment for normal cell functions (Adams and Watt, 1993). However, dysregulation of ECM production and proteolysis is often associated with the onset of pathological conditions (Duarte *et al*, 2015). TNX mRNA has been detected in many organs, such as lungs, kidneys, testis, mammary and adrenal glands. Especially in the mouse gastrointestinal tract, including the stomach, small intestine and colon, contain a higher level of TNX (Matsumoto, 1994). In addition, TNX mRNA has been detected in peripheral nerves and connective tissue structures including the epimysium, perimysium, skin dermis, *muscularis mucosa* and blood vessels (Matsumoto, 1994; Geffrotin *et al*, 1994; Valcourt *et al*, 2015; Elefteriou *et al*, 1997). Despite the TNX expressed in various organs and tissues, the function of TNX remains elusive in all species. Studies have suggested that the TNX do not play a direct role in forming structural elements, as a 'matricellular' protein, instead, they modulate the function of cells by regulating the interaction between cells and matrices (Bornstein and Sage, 2002). Yamaguchi *et al* (2017) feed the high-fat and high-cholesterol diet (HFCD) with high levels of phosphorus and calcium to wild-type and TNX-knockout mice to investigate the contribution of TNX to liver dysfunction. The results suggested that TNX deficiency suppressed hepatic dysfunction induced by HFCD administration in mice, that TNX may promote the inflammatory response thereby enhance HFCD-induced liver dysfunction (Yamaguchi *et al*, 2017). Furthermore, studies have investigated that at the initial stages of gastric emptying rate of TNX-knockout mice were significantly higher than wild-type mice. It is plausible to suggest that loss of TNX, the vagal afferent nerve endings, may indirectly disrupt sensory neurotransmission, thus cause rapid gastric emptying rates (Aktar, 2016). In the present study, we found that TNX was significantly up-regulated during the

entire breeding cycle compared with the control group. That is to say TNX changes with appetite and the rutting. This result seems to be consistent with the above results. This means that TNX may be involved to regulate the appetite, which slows down male Bactrian camels gastric emptying rates, that lead to the male camel to lose weight.

Tensin (TNS), in the form of tensin-4, was down-regulated during the breeding cycle, most significantly during stages 1 and 2. The tensin family, which comprises tensin-1, -2, -3 and -4, is involved in cell migration, and members are localised to focal adhesion sites (Tuxhorn *et al*, 2002). TNS4 is readily detected and displays a relatively unique and restricted expression pattern in normal prostate and placenta, but it is reduced or absent in advanced prostate cancers (Ibrahim *et al*, 1993), and not detectable in other tissues (Xue *et al*, 1998). Expression of TNS4 is increased significantly in gastric (Valcourt *et al*, 2015), colorectal (Lo and Tensin, 2004) and pancreatic cancers (Chen *et al*, 2013), and it may not be expressed in other normal tissues. These results suggest that overexpression of TNS4 in certain tissues may play a critical role in tumorigenesis, hence the prostate of male Bactrian camels may be affected during the breeding cycle. This could potentially influence the degree of breeding and consequent weight loss in male camels, resulting in altered inflammatory responses.

Inflammation factors in the serum proteome were also altered during the breeding cycle. Protein S100A8 plays an important role in inflammatory responses in adipose tissue in obese individuals, and contributes to pathogenesis during the early stages of obesity (Lo *et al*, 2005). SERPINF1 (PEDF), secreted by adipocytes (Sakashita *et al*, 2008), is associated with the development of insulin resistance during obesity. In the present work, SERPINF1 was least abundant during stage 1, then increased at the stage 2 and maintained at a high level throughout the rest of the breeding cycle. This protein was rapidly down-regulated in response to weight loss in a previous study (Albasri *et al*, 2011), whereas the body weight of male camels was steady during stage 1 in the present study, but lower during stages 2 and 3. Recombinant SERPINF1 was suggested to promote lipolysis in an ATGL-dependent manner, and to reduce fatty acid oxidation and thereby influence systemic fatty acid metabolism (Al-Ghamdi *et al*, 2013). Furthermore, α2M, which possesses esterase activity, may participate in ghrelin metabolism (Sekimoto *et al*, 2015). Thus, weight loss in male camels during the breeding cycle may be related to these proteins, but

further studies are required to confirm or disprove this hypothesis.

Our present research focused only on serum proteins in male Bactrian camels during the breeding cycle, and differences between female and male camels were not investigated. Additionally, a relatively small number of male camels were observed, hence future studies are needed to gain further insight into weight loss in Bactrian camels during the breeding cycle.

Acknowledgements

References

Adams JC and Watt FM (1993). Regulation of development and differentiation by the extracellular matrix. Development 117:1183-1198.

Afshari A, Wetterslev J, Brok J and Moller AM (2008). Antithrombin III for critically ill patients. Cochrane Database of Systematic Reviews CD005370.

Aktar R (2016). Multiple roles for the extracelllular matrix protein Tenascin-X in nerve gut function [J]. These awarded by Queen Mary University of London

Albasri A, Al-Ghamdi S, Fadhil W, Aleskandarany M, Liao YC, Jackson D, Lobo DN, Lo SH, Kumari R, Durrant L, Watson S, Kindle KB and Ilyas M (2011). Cten signals through integrin-linked kinase (ILK) and may promote metastasis in colorectal cancer. Oncogene 30(26):2997-3002.

Al-Ghamdi S, Cachat J, Albasri A, Ahmed M, Jackson D, Zaitoun A, Guppy N, Otto WR, Alison MR, Kindle KB, Ilyas M (2013). C-terminal tensin-like gene functions as an oncogene and promotes cell motility in pancreatic cancer. Pancreas 42(1):135-140.

Al-Qarawi AA (2005). Infertility in the dromedary bull: a review of causes, relations and implications. Animal Reproduction Science 87(1-2):73-92.

Al-Qarawi AA, Abdel-Rahman HA, El-Belely MS and El-Mougy SA (2000). Age-related changes in plasma testosterone concentrations and genital organs content of bulk and trace elements in the male dromedary camel. Animal Reproduction Science 62(4):297-307.

AmiGO2., acute-phase response (GO:0006953): the Gene Ontology; 2014. 2.1.4. Available: http://amigo.geneontology.org/amigo/term/GO:0006953/.

Borg ML, Andrews ZB, Duh EJ, Zechner R, Meikle PJ and Watt MJ (2011). Pigment epithelium-derived factor regulates lipid metabolism *via* adipose triglyceride lipase. Diabetes 60(5):1458-1466.

Bornstein P and Sage EH (2002). Matricellular proteins: extracellular modulators of cell function. Current Opinion in Cell Biology 14(5):608-616.

Chen NT, Kuwabara Y, Conley C, Liao YC, Hong SY, Chen M, Shih YP, Chen HW, Hsieh F and Lo SH (2013). Phylogenetic analysis, expression patterns, and transcriptional regulation of human CTEN gene. Gene 520(2)90-97.

Cox J, Hein MY, Luber CA, Paron I, Nagaraj N, Mann M (2014). Accurate proteome-wide label-free quantification by delayed normalisation and maximal peptide ratio extraction, termed MaxLFQ. Molecular and Cellular Proteomics 13(9):2513-2526.

Cox J, Neuhauser N, Michalski A, Scheltema RA, Olsen JV and Mann M (2011). Andromeda: a peptide search engine integrated into the MaxQuant environment. Journal of Proteome Research 10(4):1794-1805.

Cullen DA, Sword GA and Simpson SJ (2012). Optimising multivariate behavioural syndrome models in locusts using automated video tracking. Animal Behaviour 84(4):771-784.

De TG, Van EO, der Stelt Van ME, Kerstens PJ, Boerbooms AM and Van WD (1994). Effects of low dose methotrexate therapy on the concentration and the glycosylation of alpha 1-acid glycoprotein in the serum of patients with rheumatoid arthritis: a longitudinal study. The Journal of Rheumatology 21(12):2209-2216.

Duarte S, Baber J, Fujii T and Coito AJ (2015). Matrix metalloproteinases in liver injury, repair and fibrosis. Matrix Biology 44-46:147-156.

Elefteriou F, Exposito JY, Garrone R and Lethias C (1997). Characterisation of the bovine tenascinX. Journal of Biological Chemistry 272:22866-22874.

El-Hassanein E (2003). An invention for easy semen collection from dromedary camels, El-Hassanein camel dummy. In Recent advances in camel reproduction. International Veterinary Information Service (IVIS). Document (A1014):0203.

Eubanks LM, Stowe GN, De LMS, Mayorov AV, Hixon MS, and Janda KD (2011). Identification of α_2 macroglobulin as a major serum ghrelin esterase. Angewandte Chemie 50(45):10699-10702.

Famulla S, Lamers D, Hartwig S, Passlack W Horrighs A, Cramer A, Lehr S, Sell H and Eckel J (2011). Pigment epithelium-derived factor (PEDF) is one of the most abundant proteins secreted by human adipocytes and induces insulin resistance and inflammatory signaling in muscle and fat cells. International Journal of Obesity 35(6):762-772.

Fatnassi M, Padalino B, Monaco D, Khorchani T, Lacalandra GM and Hammadi M (2014). Evaluation of sexual behaviour of housed male camels (*Camelus dromedarius*) through female parades: correlation with climatic parameters. Tropical Animal Health and Production 46(2):313-321.

Foell D, Frosch M, Sorg C and Roth J (2004). Phagocyte-specific calcium-binding S100 proteins as clinical laboratory markers of inflammation. Clinica Chimica Acta 344(1-2):37-51.

Franceschini A, Szklarczyk D, Frankild S, Kuhn M, Simonovic M, Roth A, Lin J, Minguez P, Bork P, Mering CV and Jensen LJ (2012). STRING v9. 1: protein-protein interaction networks, with increased coverage and integration. Nucleic Acids Research 41(D1):D808-D815.

Gabay C and Kushner I (1999). Acute-phase proteins and other systemic responses to inflammation. New England Journal of Medicine 340(6):448-454.

Geffrotin C, Garrido JJ, Tremet L and Vaiman M (1995). Distinct tissue distribution in pigs of tenascin-X and tenascin-C transcripts. European Journal of Biochemistry 231(1):83-92.

Geyer PE, Albrechtsen NJW, Tyanova S, Grassl N, Iepsen EW, Lundgren J, Madsbad S, Holst JJ, Torekov SS and Mann M (2016). Proteomics reveals the effects of sustained weight loss on the human plasma proteome. Molecular Systems Biology 12(12):901.

Hochepied T, Berger FG, Baumann H and Libert C (2003). α1-Acid glycoprotein: an acute phase protein with inflammatory and immunomodulating properties. Cytokine and Growth Factor Reviews 14(1):25-34.

Ibrahim SN, Lightner VA, Ventimiglia JB, Ibrahim GK, Walther PJ, Bigner DD and Humphrey PA (1993). Tenascin expression in prostatic hyperplasia, intraepithelial neoplasia, and carcinoma. Human Pathology 24(9):982-989.

Kushner I (1982). The phenomenon of the acute phase response. Annals of the New York Academy of Sciences 389(1):39-48.

Lo SH (2004). Tensin. The international journal of Biochemistry and Cell Biology 36(1):31-34.

Lo SS, Lo SH and Lo SH (2005). Cleavage of cten by caspase-3 during apoptosis. Oncogene 24(26):4311-4314.

Luber CA, Cox J, Lauterbach H, Fancke B, Selbach M, Tschopp J, Akira S, Wiegand M, Hochrein H, O'Keeffe M and Mann M (2010). Quantitative proteomics reveals subset-specific viral recognition in dendritic cells. Immunity 32(2):279-289.

Martin JR (2004). A portrait of locomotor behaviour in *Drosophila* determined by a video-tracking paradigm. Behavioural Processes 67(2):207-219.

Matsumoto K (1994). The distribution of tenascin-X is distinct and often reciprocal to that of tenascin-C. The Journal of Cell Biology 125(2):483-493.

Opal SM, Kessler CM, Roemisch J and Knaub S (2002). Antithrombin, heparin, and heparan sulfate. Critical Care Medicine 30(5):S325-S331.

Sakashita K, Mimori K, Tanaka F, Kamohara Y, Inoue H, Sawada T, Hirakawa K and Mori M (2008). Prognostic relevance of Tensin4 expression in human gastric cancer. Annals of Surgical Oncology 15(9):2606-2613.

Sekimoto R, Fukuda S, Maeda N, Tsushima Y, Matsuda K, Mori T, Nakatsuji H, Nishizawa H, Kishida K, Kikuta J, Maijima K, Funahashi K and Ishii M (2015). Visualised macrophage dynamics and significance of S100A8 in obese fat. Proceedings of the National Academy of Sciences 112(16):E2058-E2066.

Skidmore JA (2000). Reproductive physiology in male and female camels: in Recent advances in camelids reproduction.

Steele AD, Jackson WS, King OD and Lindquist S (2007). The power of automated high-resolution behaviour analysis revealed by its application to mouse models of Huntington's and prion diseases. Proceedings of the National Academy of Sciences 104(6):1983-1988.

Takahashi A, Tomihara K, Shiroishi T and Koide T (2010). Genetic mapping of social interaction behaviour in B6/MSM consomic mouse strains. Behaviour Genetics 40(3):366-376.

Taylor JF, Emerson JT, Jordan R, Chang AK and Blick KE (1988). Antithrombin-III prevents the lethal effects of *Escherichia coli* infusion in baboons. Circulatory Shock 26(3):227-235.

Tuxhorn JA, Ayala GE, Smith MJ, Smith VC and Dang TD (2002). Rowley, D.R. Reactive stroma in human prostate cancer: induction of myofibroblast phenotype and extracellular matrix remodeling. Clinical Cancer Research 8(9):2912-2923.

Valcourt U, Alcaraz LB, Exposito JY, Lethias C and Bartholin L (2015). Tenascin-X: beyond the architectural function. Cell Adhesion and Migration 9(1-2):154-165.

Valcourt U, Alcaraz LB, Exposito JY, Lethias C and Bartholin L (2015). Tenascin-X: beyond the architectural function. Cell Adhesion and Migration 9:154-165.

Valcourt U, Alcaraz LB, Exposito JY, Lethias C and Bartholin L (2015). Tenascin-X: beyond the architectural function. Cell Adhesion and Migration 9(1-2):154-165.

Xue Y, Li J, Latijnhouwers MA, Smedts F, Umbas R, Aalders TW, Debruyne FM, De La Rosette JJ and Schalken JA (1998). Expression of periglandular tenascin-C and basement membrane laminin in normal prostate, benign prostatic hyperplasia and prostate carcinoma. British Journal of Urology 81:844-851.

Yamaguchi S, Kawakami K, Satoh K, Fukunaga N, Akama K and Matsumoto K (2017). Suppression of hepatic dysfunction in tenascin-X-deficient mice fed a high fat diet. Molecular Medicine Reports 16(4):4061-4067.

Zia-Ur-Rahman, Ahmad N, Bukhari SA, Akhtar N and Haq IU (2007). Serum hormonal, electrolytes and trace element profiles in the rutting and non-rutting one-humped male camel (*Camelus dromedarius*). Animal Reproduction Science 101(1):172-178.

THE ISOLATION, CULTURE AND IDENTIFICATION OF SKELETAL MUSCLE SATELLITE CELLS FROM BACTRIAN CAMEL

Tianjian Deng[1], Tuya Liu[2], Tuya[3], Bin Yang[1], Altenwula Cui[4], Surlig[5], Sharku[5], Bayartai[5] and Demtu Er[1]

[1]College of Veterinary Medicine, Inner Mongolia Agricultural University, Huhhot 010018, China; Key Laboratory of Clinical Diagnosis and Treatment Technology in Animal Disease, Ministry of Agriculture, P.R China, Huhhot 010018, China
[2]Veterinary Bureau of Alxa Left Banner, Bayanhot, 750300, Inner Mongolia Autonomous Region, P. R. China
[3]Detachment of Alxa league Agriculture and Animal Husbandry Comprehensive Administrative Law Enforcement, Bayanhot, 750306, Inner Mongolia Autonomous region, P. R. China
[4]Aminal supervision station of Agriculture and Animal Husbandry Integrated Service Centre, Barenbelle Town, Alxa Left Banner, 750308, Inner Mongolia autonomous region, P. R. China
[5]Agriculture and Animal Husbandry Integrated Service Centre of Yinggen Sumu, Alxa left banner, Inner Mongolia Autonomous Region, P.R. China

ABSTRACT

In this experiment, the skeletal muscle tissue of Bactrian camel was used as sample material. The cells of primary generation were cultured by two-step enzymatic digestion and tissue block culture. The primary skeletal muscle satellite cells were purified by differential adherence methods, and then were determined by growth curve analysis. The advantages of mode of proliferation of cells were that the cells could maintain high activity, comparatively not tend to be contaminated, and gain a long culture period, which is more suitable for the *in vitro* culture of Bactrian camel satellite cells. When using the method called LASER Confocal imaging, with immunofluorescence labeling, to identify the specific gene in skeletal muscle satellite cells, the PAX7 expression was positive in cell lines. In addition, PCR amplification bands showed that PAX7, MYF5, and Desmin genes were all clearly expressed. After induced culture, satellite cells started the myogenic differentiation process. Through the above methods, comparatively pure Bactrian camel skeletal muscle satellite cells were obtained successfully and passage proces were carried out stably. In conclusion, the *in vitro* culture system of Bactrian camel skeletal muscle satellite cells was successfully established.

Key words: Bactrian camel, *in vitro* culture, skeletal muscle satellite cells

The net weight of the Bactrian camel skeletal muscle accounts for 43% of the total weight. Bactrian camels have good meat production with 70% lean meat content, and contains more than 10 polyunsaturated fatty acids (Wenfang *et al,* 2019; Raiymbek *et al,* 2019). In-depth understanding of Bactrian camel skeletal muscle satellite cells and muscle fibre phenotypic traits have potential implications for skeletal muscle regulation and yield enhancement. Skeletal muscle satellite cell (SCs) are located between the basement membrane and the muscular basement membrane and are a specific type of myogenic stem cells (Scharner and Zammit, 2011). SCs are relatively static under normal conditions, activated under specific stress conditions, begin to divide, proliferate to form muscle precursor cells, and differentiate into new muscle fibres or fuse with original muscle fibres to form muscle tissue (Qu-

Petersen *et al,* 2002; Harel *et al,* 2009; Bellayr *et al,* 2010). Satellite cells are a kind of somatic pluripotent stem cells, have important research value in gene therapy and cell basic fields (Mohammadi-Sangcheshmeh *et al,* 2013; Evano and Tajbakhsh, 2018). This experiment aims to culture high-purity Bactrian camel skeletal muscle satellite cells, and provide a stable model for the study of skeletal muscle regulation mechanism and fibre traits in Bactrian camel.

Materials and Methods

Sample collection

The experimental animals were 2 to 4 months old healthy Bactrian camel and the sample was taken from the triceps.

Satellite cell tissue block culture

The skeletal muscle satellite cell tissue block culture step was as follows:

After taking the sample back to the laboratory, double-antibiotic PBS solution was discarded and the sample was washed three times with 75% ethanol.

Fat and fascia from the sample were removed and then sample was cut into 1mm^3 pieces. The cells were washed three times with PBS, and quickly injected the cell mass was into the cell culture flask from the plate. The sample block was ensured not be too dense.

The cell culture flask was inverted and kept it into the cell culture incubator for 2 hours.

The flask was turned back after 2 h. The solution wash was changed every 3 days, and the cells were purified by differential adherence.

When the number of cells reached 85% of the flat area, the tissue flask was taken out.

Purification of satellite cells

The skeletal muscle satellite cells were successfully separated from the muscle by two-step enzymatic digestion and differential adherence method was used to purify the satellite cells. The adherence time of the fibroblasts was usually 1-2 h, but the satellite cell attachment time was around 24h. Therefore, it was an effective method using the difference in adherence time to purify the satellite cells. In this way, the skeletal muscle satellite cells with 90% purity were acquired. Proceed as follows:

After the cells were cultured for 2 hours, cells were taken out from the incubator, the media was aspirated by a pipette, and finally the old flask was discarded and replaced with a new flask.

After 12 hours, the flask was changed, and the skeletal muscle satellite cells were obtained.

Satellite cell subculture

When the cells grew up to 80% of the flat area, the cell passaging was done as per fellowing step:

Aspirate the old culture solution, add 3 volumes of 0.25% trypsin to the culture flask, and keep the culture flask in in a 37°C constant temperature chamber for 12 mins, in case the flask gets fully vibrated and digested (drip the cell suspension every 3 min during the period, observe the cell morphology with a microscope to avoid digestion Excessive causes cell damage and death).

Terminate the digestion process by adding an equal volume of stop medium, centrifuge the flask at 2000 r/rpm for 5 min, and finally discard the supernatant.

Add three volumes of growth medium to make the cells resuspended, and culture the cells in the culture flasks labeled B1, B2, and B3, respectively, and change the liquid every 3 days.

Drawing of satellite cell growth curve

Discard old culture solution in the culture flask, add three times the volume of 0.25% trypsin, and keep the mixture in a 37°C constant temperature shaking box to ensure it shaken and digested.

FBS was added to a final concentration of 10% to stop enzyme activity, centrifuge at 2000 r/rpm for 5 min, and finally discard the supernatant.

The growth medium was gently blew into a homogenous suspension. Cells were inoculated at a density of 1*104 cells/mL per well in a 24-well plate, and solution was charged every 2 days.

The cells were counted by the method called blood cell counting from the second day of inoculation. In particular, three well cells were counted each time, three times per well, averaged, and so on, and counted continuously for 8 days.

The growth curve was plotted with the counting time as the abscissa and the average density of the 3-well cells as the ordinate.

Satellite cell immunofluorescence staining identification

The primary skeletal muscle satellite cells were washed for three times with PBS buffer, and fixed in a 4% paraformaldehyde solution for 30 min at room temperature.

These were washed 3 times with PBS buffer, 5 min each time, added with 0.1% TritionX-100, and kept for 20 min at room temperature.

Primary antibodies (Monoclonal Mouse lgG1 Clone #Pax7; dilution ratio 1:100) were added, stayed overnight at 4°C, and washed 3 times with PBS buffer for 5 min each time.

FITC-labeled secondary antibody (FITC AffinPure Goat Anti-Mouse LgG (H+L), dilution ratio 1:50) was added and incubated in the wet box at 37°C for 1 h in the dark, and washed 3 times with PBS buffer for 5 min each time.

The cell were stained with Dapi, observed under an inverted fluorescence microscope, and photographed.

Induced differentiation of skeletal muscle satellite cells

The cells cultured were taken to the 2nd generation, changed the ordinary growth medium to a differentiation medium to induce differentiation

culture. The growth and differentiation of skeletal muscle satellite cells and myotubes were observed under an inverted microscope.

PCR identification of skeletal muscle satellite cells

Total RNA from cells was extracted using the OMEGA Total RNA Extraction Kit. Reverse transcription experiments were performed using the full-gold Golden Easy one-step gDNA Removal and cDNA Synthesis Super Mix reverse transcription kit, including the AnchAnchored Oligo (dT) 18 Primer (0.5 µg•µL^{-1})/miR- cDNA synthesis was performed on 27b, U6 stem loop primer 1 µL, 2×ES Reaction Mix 10 µL, gDNA Remover 1 µL, RNase-free Water to 20 µL, and EasyScript RT/RI Enzyme Mix 1 µL.

The TaKaRa kit was used to perform PCR amplification. The reaction system consisted of 12.5 µL of Premix Taq, 3 µL of cDNA, 1 µL of each of the upstream and downstream primers (Table 1.), and 7.5 µL of ddH2O. PCR amplification conditions: pre-denaturation at 95°C for 5 min; denaturation at 95°C for 10 s; annealing at 60°C for 30 s; extension at 72°C for 1 min; total of 40 cycles; extension at 72°C for 10 min; preservation at 4°C. Detection of PCR amplification products: Firstly, a 1% agarose gel was made and after the gel was cooled and solidified, put it into an electrophoresis tank. 5 µL of PCR product per well was added, and at the same time 5 µL of DNA Marker DL2000 was added as a reference. After that, those stuff was electrophoresed in the trough, 200 V for 25 min, observed in a gel imaging system and photographed. Confirm the target band by comparison with DNA Marker.

Results and Discussion

Isolation and culture of skeletal muscle satellite cells from Bactrian camel

The newly formed Bactrian camel skeletal muscle satellite cells had a round or short fusiform shape and strong refractive index. After 48 h, adherent growth began, and the morphology of skeletal muscle satellite cells were seen as short fusiform. After 72 h of culture, the cells proliferated slowly. The skeletal muscle satellite cells did not fully expand, but the spindle-shaped or long fusiform shape began to appear, and the refractive index was strong. However, at this time, the adherent cells contained a certain amount of fibroblasts, so purification was required. On the 4th day, the solution was changed and the mixture was purified by differential adherence, and the purity of the cells increased. The 2nd generation skeletal muscle satellites had good growth status and

relatively uniform growth patterns and morphological characteristics (Fig 1).

Table 1. Primer design

Primer	Sequence
	(5`- 3`)
Pax7	Forward: GCTTCAGAGGGAGGTCAGG
	Reverse: AAGAAAGCCAAGCACAGCA
Myf5	Forward: CATCCTCGTCTGAGCCTTG
	Reverse: TGCCAGTTCTCGCCTTCT
Desmin	Forward: CAGGCTCACTCACTTCCAAC
	Reverse: CTGCTCACCGACTACCACC
Actβ	Forward: GGACTTCGAGCAGGAGATGG
	Reverse: AGGAAGGAGGGCTGGAAGAG

Cell growth curve

As can be seen from Fig 2, the number of cells did not change significantly from day 1 to day 3, and was in a delayed period. From the 4th day to the seventh day, the cells were in the logarithmic growth phase, growing rapidly and differentiating. On the eighth day, the number of cells moved from steadily growing to decreasing, which was due to the cell entering the growth stagnation period.

Immunofluorescence staining identification

Confocal laser scanning microscope for immunofluorescence staining was used and it was found that the antigen of Pax7 protein was successfully bound to the antibody, and the cells were stained red, which proved that the isolated cells were skeletal muscle satellite cells (Fig 3).

Identification of satellite cells by common PCR technology

By extracting total RNA from the cultured skeletal muscle satellite cell line and detecting it by spectrophotometer, the A260 / A280 was between 1.8 and 2.1, indicating that the RNA quality was good and the next experiment was successfully carried out. Now, the extracted RNA was inverted into cDNA with a reverse transcription kit, then PCR-amplified following the designed primer, and finally the analysis by agarose gel electrophoresis was followed. The results showed that after gel electrophoresis, a bright band appeared on the gel, indicating that Pax7, Myf5 and Desmin were expressed in the cells, and this cell line could be identified as a skeletal muscle satellite cell line (Fig 4).

Induction of differentiation of skeletal muscle Satellite cells

Myogenic induction culture to satellite cells. In 5th day, the *in vitro* induction cultured SCs started to fuse together and formed short myotube cells. As time went on, the cell density increased, and the fusion between cells became more extensive, forming a larger volume of myotubes. The length was significantly increased (Fig 5).

In the experiment on the *in vitro* culture samples of skeletal muscle satellite cells from young animals, the phenomenon could be found that the higher the age of the samples, the smaller the number of SCs. The purity of isolated SCs under Bactrian camel could reach 80% or more, but the content of SCs in Bactrian camels over 6 years old was less than 20%. The separation methods of skeletal muscle satellite cells mainly included tissue block method and enzyme digestion method. In addition to the method called differential adherence, there were also the separation and purification methods including flow sorting and density gradient centrifugation (Adhikari *et al*, 2018; Doornaert *et al*, 2019; Zhao *et al*, 2019). Flow sorting was mainly used in human and mouse studies. This method used flow cytometry to separate cells with a purity of 99%, but experimental instruments were expensive and susceptible to contamination (Ribeiro *et al*, 2019). Although the density gradient centrifugation method could obtain cells with high purity, it can cause a large amount of cell loss and

Table 2. Satellite cell count.

Time (day)	1	2	3	4	5	6	7	8
Number of cells (10^4/mL)	1.31	1.41	1.93	9.21	18.21	22.21	22.11	21.44
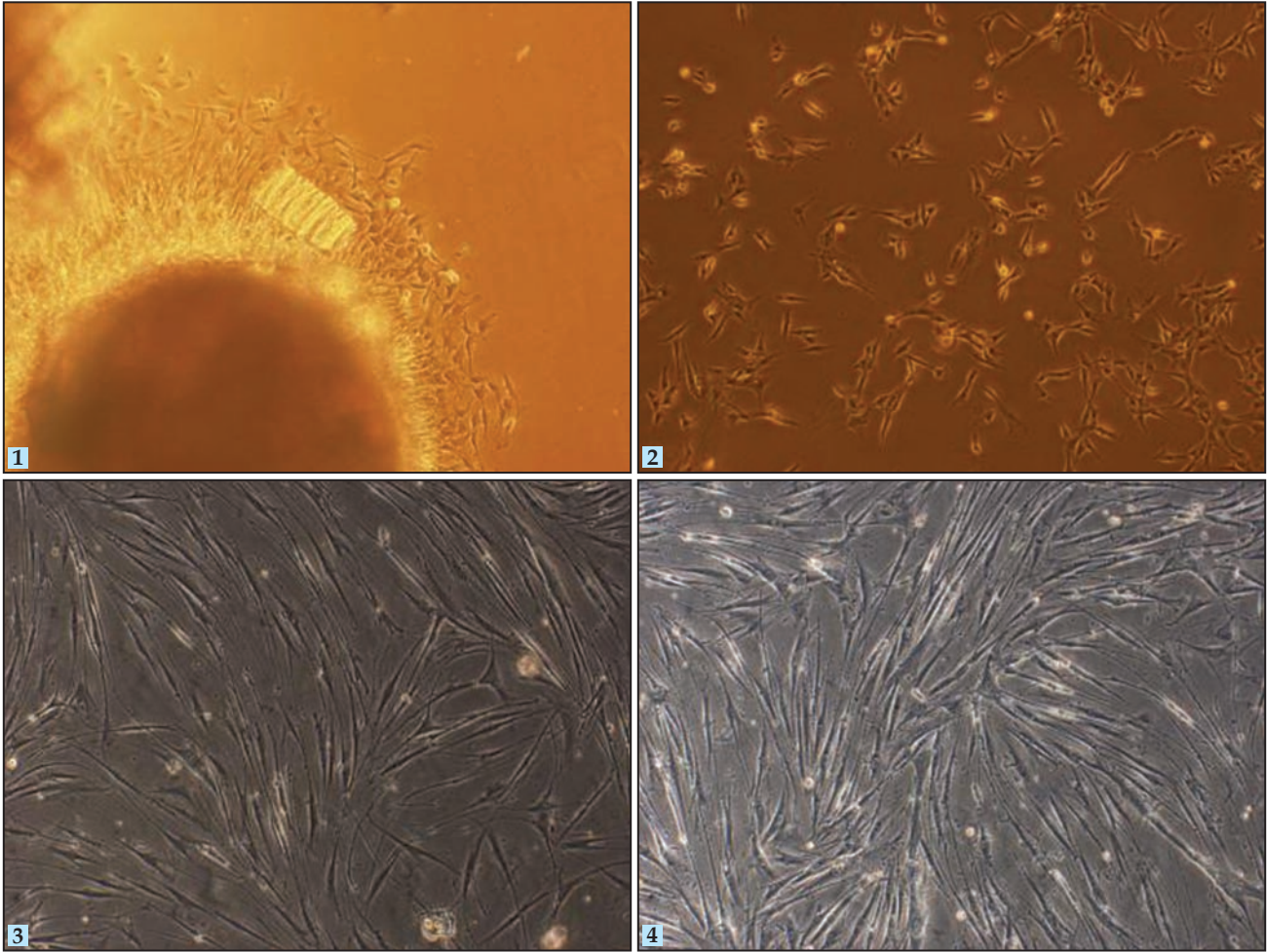
Fig 1. Bactrian camel skeletal muscle satellite cell growth pattern. **1.** Primary cells began to separate and adhere to the wall for 48 hours. **2.** The primary cells were fully adherent on the seventh day for passage. **3.** The third generation of satellite cells began to fuse, and the cell traits were long-sprung type, and the refractive index increased. **4.** The fifth generation of cells were in the third generation, and there was no major change in the cultivation.
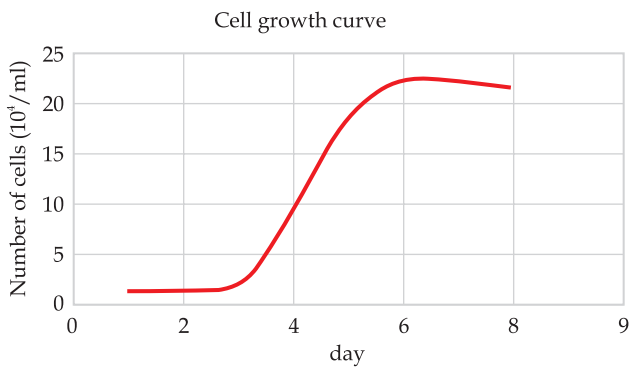
Fig 2. Satellite cell growth curve.

PAX7 has a very close relationship with the growth and repair of postnatal muscles, and is expressed during the differentiation, proliferation and activation of satellite cells (Seale *et al*, 2000; Sato *et al*, 2019). PAX7 has a maintenance effect on satellite cells and has an important anti-apoptotic effect in activated satellite cells. In this study, the markers of SCs, Desmill, Myf5 and PAX7, were tested at the RNA level (Zhao *et al*, 2019). The results were positive, and the cells isolated and purified by the experiment were proved to be Bactrian camel skeletal muscle satellite cells.
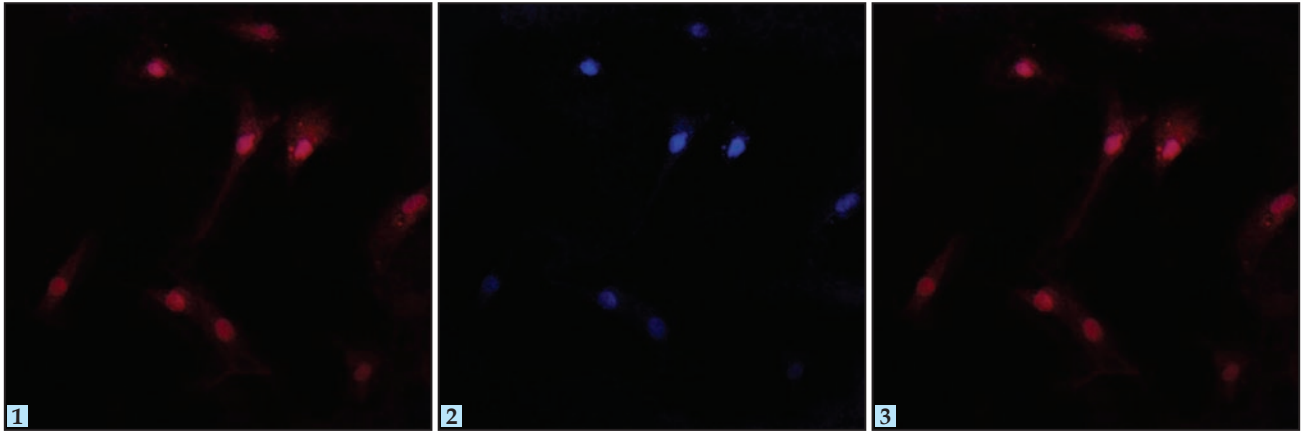
Fig 3. Identification of skeletal muscle satellite cells in Bactrian camel by immunofluorescence staining. 1. Cells labeled with pax7; 2. Cells labeled with DAPI; 3. Merged.

has a certain influence on cell activity due to repeated centrifugation, so that its application is debatable (Forcina *et al*, 2019). Therefore, in this article, young Bactrian camel were to isolate skeletal muscle satellite cells, tissue block method, and combined with differential adherence method to separate cells.

MDSCs is a category of myogenic stem cells, which contains one of the constituent components of the cytoskeleton, the intermediate filament protein Desmill, that is unique to muscle fibres. The myogenic factor MyoD gene belongs to the myogenic alkaline spiral ring and consists of 4 family members: MyoD, Myf5, MyoG, Myf6 (Lassar, 2017). Myf5 is the earliest induced expression factor in myogenic progenitor cells during embryonic development. Myf5 and MyoDl are functionally complementary to each other and activate the formation of initiate skeletal muscle. MyoDl is the earliest marker of skeletal muscle formation. It is expressed only in activated satellite cells (Qu-Petersen *et al*, 2002). It can convert many types of cells into myoblasts and promote the fusion of myoblasts into myotubes and there is no expression in the Satellite cells at rest. After activation, SCs, MyoDl and PAX7 were simultaneously expressed.
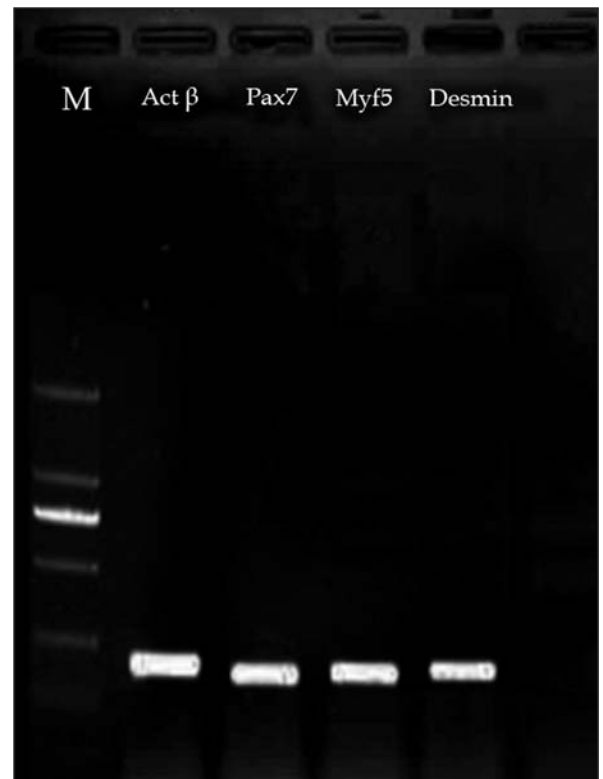
Fig 4. PCR electropherogram.
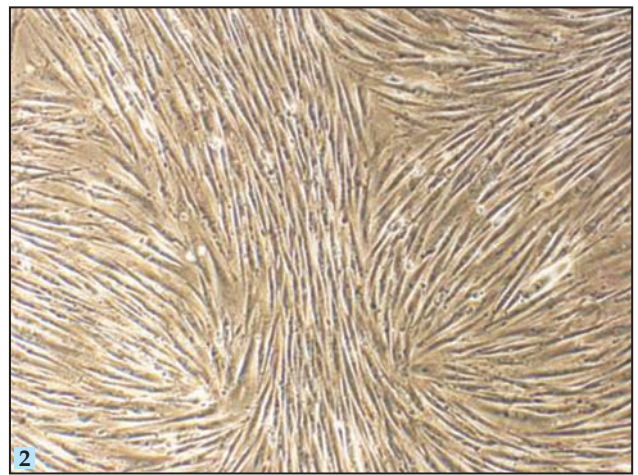
Fig 5. Induced differentiation of skeletal muscle satellite cells in Bactrian camel. **1-2.** Results of induced differentiation of skeletal muscle satellite cells.

Acknowledgements

References

Adhikari R, Chen C, Waters E, West FD and Kim WK (2018). Isolation and Differentiation of mesenchymal stem cells from broiler chicken compact bones. Frontiers in Physiology 189(2):247-254.

Bellayr I, Gharaibeh B, Huard J and Li Y (2010). Skeletal muscle-derived stem cells differentiate into hepatocyte-like cells and aid in liver regeneration. International Journal of Clinical and Experimental Pathology 3(7):681-690.

Doornaert M, De Maere E, Colle J, Declercq H, Taminau J, Lemeire K, Berx G and Blondeel P (2019). Xenogen-free isolation and culture of human adipose mesenchymal stem cells. Stem Cell Research 40(3):101-113.

Evano B and Tajbakhsh S (2018). Skeletal muscle stem cells in comfort and stress. NPJ Regen Med 24(3):27-37.

Forcina L, Miano C, Pelosi L and Musaro A (2019). An overview about the biology of skeletal muscle satellite cells. Current Genomics 20(1):24-37.

Harel I, Nathan E, Tirosh-Finkel L, Zigdon H, Guimaraes-Camboa N, Evans SM and Tzahor E (2009). Distinct origins and genetic programs of head muscle satellite cells. Developmental Cell 16(6):822-832.

Lassar AB (2017). Finding MyoD and lessons learned along the way. Seminars in Cell and Developmental Biology 72(1):3-9.

Mohammadi-Sangcheshmeh A, Shafiee A, Seyedjafari E, Dinarvand P, Toghdory A, Bagherizadeh I, Schellander K, Cinar MU and Soleimani M (2013). Isolation, characterisation, and mesodermic differentiation of stem cells from adipose tissue of camel (*Camelus dromedarius*). *In vitro* Cellular and Developmental Biology-Animal 49(2):147-154.

Qu-Petersen Z, Deasy B, Jankowski R, Ikezawa M, Cummins J, Pruchnic R, Mytinger J, Cao B, Gates C, Wernig A and Huard J (2002). Identification of a novel population of muscle stem cells in mice: potential for muscle regeneration. The Journal of Cell Biology 157(5):851-864.

Raiymbek G, Faye B, Kadim IT, Serikbaeva A and Konuspayeva G (2019). Comparativefatty acids composition and cholesterol content in Bactrian (*Camelus bactrianus*) and dromedary camel (*Camelus dromedarius*) meat. Tropical Animal Health and Production 51(7):2025-2035.

Ribeiro, AF, Souza, LS, Almeida CF, Ishiba R, Fernandes SA, Guerrieri DA, Santos ALF, Onofre-Oliveira PCG and Vainzof M (2019). Muscle satellite cells and impaired late stage regeneration in different murine models for muscular dystrophies. Scientific Reports 9(1):11842-11853.

Sato T, Higashioka K, Sakurai H, Yamamoto T, Goshima N, Ueno M and Sotozono C (2019). Core Transcription factors promote induction of PAX3-Positive skeletal muscle stem cells. Stem Cell Reports 13(2):352-365.

Scharner J and Zammit PS (2011). The muscle satellite cell at 50: the formative years. Skelet Muscle 1(1):28-29.

Seale P, Sabourin LA, Girgis-Gabardo A, Mansouri A, Gruss P and Rudnicki MA (2000). Pax7 is required for the specification of myogenic satellite cells. Cell 102(6): 777-786.

Wenfang, Yuye Fu ,Bin Yang, Hui Yang, Gerelt Borjigin, Huar Bao, Narenbatu and Demtu Er (2019). Comparative Study of Scraper Performance and Skeletal Muscle Fibre types of Alxa Gobi camel and desert camel. Journal of Camel Practice and Research 26(1):63-69.

Zhao Y, Chen M, Lian D, Li Y, Li Y, Wang J, Deng S, Yu K and Lian N (2019). Non-Coding RNA regulates the myogenesis of skeletal muscle satellite cells, injury repair and diseases. Cells 8(9):2025-2035.

PHARMACOKINETICS OF CEFQUINOME AFTER SINGLE INTRAMUSCULAR ADMINISTRATION IN DROMEDARY CAMEL (*Camelus dromedarius*)

Lakshmi Kant[1], Amita Ranjan[1], Rakesh Ranjan[2], VK Dumka[3] and Rajdeep Kaur[3]

[1]Department of Veterinary Pharmacology and Toxicology, College of Veterinary and Animal Science,
Rajasthan University of Veterinary and Animal Sciences, Bikaner 334001, Rajasthan, India
[2]ICAR-National Research Centre on Camel, Jorbeer, Bikaner 334001, Rajasthan, India
[3]Department of Veterinary Pharmacology and Toxicology, College of Veterinary and Animal Sciences,
Guru Angad Dev Veterinary and Animal Sciences, Ludhiana 141004, Punjab, India

ABSTRACT

The objective of this study was to investigate the pharmacokinetics of cefquinome in 5 healthy male dromedary camels following a single intramuscular (IM) administration at the dose rate of 1 mg/kg body weight in the caudal cervical epiaxial muscles. Blood samples were collected prior to drug administration and up to 48 h after drug administration. No clinical symptoms or signs suggestive of adverse drug reaction could be recorded in any animal. Plasma cefquinome concentration was estimated by high-performance liquid chromatography. The disposition kinetics of cefquinome best fitted to a 2 compartment open model. The peak plasma cefquinome concentration ($C_{max\ cal}$) of 1.013 ± 0.038 µg/ml^{-1} was achieved at 5.257 ± 0.067 h ($t_{max\ cal}$). The absorption half-life ($t^{1/2}_{ka}$), elimination half-life ($t^{1/2}_{\beta}$), area under plasma drug concentration-time curve (AUC) and apparent volume of distribution (Vd_{area}) of cefquinome were 3.401 ± 0.042 h, 3.754 ± 0.072 h, 14.417 ± 0.621 µg/ml^{-1} h and 0.379 ± 0.016 l/kg^{-1}, respectively. The results of the present study suggested that an intramuscular dosage regimen of 1 mg/kg body weight at 24 h interval would maintain the plasma drug levels required to be effective against the common bacterial pathogens in dromedary camel.

Key words: Camel, Cefquinome, Intramuscular, Pharmacokinetics

Cefquinome is a fourth-generation cephalosporin developed for exclusive use in animals (CVMP, 2003). It has a broad spectrum antibacterial activity, high stability against β-lactamase and enhanced potency and bioavailability. Therefore, it is a valuable antibiotic with potential use in treatment of various infectious diseases in camel. Studies on pharmacokinetics of different drugs in camel are limited, hence the doses of different drugs are usually extrapolated from those recommended for other animal species (Ali, 1998). Research reports suggest that activity of drug metabolising enzymes and the capacity to biotransform and eliminate xenobiotics in dromedary camel is lower than many other ruminants (Alquarawi and Ali, 2000). Therefore, pharmacokinetic studies to fix the appropriate dose rates are essential for rational use of any drug in this species. The present study was aimed to investigate the disposition of cefquinome following its single intramuscular administration in dromedary camel.

Materials and Methods

The study was carried out in 5 apparently healthy male dromedary camels in the age group of 3 to 4 years, weighing in between 400-450 kg. The experimental animals were kept under constant observation for 2 weeks prior to the experiment at National Research Centre on Camel, Bikaner, Rajasthan and examined periodically to exclude any possibility of localised or systemic disease. The animals were maintained under an intensive system of management and fed daily with guar (*Cyamopsis tetragonoloba*) meal (mixture of 30-33% hull, 27-30% endosperm, and 43-47% germ) and groundnut (*Arachis hypogaea*) haulms. The experimental protocol and ethical standards were followed as per guidelines of CPCSEA throughout the experiment.

Cefquinome sulphate (Cobactan 2.5% MSD Animal Health, Pune, India) was administered as single intramuscular dose of 1 mg/kg body weight in the caudal cervical epiaxial muscles located in the lower neck region after aseptic preparation of

the injection site. Blood samples (about 5 ml) were collected in heparinised vaccutainers by jugular venepuncture at 0.25, 0.5, 1.0, 2, 4, 6, 8, 10, 12, 24, 36 and 48 h after drug administration. Plasma was separated from the collected blood samples by centrifugation at 3000 rpm for 15 minutes at 4°C and stored at -80°C till analysis.

Analytical Procedure

Cefquinome concentrations in plasma samples were determined using high performance liquid chromatography (HPLC) as per the method described by Uney et al (2011). Briefly, 200 µl of plasma sample was mixed with 400 µl of methanol in a 2-ml microcentrifuge tube and vortexed for 10 seconds. The resultant mixture was centrifuged at 4000 g for 10 min, 300 µl of clear supernatant was filtered into a fresh vial and 150 µl of HPLC grade water was added and mixed for 10 seconds. The mixed clear supernatant (200 µl) was pipetted into an autosampler vial.

The HPLC system (Perkin Elmer, series 200, Waltham, USA) was fitted with a single pump, a degasser and an autosampler injector. The reverse-phase chromatography was performed with an analytic C18 column (Sun fire, Particle size 5µ, 4.6 × 150 mm, Waters, USA). In present method, binary gradient mobile phase was used with water containing 0.1% trifluroacetic acid (Sigma-Aldrich) as mobile phase A and acetonitrile (Sigma-Aldrich) as mobile phase B. The gradient elution was programmed with the ratio of mobile phases A: B as 90: 10 for 7 min, followed by 50: 50 for 3 min and 90:10 for 5 min. The injection volume was kept 50µl and flow rate was maintained as 0.9 ml min^{-1}. The detection was performed using a UV/VIS detector set at 268 nm. The Total Chrom software (version 6.1) was used for running the HPLC system and data analysis. The retention time of cefquinome was about 6.48 min and calibration curve for cefquinome was linear at concentrations of 0.05-50 µg/ ml with correlation coefficients (r) above 0.996. The limit of detection (LOD) and limit of quantification (LOQ) were determined by signal-to-noise ratio evaluations of samples spiked from 0.01 to 0.1 µg/ ml. The LOD and LOQ of cefquinome were determined to be 0.02 µg/ ml and 0.04 µg/ ml, respectively and were based on a signal-to-noise ratio of 3:1. The accuracy % for intra and inter day assay were found above 90% and above 95%, respectively. The recoveries of the 3 different concentration 0.4 µg/ ml, 6.25 µg/ ml, 25 µg/ ml were found to be 93.32 %, 89.56% and 95.51%,

respectively within the day analysis and 91.16%, 88.39% and 95.03%, respectively between the day analysis.

Pharmacokinetic Analysis

The appropriate pharmacokinetic model was determined by visual examination of plasma cefquinome concentration *versus* time curves and different pharmacokinetic parameters were calculated by PK Solver: An Add in Programme for Microsoft Excel, Version 2 (Zhang et al, 2010). The pharmacokinetic variables obtained were expressed as mean ± S.E variable.

Results and Discussion

Intramuscular administration of cefquinome at the rate of 1 mg per kg body weight appeared safe as no clinical signs suggestive of adverse effects or drug intolerance was evident in any camel. The mean plasma drug concentration-time curve for cefquinome in dromedary camel following its single intramuscular administration is depicted in Fig 1. The plasma cefquinome concentrations could be detected up to 36 h in the collected samples, but at 48h, it could not be detected. The value of different pharmacokinetic parameters obtained are presented in Table 1.

Considering the plasma drug concentration and time profile, the disposition kinetics of cefquinome after its single intramuscular administration best fitted into two-compartment open model. Atta et al (2017) also reported that after single intravenous or intramuscular injection of cefquinome in camel, the plasma drug concentration *vs* time profile followed the first order 2 compartment open model. Disposition curve of cefquinome after its intramuscular administration has also been reported and described by 2 compartment open model in sheep and goat (Dumka et al, 2013; El-Hewaity et al, 2014), sheep (Tohamy, 2011) and rabbit (Qiang et al, 2013 and Shalaby et al, 2015). However, Al-Taher (2010) described disposition of cefquinome in camel by non-compartmental analysis following its single intramuscular administration at the dose rate of 1 mg/kg body weight. Champawat et al (2018) reported that pharmacokinetics of cefquinome in goat best fitted to one compartment open model after its intramuscular administration at the dose rate of 2 mg/kg body weight. In a study, El-Sayed et al (2015) reported that plasma concentration-time curve following a single intravenous as well as intramuscular administration of cefquinome @

Parameters	Unit	Value
A	µg/ml	17.887±4.196
α	1/h	0.176±0.006
B	µg/ml	8.809±1.923
β	1/h	0.185±0.003
Ka	1/h	0.204±0.002
$T_{½\ alpha}$	h	3.965±0.144
$T_{½\ beta}$	h	3.754±0.072
$T_{½ka}$	h	3.401±0.042
CL/F	(mg/kg)/(µg/ml)/h	0.069±0.003
$T_{max\ (cal)}$	h	5.257±0.067
$C_{max(cal)}$	µg/ml	1.013±0.038
AUC_{0-t}	µg/ml*h	14.417±0.621
AUC_{0-inf}	µg/ml*h	14.548±0.633
AUMC	µg/ml*h^2	154.028±8.188
MRT	h	10.569±0.155
Vdarea	L/kg	0.379±0.016

A, zero time intercept of the least square regression line of the absorption phase; B, zero time intercept of the least square regression line of the elimination phase; α and β, distribution and elimination rate constants; Ka, first order rate constant; $T_{½α}$ and $T_{½β}$, distribution and elimination half-life; $T_{½ka}$, absorption half-life; CL/F, body clearance corrected for bioavailability; Tmax (cal), the time point of maximum plasma concentration; Cmax(cal), maximum plasma drug concentration; AUC0-t and AUC0-inf, area under plasma drug concentration *vs* time curve to 36h and to infinity; AUMC, area under the first moment curve; MRT, mean residence time; Vdarea, apparent volume of distribution of drug.

2 mg/kg body weight was best described by three compartment open model in chicken. Dissimilarities in kinetic parameters of drugs are relatively common and might be attributed to difference in assay methods, age, animal breed, health status and formulation of the used drug (El-Sayed *et al*, 1989).

In the present study, the peak plasma cefquinome concentration (C_{max}) was 1.013±0.038 µg/ml was achieved at T_{max} of 5.25±0.067 h. Likewise, a peak plasma concentration (C_{max}) of 1.23±0.08 µg/ml was reported to achieve at (T_{max}) 4.25±0.1 h after single intramuscular injection at the same dose rate in camel by Al-Taher (2010). El-Hewaity *et al* (2014) reported C_{max} of 1.80±0.09 µg/ml and 1.88±0.10 µg/ml in sheep and goat after intramuscular administration of cefquinome 2 mg/kg body weight once daily for 3 consecutive days. However, in other species, C_{max} values reported were 4.57±0.338 µg/ml and 2.60±0.14 µg/ml in sheep (Tohamy, 2011; Uney *et al*, 2011), 4.39±0.53 µg/ml in piglet (Song *et al*, 2013), 4.84±0.23 µg/ml in goat (Dumka *et al*, 2013), 5.79± 0.35 µg/ml in calf (Hemvati *et al*, 2019) and 3.04±0.71 µg/ml in chicken (Xie *et al*, 2013), which were higher than that observed in the present study. In an another report, maximum plasma concentration (C_{max}) of 3.2±0.39 µg/ml was observed after time (T_{max}) 0.82±0.06 h in camel following a single IM injection of cefquinome at the dose rate of 1 mg/kg body weight (Atta *et al*, 2017).

The absorption half-life ($t_{½Ka}$) of cefquinome after intramuscular administration in camel was found to be 3.401 ± 0.042 h suggesting delayed
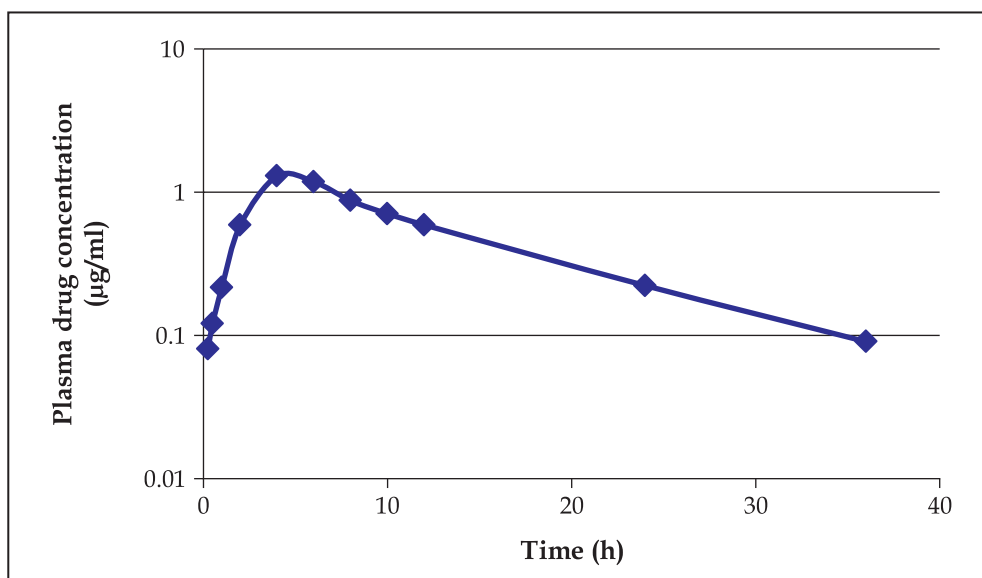

Fig 1. Drug disposition curve following a single intramuscular cefquinome administration at the rate of 1 mg/kg in dromedary camel.

absorption of cefquinome from the injection site. In corroboration with the present observation, Al-Taher (2010) also reported $t_{1/2Ka}$ equal to 4.35±0.27 h in camel after cefquinome administration at the dose rate of 1 mg/kg body weight. However, in another study (Atta *et al*, 2017) $t_{1/2Ka}$ was calculated to be 0.26±0.03 h. Variation in age group, sex and site of injection may be possible reasons behind this variation. In a study in sheep, absorption half-life of cefquinome was calculated to 1.540±0.112 h, 1.037±0.073 h and 0.664±0.071 h in one month, 6 months and one year old sheep, suggested that the age of the animal has significant influence on the absorption rate of any drug when administered at same dose rate and site (Tohamy, 2011). In a survey of literature on the kinetics of drugs used in camel, Alquarawi and Ali (2000) opined that most of drugs have longer absorption and elimination half-lives and slower systemic clearance in camel as compared to other animals. Perusal of available literature revealed large variations in $t_{1/2Ka}$ values of cefquinome among different animal species. Lower value of $t_{1/2Ka}$ indicating rapid absorption of the drug has also been reported in rabbit (0.28 ± 0.02 h, Shalaby *et al*, 2015), sheep (0.61 ± 0.10 h, Rana *et al*, 2015), goat (0.64 ± 0.23 h, Dumka *et al*, 2013), Calf (0.25±0.04 h, Hemvati *et al*, 2019) and Beagle dog (0.14±0.05 h, Zhou *et al*, 2015).

The elimination half-life ($t_{1/2\beta}$) is indicative of the overall rate of elimination of a drug from the body. In present study, the calculated value of $t_{1/2\beta}$ was 3.754±0.072 h, suggesting rapid elimination of the drug from the body of camel. The value calculated in the present study was close to the value (3.15±0.22 h) reported by Atta *et al* (2017) after single intravenous administration of cefquinome at the rate of 1 mg/kg body weight in camel. Dumka *et al* (2013) also reported $t_{1/2\beta}$ value of 5.86±0.29 h in goat receiving cefquinome at the rate of 2 mg/kg body weight intramuscularly. In pigs, $t_{1/2\beta}$ was calculated to be 4.36±2.35 h after intramuscular administration of cefquinome (Li *et al*, 2008), which was in concurrence to results of the present study. However, $t_{1/2\beta}$ values of 6.68±0.87 h and 10.24±0.8 h were reported by Atta *et al* (2017) and Al-Taher (2010), respectively, after intramuscular administration of cefquinome in camel. The elimination half-life of cefquinome after its intramuscular administration is reported to be highly variable from species to species; as low as 2.60±0.04 h in rabbit (Shalaby *et al*, 2015) to as high as 26.90±4.33 h in red-eared slider turtle (Uney *et al*, 2017).

The area under plasma concentration time curve (AUC_{0-t}) is an important parameter used to calculate clearance, volume of distribution and bioavailability of drugs in pharmacokinetic studies. The mean± S.E. value of AUC after intramuscular administration of cefquinome in camel in the present study was 14.417±0.621 µg/ml.h which was almost comparable to that reported in goat (14.42 ± 0.62 µg ml^{-1} h, Champawat *et al* (2018), in calf 16.02 ± 1.11 µg ml^{-1} h, Hemvati *et al* (2019) and 19.82 ± 2.07 µg ml^{-1} h in goat (Dumka *et al*, 2013). However, higher values of AUC were calculated as 49.582±9.173 µg ml^{-1} h in rabbit (Qiang *et al*, 2013) and 38.79 ± 1.24 µg ml^{-1} h in chicken (El- Sayed *et al*, 2015). Lower value of AUC was reported 8.24 ± 0.80 µg ml^{-1} h in Beagle dog (Zhou *et al*, 2015) and 5.13 ± 1.06 µg ml^{-1} h in chicken (Xie *et al*, 2013). After intramuscular administration, the drug is absorbed slowly resulting into significant drug elimination to occur before absorption is complete. This is why, the AUC value for a drug after intramuscular injection is lower than that reported after intravenous administration (Atta *et al*, 2017).

The value of area under moment curve (AUMC) after intramuscular administration of cefquinome in camel in the present study was found to be 154.028±8.188 µg ml^{-1} h^2. AUMC values 157.05 ± 37.93 µg ml^{-1}.h^2 in sheep (Rana *et al*, 2015), 155.85 ± 9.70 µg ml^{-1} h^2 in goat (Dumka *et al*, 2013) and 182.75 ± 5.35 µg ml^{-1} h^2 in rabbit (Shalaby *et al*, 2015) as reported in different studies were close to that observed in the present study. However, in camel, AUMC value (68.64± 14.58 µg ml^{-1} h^2) recorded after intramuscular cefquinome administration (Atta *et al*, 2017) was almost half the value calculated in the present study. This may be perhaps due to variation in age group, species, breed and sex of the animals used in different studies.

The time required for an intact drug molecule to transit through body is defined as mean residence time (MRT). The MRT calculated in the present study was 10.569 ± 0.155 h. Al-Taher (2010) reported MRT value 16.74± 0.9 h in camel after intramuscular cefquinome administration, which was greater than the value found in the present study. Hamed *et al* (2016) also reported MRT values ranged from 10.5±0.9 h to 11.9±1.2h in goat after intramuscular administration of cefquinome at the dose rate of 2 mg/kg body weight. On the other hand, Atta *et al* (2017) reported MRT as 5.14±0.27 h in camel following intramuscular administration of cefquinome at the dose rate of 1 mg/kg body weight. MRT values have been reported to vary with age from 8.157± 0.98 h (in 1 month old), 6.935±0.40 h (in 6 month old)

to 5.303±0.18 h (in 1 year old) in sheep after single intramuscular administration of cefquinome (Tohamy *et al*, 2011). Lower MRT value of cefquinome has also been reported in different animal species like 9.14 ± 1.83 h in sheep (Rana *et al*, 2015), 8.08 ± 0.50 h in goat (Dumka *et al*, 2013), 4.12 ± 0.05 h in rabbit (Shalaby *et al*, 2015) and 2.88 ± 0.23 h in calf (Hemvati *et al*, 2019).

The mean (±S.E.) value for apparent volume of distribution (Vdarea) was found 0.379 ± 0.016 L.kg^{-1} in the present study. It was close to the value 0.34 L kg^{-1} in pig (Liu *et al*, 2012) and 0.51± 0.05 L kg^{-1} in goat (Dumka *et al*, 2013). The result indicates limited distribution of cefquinome in various body fluids of camel. In the present study, values of A, B, α and β were calculated to be 17.887±4.196 µg/ml, 8.809±1.923 µg/ml, 0.176±0.006 h^{-1} and 0.185±0.003 h^{-1}, respectively. Atta *et al* (2017) reported values of A, B, α and β as 4.98± 0.77 µg/ml, 0.57±0.24 µg/ml, 0.49±0.04 h^{-1} and 0.11±0.01 h^{-1}, respectively.

The *in vitro* efficacy of cefquinome against a wide range of Gram-negative and Gram-positive pathogens has been determined in several studies. Considering the reported MIC90s (0.06-0.39 µg/ml) for *Escherichia coli, Pasteurella multocida* and *Streptococcus agalactiae*, the T>MIC has been calculated for MICs of 0.06, 0.125 and 0.39 µg/ml, respectively (Dumka *et al*, 2013). All these organisms are reported to be common pathogens in camel (Wernery and Kaaden, 2002). In the present study, plasma cefquinome levels above the MIC were maintained >24 h following single intramuscular administration of cefquinome. Therefore, a dose rate of 1 mg kg^{-1} at 24 h dosing interval may be recommended for intramuscular administration of cefquinome in camel.

References

Ali BH (1998). A survey of some drugs commonly used in the camel. Veterinary Research Communications 12:67-75.

Alquarawi AA and Ali BH (2000). A survey of the literature (1995-1999) on the kinetics of drugs in camels (*Camelus dromedarius*). Veterinary Research Communications 24:245-260.

Al-Taher AY (2010). Pharmacokinetics of cefquinome in camels. Journal of Animal and Veterinary Advances 9:848-852.

Atta AH, El-Sayed HAE, El-Hadaky AYA, Kamel E and Sdeek FA (2017). Pharmacokinetics of cefquinome following intravenous and intramuscular injection in camels. Journal of Camel Practice and Research 24:239-245.

Champawat M, Sankhala LN, Sharma P and Gaur A (2018). Pharmacokinetic of single dose intramuscular administration of cefquinome using microbiological assay in goats. Journal of Entomology and Zoology Studies 6:1825-1828.

CVMP (2003). Cefquinome (Extension to horses) Summary Report (3) EMEA/MRL/ 883/03-FINAL. European Agency for the Evaluation of Medicinal Products, London, UK.

Dumka VK, Dinakaran V, Ranjan B and Rampal S (2013). Comparative pharmacokinetics of cefquinome following intravenous and intramuscular administration in goats. Small Ruminant Research 113:273-277.

El-Hewaity M, Abd El Latif A, Soliman AA and Aboubakr M (2014). Comparative pharmacokinetics of cefquinome (Cobactan 2.5%) following repeated Intramuscular administrations in sheep and goats. Journal of Veterinary Medicine. Article ID 949642.

El-Sayed MGED, El-Komy AAEH, Mobarez EA and El-Mahdy AM (2015). Pharmacokinetics and tissue residues of cefquinome in normal and *Salmonella entretidis* infected chickens. World Journal of Pharmacy and Pharmaceutical Sciences 4:1974-1987.

El-Sayed M G, Hatem ME and El-Komy A A (1989). Disposition kinetics of gentamicin in normal and endometritic cows using a microbiological assay. Dtsch Tierarztl Wochenschr 96:412-415.

Hamed E, Mahmoud FA and Altohamy DE (2016). Pharmacokinetics of cefquinome following multiple doses intramuscular administration in goats using HPLC. Japanese Journal of Veterinary Research 64: S109-S115.

Hemvati, Sharma P and Gaur A (2019). Disposition kinetics of cefquinome in calves after a single intramuscular bolus dose. International Journal of Current Microbiology and Applied Sciences 8:494-500.

Li XB, Wu WX, Su D, Wang ZJ, Jiang HY and Shen JZ (2008). Pharmacokinetics and bioavailability of cefquinome in healthy piglets. Journal of Veterinary Pharmacology and Therapeutics 31:523-527.

Liu B, Zhang C, Zhang X, Yang S, YuJ, Sun J and Liu Y (2012). Pharmacokinetics and bioavailability of cefquinome in crossbred wild boars. Journal of Veterinary Pharmacology and Therapeutics 35:611-614.

Qiang FU, HuaLin FU, Huan LUO, Zhang W, Guang SHU, Meng-Jiao LIU, Feng-Ying D and Jun HU (2013). Preparation of cefquinome sulphate proliposome and its pharmacokinetics in rabbit. Iranian Journal of Pharmaceutical Research 12:611-621.

Rana MP, Sadariya, KA and Thaker AM (2015). Effect of tolfenamic acid co-administration on pharmacokinetics of cefquinome following intramuscular administration in sheep. Veterinarski Arhiv 85:283-292.

Shalaby MA, Goudah A, Kamel GM and Shaheen HA (2015). Disposition kinetics of cefquinome in healthy rabbits following intramuscular and oral administration. World Journal of Pharmacy and Pharmaceutical Sciences 4:263-274.

Song IB, Kim TW, Lee HG, Kim MS, Hwang YH, Park BK, Lim JH and Yun HI (2013). Influence of the injection site on the pharmacokinetics of cefquinome following intramuscular injection in piglets. Journal of Veterinary Medical Science 34:22-26.

Tohamy MA (2011). Age-related intramuscular pharma-cokinetics of cefquinome in sheep. Small Ruminant Research 99:72-76.

Uney K, Altan F and Elmas M (2011). Development and validation of a high-performance liquid chromatography method for determination of cefquinome concentrations in sheep plasma and its application to pharmacokinetic studies. Antimicrobial Agents and Chemotherapy 55:854-859.

Uney K, Altan F, Cetin G, Aboubakr M, Dik B, Sayin Z, Er A and Elmas M (2017). Pharmacokinetics of cefquinome in red-eared slider turtle (*Trachemys scripta elegans*) after single intravenous and intramuscular injections. Journal of Veterinary Pharmacology and Therapeutics 41:e40-e44.

Wernery U and Kaaden OR (2002). Infectious Diseases in Camelids. Blackwell Science, Berlin.

Xie W, Zhang X, Wang T and Du S (2013). Pharmacokinetic analysis of cefquinome in healthy chickens. British Poultry Science 54:81-86.

Zhang Y, Huo M, Zhou J and Xie S (2010). PK Solver: An add-in program for pharmacokinetic and pharmacodynamic data analysis in Microsoft Excel. Computer Methods and Programs in Biomedicine 99:306-314.

Zhou YF, Zhao DH, Yu Y, Yang X, Shi W, Peng YB and Liu YH (2015). Pharmacokinetics, bioavailability and PK/PD relationship of cefquinome for *Escherichia coli* in Beagle dogs. Journal of Veterinary Pharmacology and Therapeutics 38:543-548.

DIAPLACENTAL INFECTION OF A BACTRIAN CAMEL (*Camelus Bactrianus*) WITH THE FILARIAL WORM *Dipetalonema evansi*: A CASE REPORT

Rolf K. Schuster, Gudrun Wibbelt[1], Elisa Maio, Ulrich Wernery and Saritha Sivakumar

Central Veterinary Research Laboratory, Dubai, U.A.E.
[1]Leibnitz Institute for Zoo and Wildlife Research, Berlin, Germany

ABSTRACT

This case report describes the first finding of the filarial worm *Dipetalonema evansi* in the United Arab Emirates. This case is also the first description of a diaplacental infection with *D. evansi*. Three adult nematodes were found at necropsy in the cranial mesentery artery of a newborn Bactrian camel (*Camelus bactrianus*). Scanning electron microscopy images were used to describe morphological details of this parasite. The pregnant mother was imported 4 months earlier from a farm in South Western Kazakhstan. Considering the climatic conditions in Kazakhstan, it is believed that the infection happened before October 2018.

Key words: *Camelus bactrianus*, diaplacental infection, *Dipetalonema evansi*, microfilaria

Dipetalonema evansi (Syn. *Deraiophora evansi*) is a filarial worm of the family Onchocercidae that inhabits blood vessels of Old World camelids. The first description of the parasite under the name of *Filaria evansi* was made by Lewis (1882) on material found by Griffith Evans in pulmonary arteries of a dromedary in Dera Ismail Khan (Khyber Pakhtunkhawa Province of Pakistan). Baylis and Daubney (1922) found the same filarial nematodes in the spermatic arteries of a camel in Lahore (Punjab district of Pakistan) and transferred this species into the genus *Acanthocheilonema*, based on characters of the oesophagus, the spicules and the caudal papillae of the male. Boulenger (1924) completed the description of *A. evansi* by a detailed description of the position of the papillae at the anterior end and the male posterior end. Yorke and Maplestone (1926) considered the genus *Acanthocheilonema* a junior synonym of *Dipetalonema* and subsequently transferred *A. evansi* into that genus. The first description of these filarial worms in a Bactrian camel was made by Romanovic (1916). The author found fragments of *D. evansi* in the lungs of a camel in Kyrgyzstan and described them under the name of *Deraiophoronema cameli*.

G. Evans was the first who reported microfilariae of *D. evansi* in the blood of camels and found that they are indistinguishable from those found in human blood (Lewis, 1882). Nagaty (1947) described a severe case of cardiac dipetalonemosis with 216 coiled nematodes in the right ventricle of a camel in Egypt. At a Cairo camel abattoir, he obtained further *D. evansi* specimens from blood vessels of testicles and lungs and examined blood samples for microfilariae. As a result, the author gave the most comprehensive description of adults and their microfilariae. He also listed references that detected microfilariae in dromedaries in Tunisia, Algeria, Morocco, Mali and Sudan, and in Bactrian camels in Turkestan.

The aim of this case report is to describe findings of adult *D. evansi* in a newborn Bactrian camel and microfilaria in a herd of Bactrian camels originated from Kazakhstan in the UAE.

Materials and Methods

A freshly dead Bactrian camel calf was sent for necropsy to the Central Veterinary Research Laboratory in Dubai in March 2019. According to the sender, the calf originated from a farm in Fujairah on the East coast of the United Arab Emirates that had imported pregnant Bactrian camels from South Western Kazakhstan in December 2018. The calf was one week old and suffered from bloody diarrhoea with soiled tail and legs. An open ductus arteriosus confirmed the neonatal age of the animal. The main pathological alterations were seen in the distal intestinal tract and consisted of petechiae at large

and circular colon and red stripes in the mucosa of the distal colon. Parasitological examination of a watery faecal sample revealed *Cryptosporidium* sp. and *Cystoisospora orlovi* oocysts in large numbers. These parasitological results were confirmed by histopathology. Three white coloured nematodes were removed from the cranial mesentery artery (Fig 1).

The nematodes (one male and two females) were fixed in hot (70°C) 10% formalin, examined and measured by light microscopy, followed by scanning electron microscopy examination to identify relevant structures for species determination. For this, the nematodes were dehydrated by increasing alcohol concentration, followed by critical point drying and subsequent sputter-coating with gold-palladium.

EDTA blood samples from 20 Bactrian camels of the imported herd (11 adult females and 9 calves) were examined with the modified Knott's test (Deplazes, 2006). For this, 1 ml of anticoagulated blood was mixed with 10 ml of 2 % formalin. After thorough mixing, the liquid was centrifuged for 3 min at 1500 rpm. Examination of methylene blue stained sediment was made at a magnification of 100 x by light microscopy. In addition, Giemsa stained blood smears were also examined.

Results and Discussion

The male specimen measured 11.5 cm with a maximum width of 400 µm. The intact female worm was 19 cm long and up to 650 µm in width. Of the second female specimen, only a fragment of 17 cm with missing anterior end was present. In light microscopy, the body surface was smooth but with high magnification of scanning electron microscope a fine transverse striation was recognisable (Fig 2). Spongy structures were present at both lateral sites of the mouth opening, around cervical papillae and at the posterior end of the female. The width of head of the male and female specimens in dorso-ventral projection was 110 and 120 µm, respectively. Scanning electron microscopy showed that the anterior end in both sexes was oblong rather than round and consisted of a circular, tire-like mouth opening and 12 papillae arranged in 2 levels (Fig 3). Four conical papillae were situated on the outer level on each corner of the rectangular shaped anterior end and 8 further papillae on lateral sites were located closer to the mouth opening. Of these, 4 were close to those of the outer level and 4 were arranged in pairs on each lateral site. There was a pair of cervical papillae (Fig 4) situated at unequal distances from the anterior end (305 and 350 µm in the male and 325 and 410 µm in the female specimen). The 1½ times spirally twisted posterior end of the male beared 4 pairs of pre-cloacal papillae (Fig 5). Between the last pair there was an unpaired median papilla. Four pairs of post-cloacal papillae were situated caudal to the anal opening. Spicules were of noticeable unequal length and shape. The longer spicule (810 µm) consisted of two parts (Fig 6). Its proximal 3rd was more massive and at a fracture like structure it proceeded as a thin curved and sharply pointed peak. The shorter and broader spicule was slightly curved and the pointed tip was kinked in an obtuse angle. The female ends blunted with 4 protrusions on the posterior end (Fig 7). The anal opening was at a distance of 250 µm from the posterior end (Fig 8). The uteri of both female worms were filled with sheathed microfilariae.

The Knott's test revealed microfilariae (Fig 9) in the blood of 4 out of 11 adult camels including the mother of the deceased calf. The 9 blood samples from camel calves were negative. Sheathed microfilariae in Giemsa stained blood samples (Fig 10) measured 266 - 320 µm in length with a maximum width of 6 - 7 µm.

To the best of our knowledge, this is the first case of a congenital infection with this filarial worm and it is the first case of finding of *D. evansi* in a camel in the UAE. Also, the location of the nematodes in the mesenterial arteries is rather unusual. Sazmand *et al* (2013) described testes, hearts and lungs as predilection sites.

Of the 4 filarial nematodes detected in camels, *D. evansi* and *Onchocerca fasciata* are camel specific while *O. gutturosa* and *O. armillata* despite parasitise camels were more often found in cattle. While adults of *D. evansi* and *O. armillata* inhabit blood vessels, macrofilariae of the two other species are located in connective tissues: *O. fasciata* forms nodules in subcutaneous fasciae and *O. gutturosa* is found in the nuchal ligament (Cheema and Ivoghli, 1978, Pathak *et al*, 1998; Moghaddar and Zahedi, 2006; Chhabra and Gupta, 2006). While *Onchocerca* species were transmitted by blackflies (Simuliidae) vectors of *D. evansi* are mosquitos of the genus *Aedes*. Investigations on the life cycle of *D. evansi* were carried out in a camel farm in the Mary district of Turkmenistan where 157 out of 681 camels were positive for blood microfilariae. Katajceva (1969) examined 3,792 *Aedes caspius* caught at the camel farms territory and detected larval stages of *D. evansi* in 505 (=13.3%). Positive mosquitos were present between May and September but not in October anymore. Experimental infection of *A. caspius* at a temperature of 26 to 28°C showed that it takes 10 days from uptake of blood
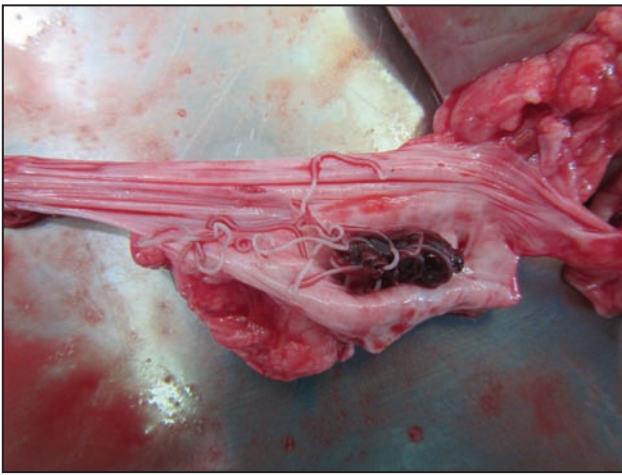
Fig 1. Filarial worms (*Dipetalonema evansi*) in the cranial mesentery artery.
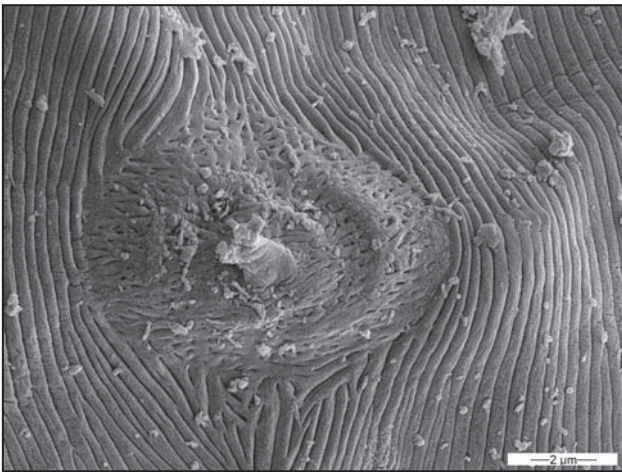
Fig 2. Cervical papillae of *D. evansi* is surrounded by a sponge like structure. The anterior body of the nematode shows a fine transverse striation (SEM).
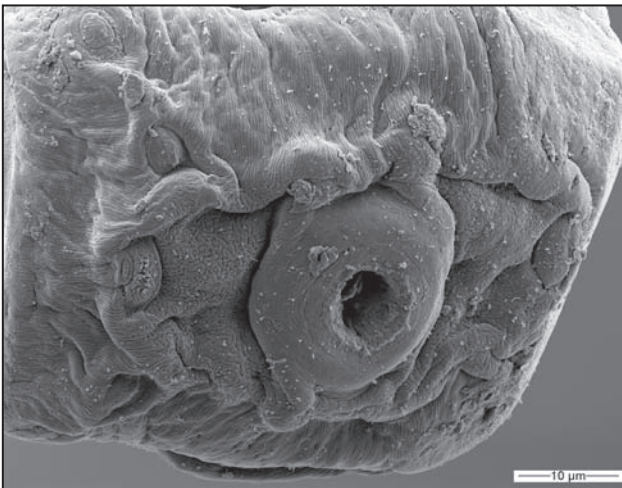
Fig 3. Apical view on the anterior end of *D. evansi*. The tire shaped mouth opening is surrounded by 12 papillae (SEM).
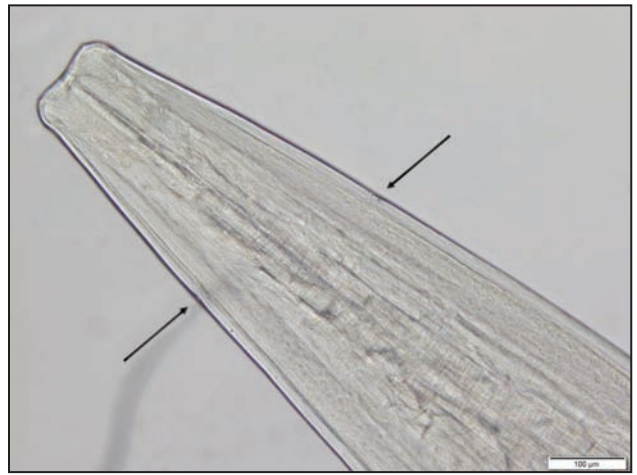
Fig 4. Asymmetrical cervical papillae (arrows) in a female *D. evansi.*

Fig 5. Posterior end of the male *D. evansi* with pre and post cloacal papillae (SEM).

Fig 6. Posterior end of the male *D. evansi* with two spicules of uneven length and shape. The longer spicule has a fracture like structure at its proximal end (arrow).
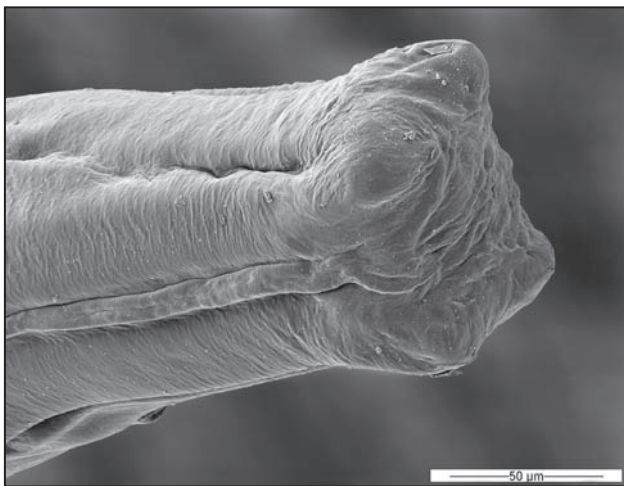
Fig 7. Posterior end of the female *D. evansi* (SEM)..
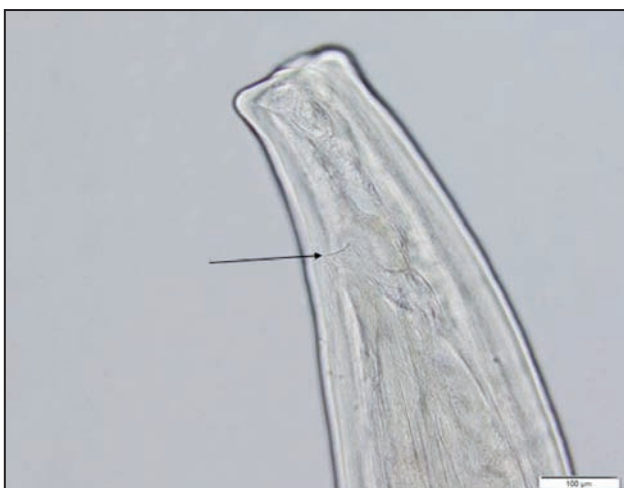
Fig 8. Anal opening (arrow) of the female *D. evansi*.

Fig 9. Sheathed *D. evansi* microfilaria (Knott's test).
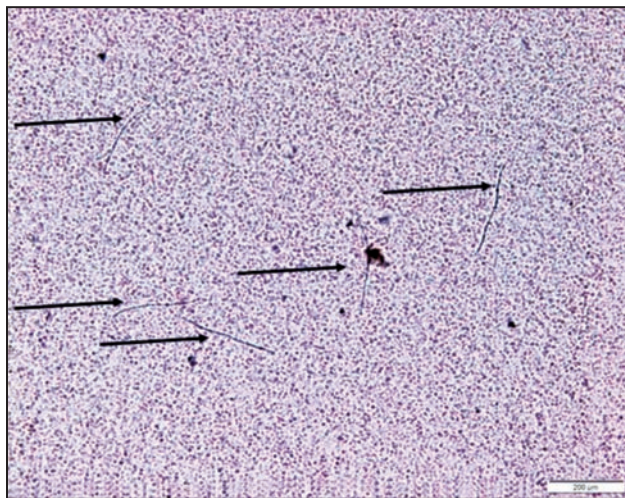
Fig 10. Five *D. evansi* microfilaria (arrows) in a stained blood smear (low magnification).

microfilariae to the development of infective 3rd stage larvae (Katajceva, 1969).

Finding adult macrofilariae in a neonatal camel calf can only be explained by a congenital infection. There are only few reports of diaplacental infections with filarial worms. Auer and Aspöck (2004) listed cases of microfilaria detection in human placenta and umbilical cord blood samples and thus, demonstrated that microfilariae can migrate though the human placenta. In our case, however, not only microfilariae but also infective 3rd stage larvae must have passed through the placental barrier. Real congenital filarial infections were reported for *Setaria digitata* by Kim *et al* (2010) in cattle and for *S. bidentata* by Gomez-Puerta and Mayor (2017) in a deer.

Although, there are no data on the development of *D. evansi* in the camel host, the prepatent period of *Dipetalonema reconditum* in dogs lasted more than two months (Farnell and Faulkner, 1978) and for

other filarial nematodes prepatent periods of 8 – 10 months were given (Taylor *et al,* 2015). Since a survey of Camp *et al* (2019) revealed that the vector mosquito *A. caspius* is rare in the UAE and was not detected in Fujairah, it is most likely that the infection took place in Kazakhstan and in this case, considering the temperature profile that influence the activity of mosquitos in Kazakhstan it can be concluded that the infection of the most had taken place not later than September 2018.

It is noteworthy that this is also the first proven evidence that Bactrian camels can be a host for *C. orlovi*. Although, the parasite was described for the first time in camel calves in Kazakhstan by Cygankov

(1950), the author did not mention the species of the camel.

Acknowledgements

References

Auer H and Aspöck H (2004). Verticale Transmission von Helminthen beim Menschen. Nova Acta Leopoldina NF 89:334-363.

Baylis HA and Daubney R (1923). A further report on parasitic nematodes in the collection of the Zoological Survey of India. Records of the Indian Museum 25:551-578.

Boulenger CL (1924). The filariid of the camel, *Acanthocheilonema evansi* (*Lewis*). Parasitology 16:419-423.

Camp JV, Karuvantevida N, Chouhna H, Safi E, Shah JN and Nowotny N (2019). Mosquito biodiversity and mosquito-borne viruses in the United Arab Emirates. Parasites and Vectors 12:153 https://doi.org/10.1186/s13071-019-3417-8

Chhabra MB and Gupta SK (2006). Parasitic diseases of camels – an update: 2. Helminthoses. Journal of Camel Practice and Research 13:81-87.

Cheema AH and Ivoghli B (1978). Bovine onchocerciasis caused by *Onchocerca armillata* and *O. gutturosa*. Veterinary Parasitology 15:495-505.

Cygankov AA (1950). Revision of coccidian species of camels. Izvestia Akademii Nauk Kazakhskoj SSR [In Russian]. Seria parazitologiceskaja 75:174-185.

Deplazes P (2006). Helminthosen von Hund und Katze. In: Veterinärmedizinische Parasitologie., Ed., Schnieder, T. 6th Edition, Parey in MVS Medizinverlage, Stuttgart. pp 444-518.

Farnell WH and Faulkner AJ (1978). Prepatent period of *Dipetalonema reconditum* in experientally-infected dogs. Journal of Parasitology 64:565-567.

Gomez-Puerta LA and Mayor P (2017). Congenital filariasis caused by *Setaria bidentata* (Nematoda: Filaroidea) in the Red Brocket Deer (*Mazama americana*). Journal of Parasitology 103:123-126.

Katajceva TV (1969). On the biology of *Dipetalonema evansi* Lewis, 1882 – A parasite of camels. [In Russian] Parazitologiya 3:76-80.

Kim NS, Kim HC, Sim C, Ji JR, Kim NS and Park BK (2010). Congenital infection with *Setaria digitata* and *Setaria marshalli* in the thoracic cavity of a Korean calf: a case report. Veterinarni Medicina 55:275-280.

Lewis TR (1882). Remarks on a Nematoid Haematozoon Discovered by Dr. Griffith Evans in a Camel. Proceedings of the Asiatic Society of Bengal. pp 63-64.

Moghaddar N and Zahedi A (2006). Prevalence and pathogenesis of *Onchocerca fasciata* infection in camels (*Camelus dromedarius*) in Iran. Journal of Camel Practice and Research 13:31-35.

Nagaty HF (1947). *Dipetalonema evansi* (Lewis, 1982) and its microfilaria from *Camelus dromedarius*. Parasitology 38:86-92.

Pathak KLM, Singh Y and Harsh DL (1998). Prevalence of *Dipetalonema evansi* in camels of Rajasthan. Journal of Camel Practice and Research 5:166.

Romanovic MI (1916). *Deraiophora cameli* (n.g., n.sp.). Comptes Rendus des Seances de la Society de Biologie et des Filiales 68:745-746.

Sazmand A, Anvari Tafti MH, Hekmatimoghaddam S and Moobedi I (2013). *Dipetalonema evansi* infection in camels of Iran's Central Area. Pakistan Journal of Biological Sciences 16: 647-650.

Taylor MA, Coop RL and Wall RL (2015). Veterinary Parasitology 4th Ed. Blackwell Publishing. pp 1032.

Yorke W and Mapelstone PA (1926). The Nematode parasite of Vertebrates. J. and A. Churchill, London. pp 536.

SELECTED RESEARCH ON CAMELID IMMUNOLOGY

(Hard Bound, 392 pages, few figs coloured, Edition 2016)

In 1989 a group of biologists led by Raymond Hamers at the Free University Brussels investigated the immune system of dromedaries. This discovery was published in Nature in 1993. Based on their structure, these peculiar camelid antibodies have been named Heavy Chain Antibodies (HCAb), as they are composed of heavy chains only and are devoid of light chains. Sera of camelids contain both conventional heterotetrameric antibodies and unique functional heavy (H)-chain antibodies (HCAbs). The smaller size and monomeric single domain nature make these antibodies easier to transform into bacterial cells for bulk production, making them ideal for research purposes. Camelid scientists world over were greatly fascinated by a new field of research called "Camelid Immunology". Significant research has been done on camelid immunology in recent decade. In order to benefit future camelid immunology researchers, this book was planned in the series of "Selected Topics" by Camel Publishing House with a title- "Selected Research on Camelid Immunology" edited by T.K. Gahlot, U. Wernery and Serge Muyldermans. This book is a unique compilation of research papers based on "Camelid Immunology" and published in Journal of Camel Practice and Research between 1994-2015. Research on this subject was done in 93 laboratories or institutions of 30 countries involving about 248 scientists. In terms of number of published papers in JCPR on the immunology the following countries remain in order of merit (in parenthesis), i.e. Iran (1), India and UAE (2), China and Saudi Arabia (3), Sudan (4), Kenya and Belgium (5), USA (6), Germany (7) and so on. The book contains 11 sections and is spread in 384 pages. The diverse sections are named as overview of camel immune system; determinates of innate immunity, cells, organs and tissues of immune system; antibodies; immunomodulation; histocompatibility; seroprevalence, diagnosis and immunity against bacteria, viruses, parasites and combination of other infections; application of camel immunoglobulins and applications of immune mechanisms in physiological processes. The camelid immunology has to go a long way in its future research, therefore, this reference book may prove quite useful for those interested in this subject. Book can be seen on www.camelsandcamelids.com.
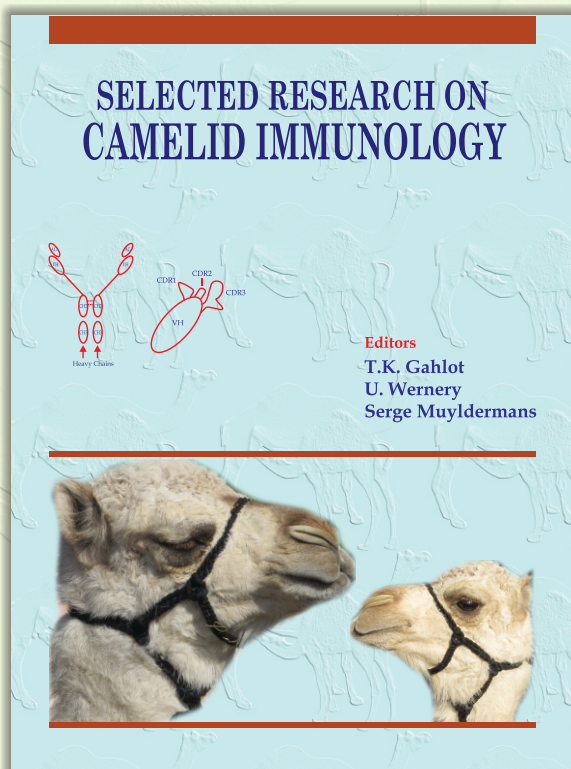
Editor:
T.K. Gahlot
U. Wernery
Serge Muyldermans

Edition: 2016

© Camel Publishing House

Publisher:
Camel Publishing House
67, Gandhi Nagar West, Near Lalgarh Palace,
Bikaner-334001 Rajasthan, India
email: tkcamelvet@yahoo.com

Website:
www.camelsandcamelids.com
www.tkgahlotcamelvet.com

Price: US $ 475
        INR 12500

ISBN 81-903140-4-1

A MORPHOMETRIC STUDY ON THE PANCREAS OF THE CAMEL FOETUS (*Camelus dromedarius*)

T.E.A. Mohammed[1], H.I. Ismail[2] and H.A. Ali[3]

[1]Department of Anatomy, Faculty of Veterinary Sciences, University of Gadarif, Sudan
[2]Department of Anatomy, College of Veterinary Medicine, University of Bahri, Sudan
[3]Department of Biomedical Sciences, Faculty of Veterinary Medicine,
Sudan University of Science and Technology, Khartoum, Sudan

ABSTRACT

Standard Stereological methods of the point-counting techniques were applied to study certain components of the camel foetus pancreas at different embryological stages (First, second and third trimester). The volume densities (Vv) of the acini, ducts, islets of Langerhans, connective tissue and blood vessels were determined and hence the percentage volume for each component. Both ducts and islets of Langerhans were not observed in the first trimester hence they were excluded. In the first trimester the acini occupied less than half the volume of the pancreas followed by connective tissue (44.62% and about 0.71 cm^3 absolute volume). In the second trimester the acini occupied half of the volume of the pancreas (54.98% and about 1.48 cm^3 absolute volume) at the expense of the connective tissue. The ducts and islets of Langerhans which were first appeared in the second trimester showed results of 3.30%, 0.1 cm^3 and 1.82% , 0.05 cm^3, respectively. In the third trimester the acini and islets of Langerhans underwent further increase in size and occupied 60.95%, 2.55 cm^3 and 2.48, %, 0.10 cm^3, respectively.

Key words: Camel, development, embryology, morphometry, pancreas

The pancreas in the adult camel was extensively studied by many authors (Adeghate, 1997; Al-Ajlan and Bailey, 2000; Masaad, 2007; Baragob *et al,* 2011; Elamin *et al,* 2014; Hafez *et al,* 2015). Recently, the endocrine portion had been studied by few investigators (Hafez *et al,* 2015; Zghair, 2016).

Investigators have studied the development and slightly the morphometry of the pancreas in man, mammals and birds (Dean, 1973; Bock *et al,* 1997; Zharkov *et al,* 1996; Taga *et al,* 1998; Jay *et al,* 1997; Ober *et al,* 2003; Yee *et al,* 2005; Jorgensen *et al,* 2007; Tehrani and Lin, 2011; Cleaver and Dor, 2012; Jennings *et al,* 2015).

However, from the available literature, morphometric studies on the development of the pancreas in camel foetus were virtually lacking. Hence the current research was undertaken to give insight on the morphometry of the pancreas of the camel fetuses at different stages of pregnancy.

Materials and Methods

A total of 15 camel foetuses were used for the morphometric study, 5 for each trimester. The approximate age of the foetuses was estimated by using the following formula adopted by El-Wishy *et al,* (1981).

$$GA = \frac{(CVRL+23.99)}{0.366}$$

where GA is age in days and CVRL is the Crown Vertebral Rump Length. Crown Vertebral Rump Length (CVRL) was measured (cm) as a curved line along the vertebral column from the point of the anterior fontanel or the frontal bone following the vertebral curvature to the base of the tail. Foetuses less than 130 days were designated as first trimester, 130-260 days as second trimester and 261-390 days as third trimester (Bustinza, 1979).

Tissue samples

The entire pancreas was removed by blunt dissection. The volume of the pancreas was measured by the water displacement method (Scherle, 1970). Tissue Sample were taken randomly from the different parts of the pancreas (4 regions for the first trimester, 7 regions for the second trimester and 12 regions for the third trimester representing the different lobes of the gland). They were fixed in 10% formalin and processed for routine histology. Paraffin sections were prepared and stained with haematoxylin and eosin.

The microscopic fields were selected blindly by moving the stage of the microscope. Chosen fields

were photographed at two magnifications (X10 and X40). The obtained images were saved as PowerPoint slides in the computer. Later, quantitative analysis was performed by the stereological methods of the point-counting techniques (Weibel, 1963).

Sampling

As it is impossible to examine the histological sections of the entire organ, sampling is being necessary and should represent the whole pancreas. Hence, the accuracy of the results obtained by the point-counting technique depends on the sample size. The larger the sample size the better values for each selected parameter to be obtained. A high degree of accuracy can be attained by the procedure of systematic random sampling (Weibel, 1969). The sampling process adopted is shown in Table 1. The sampling procedure gave a final size of 230 microscopic fields that were saved as PowerPoint images and analyzed by stereological methods to determine the volume densities (Vv) of the components of the parenchyma of the pancreas. These parameters were used to calculate the absolute volumes.

Determination of the volume densities

Point-counting methods

The determination of the volume density Vv (hence the percentage volume) of the tissue component and derivation of the formula to be applied was used according to the method reported by Weibel *et al* (1966) and Dunnill (1968). According to the point-counting principle the percentage number of points falling on a given parameter is equivalent to the percentage volume occupied by the component.

To determine the Vv (percentage volume), the microscopic fields were photographed at X40 as the components of the pancreas were easily identified at this magnification. A grid of 1 cm square lattice was installed and superimposed randomly on the PowerPoint image of each of the 230 fields of the parenchyma of the pancreas (Fig 1). The intersections of the lines at the corners of the squares constituted the points for counting, the total number of points on the grid being 100 points.

The number of points for each component was counted directly on the computer screen and the volume density (Vv), hence the percentage volume was calculated for each of the following parameters of the parenchyma of the pancreas; acini, islets of Langerhans, ducts, connective tissue and blood vessels.

Table 1. Showing the procedure used for sampling.

No.	Stage	Specimens number
1	5 pancreas (animals)	5
2	4,7 and 12 tissue blocks (slide) per pancreas for the 1st, 2nd and the 3rd trimester, respectively	5x4 5x7 5x12
3	Each sections 2 fields (images) per slide (block). 5x4x2= 40 fields (images) 1st trimester. 5x7x2= 70 fields (images) 2nd trimester. 5x12x2= 120 fields (images) 3rd trimester.	40+70+120=230
4	100 lattice (grid) points per field	100x230=23000

Calculation of the volume densities

The volume density (Vv) was calculated for each of these components using the formula given by Weibel *et al* (1966) as follows: Vv = P/PT

where P is the number of points falling on the component and PT is the total number of grid points. The number of points to be counted for each component depends on the volumetric proportion itself (i.e. Vv). Vv is volume density (volume fraction).

Calculation of the absolute volumes

The absolute volumes of the pancreas components were calculated from the volume densities (Vv) of the components and the total volume (V) of the fresh pancreas (i.e Absolute volume = Vv.V) according to Weibel *et al* (1966).

Statistical analysis

In this investigation the means and standard deviation (SD) was calculated for the Vv of each component of the pancreas as recommended by Weibel *et al* (1963).
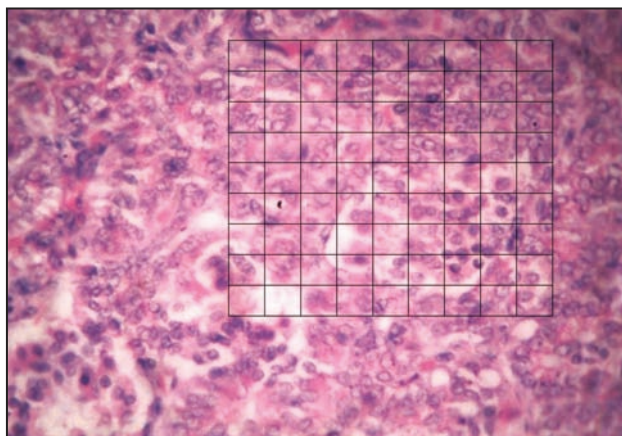

Fig 1. Showing the grid superimposed on the images of parenchyma of pancreas.

Results

The first trimester

At this trimester only the acini, connective tissue and blood vessels could be observed in the pancreas of the camel foetus. Hence, only these parameters were considered in this study. The results obtained from analysis of histological sections by point-counting technique for this stage were shown in Tables 2 and 3.

The mean volume of the pancreas was calculated to be 1.66 cm^3. The total number of points falling on the acini and connective were more or less similar, the acini were slightly higher (357 for the acini and 310 for the connective tissue). Accordingly, in this stage the acini accounted for about 44.62% of the total volume of the pancreas, whereas the connective tissue occupied about 38.82%; the absolute volumes being 0.71 cm^3 and 0.61 cm^3, respectively (Tables 2 and 3). The number of points falling on the blood vessels were less compared with the other two parameters, being 132. Hence, giving only 16.55% of the total volume of the pancreas and an absolute volume of 0.26 cm^3 (Tables 2 and 3).

The Second trimester

In this trimester the following parameters were calculated for morphometry (Acini, islets of Langerhans, ducts, connective tissue and Blood vessels). The mean volume of the pancreas was 2.7 cm^3. The number of points falling on the acini increased at the expense of the connective tissue, being 931 and 306, respectively (Table 4). Hence, the acini occupied about 54.98% and the connective tissue about 27.70% of the volume of the pancreas which represented 1.48 cm^3 and 0.70 cm^3 of the total volume of the pancreas, respectively (Table 6 and 8). The ducts and islets of Langerhans were first observed in this trimester. The points falling on them were only 35 and 30, respectively. These gave volume densities of about 3.30% for the ducts and 1.82% for the islets of Langerhans. Accordingly the absolute volumes were calculated as 0.09 cm^3 and 0.05 cm^3, respectively (Table 6). The number of points falling on the blood vessels showed an increment compared to the first trimester and calculated to be 142. Hence, giving a volume density of about 12.20% and an absolute volume of about 0.32 cm^3 (Table 6 and 8).

The third trimester

The mean volume of the pancreas was 4.18 cm^3. Similar parameters to those of the second trimester were calculated in this stage. The numbers of points falling on the acini and the connective tissue were found to the highest. They were found to be 1300

Table 2. Showing points falling on each parameters, the volume densities and the absolute volumes of the different components of the pancreas at the first trimester for 5 sections shown as Means ± Standard Deviation.

Section No.	No. of fields counted	Acini	Connective Tissue	Blood Vessels	Total No. of Points
1	8	369	361	70	800
2	8	262	483	55	800
3	8	425	111	264	800
4	8	352	318	130	800
5	8	377	280	143	800
Total	40	1785	1553	662	4000
Mean	357		310.6	132.4	
Volume density	44.62%		38.82%	16.55%	100%
Absolute Volume	0.71 cm^3		0.62 cm^3	0.26 cm^3	

Table 3. Showing the volume of fresh pancreas, volume densities and absolute volumes of the main components in 5 camels foetuses at the first trimester expressed as Means ± Standard Deviations (SD).

Animal No.	Volume of fresh pancreas	Acini		Connective tissue		Blood vessels	
		Vv %	Abs V cm^3	Vv %	Abs V cm^3	Vv %	Abs V cm^3
1	2 cm^3	46	0.92	45	0.9	8.75	0.17
2	1.5 cm^3	32.75	0.49	60.77	0.91	6.87	0.1
3	1.9 cm^3	53.12	1	13.87	0.26	33	0.62
4	1.7 cm^3	44	0.74	39.75	0.67	16.25	0.27
5	1.2 cm^3	47.12	0.56	35	0.42	17.87	0.21
Mean	1.66±0.32	44.59±7.44	0.74±0.22	38.87±17.01	0.63±0.29	16.54±10.33	0.27± 0.20

Table 4. Showing the data obtained by point-counting of fields on seven sections of the pancreas at the second trimester.

Section No.	No. of fields counted	Acini	Islets of Langerhans	Ducts	Connective tissue	Blood vessels	Total
			Number of points falling on				
1	1	80	0	0	19	1	100
	2	69	0	0	31	0	100
2	1	48	1	5	34	12	100
	2	86	3	7	3	1	100
3	1	70	1	0	20	9	100
	2	59	1	1	35	4	100
4	1	54	0	5	34	7	100
	2	62	0	3	20	15	100
5	1	80	4	0	16	0	100
	2	71	4	1	9	15	100
6	1	72	2	4	13	9	100
	2	56	5	1	30	8	100
7	1	34	6	8	36	16	100
	2	90	3	0	6	1	100
Total	14	931	30	35	306	142	1400

Table 5. Showing the data obtained by point-counting of fields on twelve sections of the pancreas at the third trimester.

Section No.	No. of fields counted	Acini	Islets of Langerhans	Ducts	Connective tissue	Blood vessels	Total
			Number of points falling on				
1	1	70	5	0	20	5	100
	2	40	1	2	44	13	100
2	1	59	0	1	31	9	100
	2	32	0	0	50	18	100
3	1	57	4	3	26	10	100
	2	33	2	2	60	3	100
4	1	60	6	4	21	9	100
	2	40	5	2	35	18	100
5	1	51	2	1	10	36	100
	2	80	0	6	12	2	100
6	1	36	4	2	52	6	100
	2	80	1	0	19	0	100
7	1	42	2	3	51	2	100
	2	50	3	5	39	3	100
8	1	80	4	0	10	6	100
	2	36	0	2	60	2	100
9	1	50	4	1	30	15	100
	2	48	2	2	36	12	100
10	1	74	1	0	22	3	100
	2	39	0	3	50	8	100
11	1	54	1	0	33	12	100
	2	66	3	0	30	1	100
12	1	90	2	1	2	5	100
	2	33	2	0	42	23	100
Total	24	1300	54	40	785	221	2400

Table 6. Showing points falling on each parameters, the volume densities and the absolute volumes of the different components of the pancreas at the second trimester 5 sections shown as Means ± Standard Deviation.

Section No.	No. of fields counted	Acini	Islets of Langerhans	Ducts	Connective tissue	Blood vessels	Total of points
1	14	659	50	80	305	306	1400
2	14	714	13	20	552	101	1400
3	14	931	30	35	306	98	1400
4	14	705	19	55	369	252	1400
5	14	840	16	40	407	97	1400
Total	70	3849	128	230	1939	854	7000
Mean	769.8	25.6	46	387.8	170.8		100%
Volume densities	54.98%	1.82%	3.3%	27.7%	12.2%		
Absolute volumes	1.48 cm^3	0.049 cm^3	0.089 cm^3	0.74 cm^3	0.32 cm^3		

Table 7. Total data obtained by point-counting of fields of five histological sections at the third trimester.

Section No.	No. of fields counted	Acini	Islets of Langerhans	Ducts	Connective tissue	Blood vessels	No. of points
1	24	1300	54	40	785	221	2400
2	24	1654	67	55	502	122	2400
3	24	1504	49	80	579	188	2400
4	24	1486	62	60	602	190	2400
5	24	1370	70	58	742	160	2400
Total	120	7314	302	293	3210	881	12000
Mean	1462.8	60.4	58.6	642	176.2		100%
Volume densities	60.95%	2.51%	2.44%	26.75%	7.34%		
Absolute volumes	2.55 cm^3	0.1 cm^3	0.1 cm^3	1.12 cm^3	0.3 cm^3		

and 785, respectively. The volume density for the acini was about 60.95% and that for the connective tissue was about 26.75%. Hence the absolute volumes calculated for the two parameters were 2.55 cm^3 and 1.12 cm^3, respectively (Tables 5,7 and 9). The number of points falling on ducts and islets of Langerhans showed further increase being 54 and 40 respectively. The calculated volume densities and absolute volumes for the ducts were 2.44% (0.10 cm^3) and those for islets of Langerhans were 2.51% (0.10 cm^3).

Discussion

The morphometric data on the pancreas of the camel foetus were investigated with the view of estimating the volume of the pancreas and the volume densities of its main components namely acini, ducts, islets of Langerhans, connective tissue, and blood vessels. The results of this stereological study of the pancreas of the camel foetus presented in this research are the first report regarding morphometry in the camel foetus. Stereological data obtained in this investigation are prerequisite to understand the structure and function correlation. The plots of Weibel

et al (1963) and Dunnil (1968) were used to insure the sufficiency of the number of points counted for each component studies.

To the best of our knowledge data on morphometric development of the camel foetus pancreas is virtually lacking. Even in other animals the data found in the literature was only estimation of the biometric parameters namely weight, length and width (Singh *et al,* 2017) and the islets tissue (Edwin, 1986).

First trimester

As ducts and islets of Langerhans were not observed in this stage they were excluded from the study. The acini occupied approximately half the volume of the pancreas in this trimester (44.62% which was 0.71 cm^3 of the total volume) whereas the connective tissue occupied about 38.82% of the whole pancreas. The blood vessels percentage was to be 16.55% of the total volume of fresh pancreas. No comparative data was available on the camel or other animals. Taga *et al* (1998) studied the body mass of the pancreas in the mouse. Numerous studies on

Table 8. Showing the volume of fresh pancreas and volume densities of their main components in 5 camel foetuses at the second trimester expressed as mean and standard deviations, Mean absolute volumes of components indicated in cm³.

Animal number	Volume of pancreas	Acini		Islets of Langerhans		Ducts		Connective tissue		Blood vessels	
		Vv %	Abs V cm³	Vv %	Abs V cm³	Vv %	Abs V cm³	Vv %	Abs V cm³	Vv %	Abs V cm³
1	3.5 cm³	47.00	1.60	3.50	0.12	5.70	0.20	21.70	0.76	22.00	0.80
2	2.5 cm³	51.00	1.27	1.00	0.02	1.40	0.03	39.40	0.98	7.20	0.18
3	1.5 cm³	66.50	0.99	2.10	0.03	2.50	0.037	21.80	0.32	7.00	0.10
4	2.8 cm³	50.30	1.40	1.35	0.04	3.90	0.10	26.30	0.73	18.00	0.50
5	3.2 cm³	60.00	1.90	1.14	0.04	2.85	0.09	29.00	0.92	6.92	0.20
Mean	2.7± 0.77	54.90± 8.05	1.43± 0.34	1.82± 1.03	0.05± 0.04	3.27± 1.62	0.09± 0.06	27.64± 7.26	0.74± 0.25	12.22± 7.23	0.36± 0.29

Table 9. Showing the volume of fresh pancreas and volume densities of their main components in 5 camel foetuses at the third trimester expressed as mean and standard deviations, Mean absolute volumes of components indicated in cm³.

Animal number	Volume of fresh pancreas	Acini		Islets of Langerhans		Ducts		Connective tissue		Blood vessels	
		%	cm³	%	cm³	%	cm³	%	cm³	%	cm³
1	6.1 cm³	54	3.20	2.20	0.13	1.60	0.10	32.7	1.90	9.20	0.60
2	5 cm³	68.90	3.40	2.70	0.13	2.30	0.10	20.90	1.00	5.00	0.25
3	4 cm³	62.60	2.50	2.00	0.08	3.30	0.13	24.10	0.96	7.80	0.30
4	3.5 cm³	61.90	2.16	2.58	0.09	2.50	0.08	25.00	0.87	7.90	0.24
5	2.3 cm³	57.00	1.30	2.91	0.06	2.40	0.05	30.90	0.71	6.60	0.15
Mean	4.18± 1.44	60.88± 5.71	2.51± 0.84	2.48± 0.37	0.10± 0.03	2.42± 0.61	0.09± 3.54	26.72± 4.92	1.10± 0.47	7.30± 1.58	0.31± 0.17

the morphometry of the islets of Langerhans were reported (Dean, 1973; Zharkov, 1996; Yorde and Kalkhoff, 1986; Elayat *et al*, 1995).

Second trimester

In this stage the presence of ducts and islets of Langerhans was first observed. Hence, they were included in the parameters (components) studied in this trimester. The acini also occupied half of the volume of the pancreas (54.98% and about 1.48 cm³ absolute volume). An accompanied decrease in the size of the connective was observed (27.70% and absolute volume of 0.74 cm³). The ducts and islets of Langerhans showed results of 3.30% and 1.82%, respectively. The blood vessels exert slight decrease as a result of the development of the other parameters, being 12.20% and absolute volume of 0.32 cm³. Similarly, no comparative data was available concerning the camel foetus.

Third trimester

The current research showed that the acini underwent further increase in size and showed a percentage of 60.95% and absolute volume of 2.55 cm³. The connective tissue presented more or less similar data to the previous trimester showing a sort of consistency, occupying about 26.75% of the volume of the pancreas with absolute volume of 1.12 cm³. Further increase was shown by islets of Langerhans which occupied 2.5% of the volume of the pancreas giving absolute volume of about 0.1 cm³. No increase was noticed on the volume of the ducts. This may suggest that the ducts reached their maximum growth at the end of the second trimmer and at beginning of the third trimester. The volume density for the ducts was 2.44% and absolute volume of about 0.1 cm³. A marked decrease on the percentage of the volume occupied by the blood vessels was noticed. They occupied 7.34% of the volume of the pancreas and showed an absolute volume of 0.3 cm³. This could be attributed to the vast development of the other components of the foetus pancreas. Further morphometric study to investigate the postnatal development of the camel foetus pancreas is required.

References

Adeghate E (1997). Immunohistochemical identification of pancreatic hormones, neuropeptides and cytoskeletal

proteins in pancreas of the camel (*Camelus dromedarius*). Journal of Morphology 231(2):185-193.

Al-Ajlan A and Bailey GS (2000). Purification and some properties of camel carboxypeptidase B. Molecular and Cellular Biochemistry 201:105-110.

Baragob AEA, Mohammed OY, Hana AEA, Somia HA, Khojali SME and Alkari SM (2011). Extraction, purification, drying and analysis of camel insulin. Research Journal of Pharmacology 5:43-46.

Bock P, Abdel-Moneim M and Egerbacher M (1997). Development of pancreas. Microscopy Research and Technique 17:374-383.

Bustinza V (1979). The Cameli of South America. The Camelid. pp 112-143.

Cleaver O and Dor Y (2012). Vascular instruction of the pancreas development. Development 139:2833-2843.

Dean PM (1973). Ultrastructural morphometry of the pancreatic β cell. Diabetologia 9(2):115-119.

Dunnill P (1968). The use of helical net-diagrams to represent protein structures. Biophysical Journal 8(7):865-875.

Elamin BA, Al-Malki A, Ismael MA and Ayoub MA (2014). Purification and functional characterisation of pancreatic insulin from camel (*Camelus dromedarius*). Saudi Journal of Biological Sciences 21(6):574-581.

El-wishy AB, Hemeida NA, Omar MA, Mobarak AM and El Sayed MA (1981). Functional changes in the pregnant camel with special reference to foetal growth. British Veterinary Journal 137:527-537.

Hafez SA, Zaghloul DM and Caceci T (2015). Immuno-histochemical identification of the endocrine cells in the pancreatic islets of the camel, horse and cattle. European Journal of Anatomy 19(1):27-35.

Jay TR, Heald KA and Downing R (1997). Histologic study of β cells in the porcine pancreas aged 5, 12, and 24 weeks. Transplant Proceeding 29(4)2024-25.

Jennings RE, Berry AA, Strutt JP, Gerrard DT and Hanley NA (2015). Human pancreas development. Development 142: 3126-3137.

Jorgensen MC, Ahnfelt-Ronne J, Hald J, Madsen OD, Serup P and Hecksher-Sorensen J (2007). An illustrated review of early pancreas development in the mouse. Endocrine Reviews 28(6):685-705.

Masaad GAM (2007). A comparative morphological study on the pancreas of the dromedary and the donkey. M.V.Sc. Thesis, University of Khartoum, Sudan.

Ober EA, Field HA and Stainier YR (2003). From endoderm formation to liver and pancreas development in zebrafish. Mechanisms of Development 120:5-18.

Scherle WF (1970). A simple method for volumetry of organs in quantitative stereology. Mikroskopie 26:57-60.

Singh D, Prakash A, Farooqui MM, Singh SP and Pathak SK (2017). Gross anatomical studies on the pancreas in prenatal goat (*Capra hircus*). International Journal of Current Microbiology and Applied Sciences 6(2):823-830.

Taga R, Bispo LB, Bordin RA and Hassunuma RM (1998). Morphometric and allometric study of the mouse exocrine pancreas growth during the postnatal life. Okajimas Folia Anatomica Japonica 74(6):271-278.

Tehrani Z and Lin S (2011). Endocrine pancreas development in zebrafish. Cell Cycle 10(20):3466-3472.

Weibel ER, Kistler GS and Scherle WF (1966). Practical stereological methods for morphometric cytology. The Journal of Cell Biology 30:23-38.

Weibel ER, Cournand AF and Richards DW (1963). Morphometry of the Human Lung (Vol. 1). Berlin: Springer.

Yee NS, Lorent K and Pack M (2005). Exocrine pancreas development in zebrafish. Developmental Biology 284: 84-101.

Zghair FS (2016). Immunofluorescence Identification of the Endocrine Cells in the Pancreatic Islets of the Camel (*Camelus dromedarius*). Kufa Journal For Veterinary Medical Sciences 7(1):138-146.

Zharkov VP, Yarygin VN and Dolzhikov AA (1996). Morphometric analysis of the pancreas regenerating after resection. Bulletin of Experimental Biology and Medicine 122(3):953-955.

Bulletin of Camel Diseases in The Kingdom of Bahrain

This is a unique book which contains chapters on infectious and non-infectious diseases. The chapter on infectious diseases contains six sections. The section of bacterial diseases is subclassified as corynebacterium abscesses, paratuberculosis, hepatic necrobacillosis, mastitis, *Streptococcus zooepidemicus*, bacterial Infection in young camels, uterine Infection, infection of the vagina and vulva and other disorders. The section of protozoal diseases has narrations on trypanosomiasis, anaplasmosis and babesiosis. The section on parasitic infections is composed of gastrointestinal parasites in young camels, echinococcosis and mange. The section of mycotic diseases contains phycomycosis and ringworm. The section of viral diseases contains subsections on camel pox and contagious ecthyma. Edema Disease is described in miscellaneous section. The chapter on noninfectious diseases has three sections. Other section on poisoning describes pyrethroid, nitrate and toxic jaundice. The section describes zinc deficiency. The miscellaneous section describes foreign bodies, sand colic, bloat, caecal impaction, hydrocephalus, corneal opacity and osteochondroma.

About the Author

Dr. Abubakr Mohamed Ibrahim is a Veterinary Pathologist and worked for a long period as head of Royal Court Veterinary Laboratory. Kingdom of Bahrain which led to genesis of this publication out of his rich experience in diagnosing camel diseases in the Kingdom of Bahrain. This would be counted as his significant contribution and future researchers will find it easy to understand the pattern of camel diseases in this part of the world. Dr. Abubakr had majority of his publications based on camel diseases of Bahrain. Thus publication of this book would prove an important reference book for the camel practitioners and researchers.

ANALYSIS OF BETA CASEIN GENE POLYMORPHISM IN INDIAN CAMEL BREEDS

S.A. Jadhav[1], U.D. Umrikar[1], M.P. Sawane[1], V.D. Pawar[1] R.S. Deshmukh[1], S.S. Dahiya[2] and S.C. Mehta[2]

[1]Bombay Veterinary College, Parel, Mumbai- 400 012, Maharashtra
[2]ICAR-National Research Centre on Camel, Post Box-07, Bikaner-334001, Rajasthan, India

ABSTRACT

The present study was carried out on 118 camels belonging to the 4 major breeds *viz.* Bikaneri, Jaisalmeri, Kachchhi and Mewari to detect polymorphism in the promoter region of β-casein gene by PCR-RFLP. The PCR amplification of 659 bp fragment spanning the promoter (-428bp) and the 5' flanking region (+231) of β-Casein gene was carried out and restriction digestion with *Hph*I was done to study the transition g.2126A>G in the promoter region of dromedary camel. This transition removes the restriction site for the *Hph*I. The restriction patterns were characterised by the 2 fragments of 608 bp and 51 bp (GG), 4 fragments of 608 bp, 352bp, 256 bp and 51 bp for the heterozygous (AG) and 3 bands of 352bp, 256 bp and 51 bp (AA). The genotype frequency in the Indian dromedary was observed as 0.195, 0.525 and 0.280, respectively for the GG, AG and AA genotypes. The allele frequency was 0.458 and 0.542 for the G and A alleles, respectively. All the 4 Indian dromedary breeds were polymorphic for this variation. This transition of amino acid in the promoter region has impact on the affinity of the TATA box binding site in the gene transcription process. However, further investigations are required to verify the influence of this allelic variant in the gene regulation process.

Key words: Beta-Casein, camel, dromedary, milk, polymorphism

The protein content in Indian dromedary breeds has been estimated to be 2.3%, however, it ranges from 2.3 to 4.9% in different camel rearing countries (Singh *et al*, 2017). The casein is the major protein (1.63 to 2.76%) in camel milk and constitutes about 52 to 89%. In camel milk, β-CN (65%) is the main fraction followed by α_{s1}-CN (22%), α_{s2}-CN (9.5%) and κ-CN (3.5%) (El Agamy, 2006). It is hypothesised that since β-CN is more sensitive to peptic hydrolysis than α_{s1} and α_{s2} –casein, the higher percentage of this casein fraction in camel milk as compared to bovine milk (45%) (Farrell *et al*, 2004) could reflect its higher rate of digestibility and lower the incidence of allergy in the infants nourished with camel milk (El Agamy *et al*, 2009). The β-Casein encoding gene is considered as a major gene for the presence of alleles associated to different levels of expression in other species like sheep, goat and cattle (Chessa *et al*, 2010; Caroli *et al*, 2006; 2009; Cosenza *et al*, 2005; Cosenza *et al*, 2007). However, the information about the DNA sequence of dromedary β-Casein is coming at a slow pace. The cDNA and promoter sequences (Kappeler *et al*, 1998; 2003; Bhure *et al*, 2008) along with full length sequence of CSN2 gene and promoter with annotation is now available (Pauciullo *et al*, 2014). Looking at the increased importance of camel milk due to its nutritional and therapeutic utility, this study was carried out to investigate the polymorphism in beta casein gene promoter of Indian dromedary breeds.

Materials and Methods

Experimental animals

The blood samples were collected from 118 camels belonging to Bikaneri, Jaisalmeri, Kachchhi and Mewari breeds (Table 1) of Indian dromedary herd maintained at the ICAR-National Research Centre on Camel, Bikaner, Rajasthan. Ten ml of venous blood from jugular vein was collected in EDTA. The samples were transported to the laboratory in ice box and stored at 4°C until use.

PCR conditions

DNA was isolsated using phenol-chloroform method (Sambrook *et al*, 1989) with minor modifications. The PCR primers; forward: GTTTCTCCATTACAGCATC and reverse TCAAATCTATACAGGCACTT were utilised (Pauciullo *et al*, 2014). PCR amplifications were carried

out in 25 μl reactions containing 50 ng DNA, 25 pmol each primer (Sigma-Aldrich), 1.0 U *Taq* DNA polymerase, 0.2 mM each dNTP, 2.5 μl 10X *Taq* DNA polymerase buffer containing 10 mM Tris – HCl (pH 9.0), 1.5 mM MgCl$_2$, 50 mM KCl and 0.01% gelatin. The PCR amplification programme, performed on Eppendorf Mastercycler Gradient, consisted of an initial denaturation temperature of 95°C for 5 min, then 34 cycles at 94°C for 30s, 58°C for 30s and 72°C for 1 min. Final extension was carried out at 72°C for 5 min. The β-Casein bands were visualised in 1% agarose gel containing ethidium bromide. The electrophoresis was carried out in 1XTBE at 80 Volts and the results were recorded using UVP gel-documentation system.

Restriction digestion

Around 250-500 ng of amplified PCR products were digested in 20 μl reaction using 5 units of *Hph*I restriction enzyme (BioLabs) with CutSmart Buffer and incubating at 37°C for 15 minutes. The restriction bands were analysed on 2% Agarose gel electrophoresis with appropriate marker DNA.

Statistical Analysis

The Chi-square test (χ^2) was performed using IBM SPSS Statistics 20 software to test the statistical significance of the differences between observed and expected frequencies in genotypic classes.

Sequencing and Sequence Analysis

The PCR products were got sequenced on ABI3730 DNA Sequencer. The SNPs were visualised on chromatograms using Chromas 2.6.6 software. The sequences were analysed using multi-align editor of GeneTool Lite software. Sequence phylogeny was derived using Nucleotide BLAST programme of NCBI.

Results and Discussion

PCR amplification of β-Casein gene promoter

The PCR amplification of 659 bp fragment spanning the promoter (-428bp) and the 5′ flanking region (+231) of β-Casein gene was successfully achieved in Bikaneri, Jaisalmeri, Kachchhi and Mewari Camels (Fig 1). The present results agree with the findings of Pauciullo *et al* (2014), where PCR amplification of 659 bp fragment spanning the promoter (-428bp) and the 5′ flanking region (+231) of β-Casein gene in Sudanese camel (*Camelus dromedarius*) was achieved using the same primer pair.

PCR-RFLP of β-Casein gene fragment

To study the transition g.2126A>G in the promoter region of dromedary camel, restriction digestion of PCR product (659 bp) of β-Casein gene promoter was carried out using *Hph*I restriction enzyme and the restriction bands were resolved in 2% Agarose gel. The restriction digestion lead to 2 digested daughter bands of fragments of 608 bp and 51 (GG genotype); 4 fragments of 608 bp, 352bp, 256 bp and 51 bp for the heterozygous (AG genotype) and 3 bands of 352bp, 256 bp and 51 bp (AA genotype). This transition g.2126A>G removes the restriction site for the *Hph*I. The results are presented in Fig 2.

The breed-wise observation of data indicated that the GA genotype was present in all 4 Indian camel breeds showing that the nucleotide substitution at g.2126A>G SNP was widespread. The frequency of GA genotype in Bikaneri, Jaisalmeri, Kachchhi and Mewari was observed to be 0.607, 0.515, 0.414, and

Table 1. Genotype frequency in Indian dromedary at β-Casein gene promoter.

Genotype	Bikaneri			Jaisalmeri			Kachchhi			Mewari		
	M	**F**	**P**	**M**	**F**	**P**	**M**	**F**	**P**	**M**	**F**	**P**
N	13	15	28	6	27	33	14	15	29	13	15	28
GG	0.15	0.2	0.18	0.17	0.11	0.12	0.21	0.13	0.17	0.30	0.33	0.32
GA	0.70	0.53	0.61	0.50	0.52	0.52	0.29	0.54	0.41	0.62	0.54	0.57
AA	0.15	0.27	0.21	0.33	0.37	0.36	0.50	0.33	0.42	0.08	0.13	0.11

M-Male; F-Female; P-Pooled Sex; N-Number of Animals

Table 2. Genotype and allele frequency in Indian dromedary at β-Casein gene promoter.

Genotype	Male	Female	Pooled	Allele	Frequency
GG	0.22	0.18	0.19	G	0.458
GA	0.52	0.53	0.53	A	0.542
AA	0.26	0.29	0.28		

0.572, respectively. The frequency of the GG, GA and AA genotypes pooled over breeds was 0.195, 0.525 and 0.28, respectively, indicating that the 2 alleles at the locus in Indian dromedary are segregating in typical Mendelian ratio of 1:2:1. The same was substantiated by the chi-square test (χ^2= 1.921; P >0.05 at 2 degrees of freedom). Almost comparable polymorphism was observed in both the sexes. The three genotypes (GG, GA, AA) were almost equally distributed among the 4 Indian breeds (χ^2=10.6013; P = 0.10151). The frequency of allele G was observed to be 0.458 and that of A was observed to be 0.542. The lower frequency of G allele is an indication that this genetic variant, responsible for the lower affinity of the TATA box binding site, might be less facilitated in gene transcription process. Further, here it may be pertinent to mention that the Bikaneri, Jaisalmeri, Kachchhi and Mewari camels were mainly used for their draught potential (Rathore, 1986). The breeds differed significantly in terms of milk production (Sahani *et al*,1998), draught potential and speed and stride (Rai *et al*, 1992), etc. Further, these breeds have been recently selected for their milk production potential (Mehta *et al*, 2011; 2014). Thus, the existence
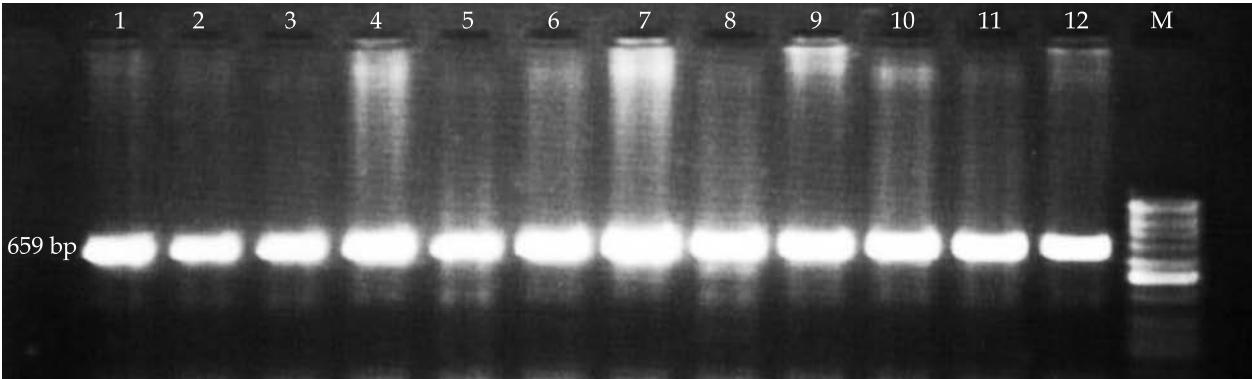
Fig 1. Amplification of 659 bp fragment of β-Casein gene promoter in Indian camel (Lane 1 – 12) ; M-100 bp marker.
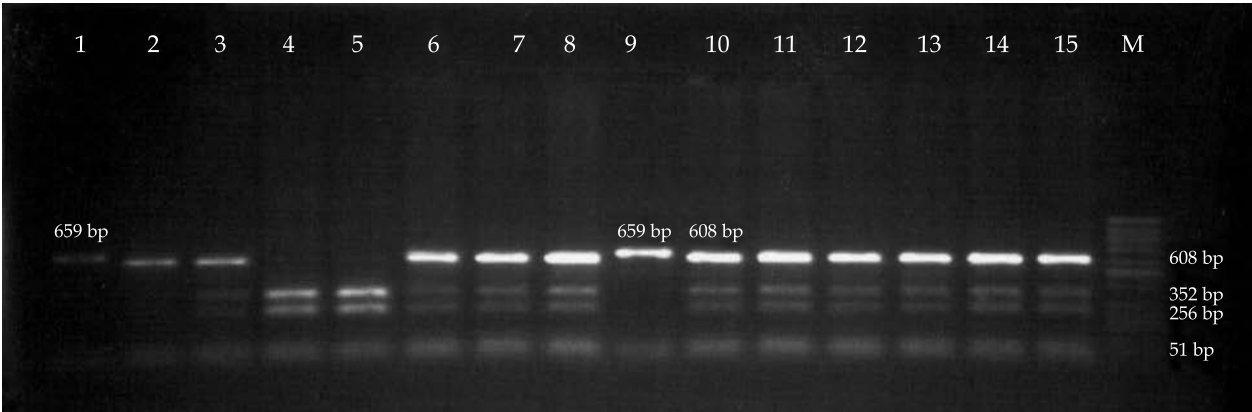

Fig 2. PCR-RFLP genotyping of camel β-Casein gene promoter with *Hph*I. Lane 1,9 : Undigested Product of 659 bp; Lane 2 : GG genotype (608 bp and 51 bp) ; Lane 3,6-8,10-15 : GA genotype (608 bp, 51 bp and 352 bp, 256 bp, 51 bp); Lane 4-5 : AA genotype (352 bp, 256 bp and 51 bp) ; M-100 bp marker.

Fig 3. SNP g.2126A>G in the promoter region of CSN2 gene in the Indian camel population.
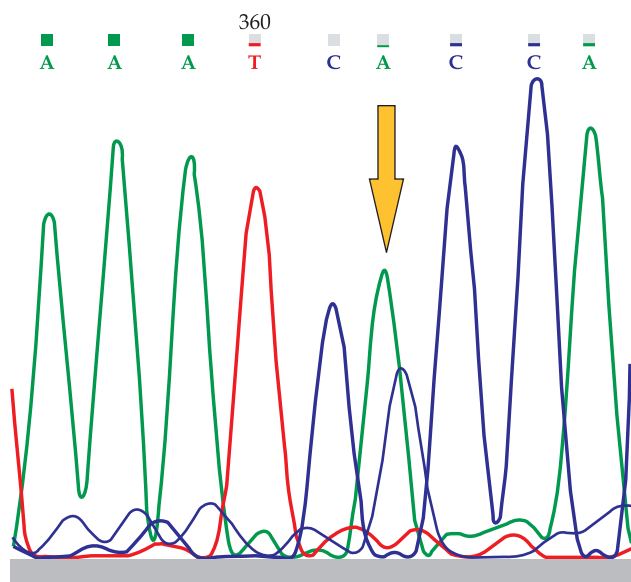
Fig 4. A four-colour chromatogram showing GA genotype in the promoter region of CSN2 gene in Indian dromedary.

of this single nucleotide polymorphism at g.2126A>G SNP in all 4 Indian dromedary breeds in uniform pattern indicate that it is independent of the selection of the Indian camel breeds for various purposes, especially the milk production.

However, Pauciullo *et al* (2014) reported little higher frequency of allele A (0.65) in Sudanese camel breeds with the variation among the ecotypes ranging between 0.59 and 0.72. Since, the β-casein is the most abundant protein in camel milk and its encoding gene (CSN2) in other species is considered as a 'major' gene for the presence of alleles associated to different level of expression, the present results indicated the existence of genetic variation in the Indian dromedary breeds at this locus and further investigation with regard to its association with the expression of β-casein gene in terms of diversity and concentration in the camel milk might possibly pave the way for its utilisation for the production of diversified milk.

Nucleotide-substitution: SNP verification by sequencing

The samples identified as representing GG, GA and AA genotype with respect to the single A >G nucleotide substitution in promoter region of CSN2 gene were sequenced. The analysis of sequences confirms the specificity of the sequences for the identified SNP genotypes (Figs 3 and 4). The phylogenetic analysis of the sequence containing A>G substitution formed a separate node between Llama
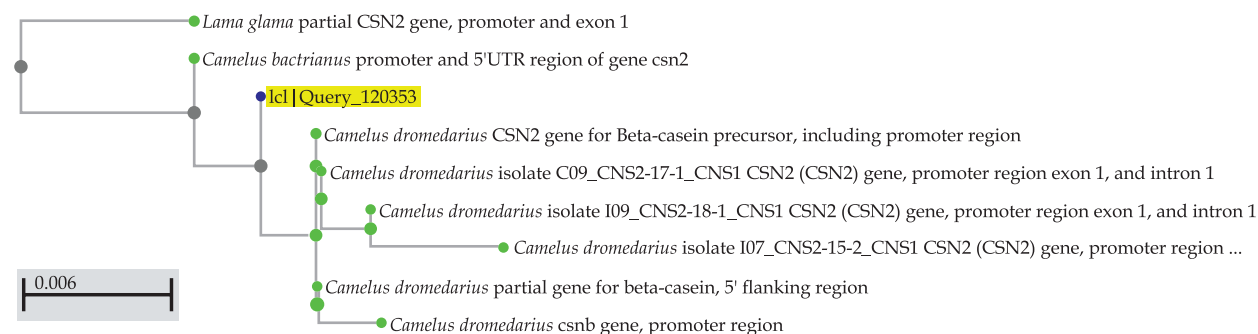
(a)
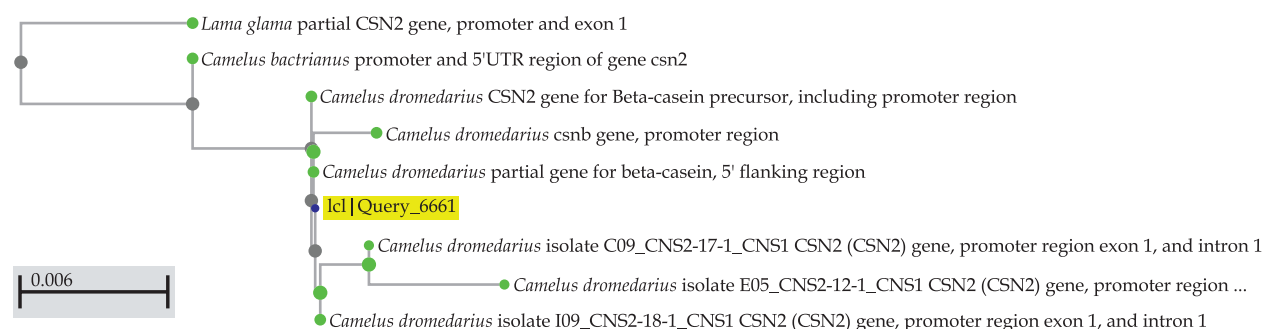
(b)

Fig 5. Phylogenetic analysis of sequence containing G allele (Fig 5a) and A allele (Fig 5b) at SNP g.2126A>G in the promoter region of CSN2 gene in the Indian camel.

(*Lama glama*) and double-humped camel (*Camelus bactrianus*) on one side and single-humped camel (*Camelus dromedarius*) sequences on the other side (Fig 5a); whereas, the sequence containing A allele were placed within the single-humped camel (*Camelus dromedarius*) sequences (Fig 5b).

The study documents the existence of genetic polymorphism in Indian dromedary breeds at the promoter region of CSN2 gene. This DNA based PCR-RFLP test can be used for typing camel CSN2 variability independent of age, sex and stage of lactation of animals for selecting them in breeding and production programmes. The information generated can be utilised to produce diversified camel milk to increase the economic value of camel milk and the income of the poor camel owners.

Acknowledgement

References

Bhure SK, Mehta SC and Singh R (2008). Comparative genomic organisation of camel beta casein gene promoter: a computer aided gene regulation study. Journal of Camel Research and Practice 15(1):25-33.

Caroli A, Chiatti F, Chessa S, Rignanese D, Bolla P and Pagnacco G (2006). Focusing on the goat casein complex. Journal of Dairy Science 89:3178-3187.

Caroli AM, Chessa S and Erhardt GJ (2009). Milk protein polymorphisms in cattle: effect on animal breeding and human nutrition. Journal of Dairy Science 92:5335-5352.

Chessa S, Rignanese D, Berbenni M, Ceriotti G, Martini M, Pagnacco G and Caroli A (2010). New genetic polymorphisms within ovine β- and αs$_2$-caseins. Small Ruminant Research 88:84-88.

Cosenza G, Pauciullo A, Gallo D, Di Berardino D and Ramunno L (2005). A SspI PCR-RFLP detecting a silent allele at the goat CSN2 locus. Journal of Dairy Research 72:456-459.

Cosenza G, Pauciullo A, Colimoro L, Mancusi A, Rando A, Di Berardino D and Ramunno L (2007). An SNP in the goat CSN2 promoter region is associated with the absence of β-casein in milk. Animal Genetics 38:655-658.

El Agamy E I (2006). Camel milk. In: Handbook of Non-Bovine Mammals, Eds., Park Y W and Haenlein F W, Blackwell Publisher Professional, Iowa, NJ, USA. PP 297-344.

El-Agamy EI, Nawar M, Shamsia SM, Awad S and Haenlein GFW (2009). Are camel milk proteins convenient to the nutrition of cow milk allergic children. Small Ruminant Research 82:1-6.

Farrell Jr HM, Jimenez-Flores R, Bleck GT, Brown EM, Butler JE, Creamer LK, Hicks CL, Hollar CM, Ng-Kwai-Hang K Fand Swaisgood HE (2004). Nomenclature of the proteins of cows' milk—6th revision. Journal of Dairy Science 87:1641-1674.

GeneTool Lite 1.0. Release (2000). Bio Tools Incorporated, Advanced Bioinformatic Solutions.

IBM Corp. Released (2017). IBM SPSS Statistics for Windows, Version 20.0. Armonk, NY: IBM Corp.

Kappeler S, Farah Z and Puhan Z (2003). 5' Flanking regions of camel milk genes are highly similar to homologue regions of other species and can be divided into 2 distinct groups. Journal of Dairy Science 86:498-508.

Kappeler S, Farah Z and Puhan Z (1998). Sequence analysis of *Camelus dromedarius* milk caseins. Journal of Dairy Research 65:209-222.

Mehta SC, Bissa UK, Patil NV and Pathak KML (2011). Importance of camel milk and production potential of dromedary breeds. Indian Journal of Animal Science 81(11):1173-1177.

Mehta SC, Yadav SBS, Singh S and Bissa UK (2014). Sire evaluation and selection of Indian dromedary for milk production: issues and strategies. Journal of Camel Practice and Research 21(1):93-98.

Pauciullo A, Giambra IJ, Iannuzzi L and Erhardt G (2014). The β-casein in camels: molecular characterisation of the CSN2 gene, promoter analysis and genetic variability. Gene 547:159-168.

Rai AK, Roy AK and Khanna ND (1992). Speed and strides of different breeds of camel. Indian Journal of Animal Science 62:91-92.

Rathore GS (1986). Camels and Their Management. ICAR Publication, New Delhi, India

Sambrook J, Fritsh EF and Manities T (1989). Molecular cloning: A Laboratory Manual, 2nd Edn. Cold Spring Harbour Laboratory Press, New York.

Sahani MS, Rathinasabapathy M, Gorakhmal and Khanna N D (1998). Milking technique and other factors affecting milk production potential in different breeds of camels under farm conditions. Indian Journal of Animal Science 68:54-56.

Singh R, Mal G, Kumar D, Patil NV and Pathak KML (2017). Camel milk: an important natural adjuvant. Agricultural Research 6(4):327-340.

THE CAMEL
THE ANIMAL OF THE 21ST CENTURY

This book authored by Dr Alex Tinson is an acknowledgement to the support and inspiration that His Highness Sheikh Khalifa Bin Zayed Al Nahyan has provided to the centre and to research in general. The last 25 years has been an incredible adventure for us, the noble camel and the people of the U.A.E. Dr Tinson has been involved with many world first's since moving to Abu Dhabi 25 yrs ago. First there was the establishment of pioneering centres in exercise physiology and assisted reproduction. The establishment of the Hilli Embryo Transfer Centre led to five world firsts in reproduction. The world's first successful embryo transfer calf birth in 1990, followed by frozen embryo transfer births in 1994, twin split calves in 1999, pre-sexed embryo births in 2001 and world's first calf born from A.I. of frozen semen in 2013. The hard bound book is spread in 288 pages with 5 chapters. The first chapter involves early history of the centre, world's firsts, world press releases, history of domestication and distribution, evolution of camel racing in the U.A.E. and historical photos the early days. Second chapter comprises camel in health and disease and it involves cardiovascular, haemopoetic, digestive, musculoskeletal, reproductive, respiratory, urinary and nervous systems in addition to the description of special senses. This chapter describes infectious, parasitic and skin diseases in addition to the nutrition. The third chapter is based on Examination and Differential Diagnosis. The fourth chapter is based on special technologies bearing description of anaesthesia and pain management in camels, diagnostic ultrasound and X-Ray, assisted reproduction in camels, drug and DNA testing and surgery. The last chapter entailed future scope of current research.

THE CAMEL
THE ANIMAL OF THE 21ST CENTURY
Dr Alex Tinson

MANAGEMENT OF SCIENTIFIC CENTRES AND PRESIDENTIAL CAMELS
25TH ANNIVERSARY 1989-2014

ANTIBACTERIAL FUNCTIONS OF NEUTROPHIL AND MONOCYTE IN NEWBORN DROMEDARY CAMEL CALVES

Jamal Hussen

Department of Microbiology and Parasitology, College of Veterinary Medicine,
King Faisal University, Al Ahsa, Saudi Arabia

ABSTRACT

Newborn camel calves show recurrent infections with higher mortality rates in comparison to adult camels. It is unknown, whether these infections are related to reduced antimicrobial function of innate immune cells. The objective of the current study was to evaluate the impact of age on the phagocytosis function of neutrophils and monocytes in dromedary camel. Phagocytosis of *Staphylococcus aureus* by blood neutrophils and monocytes collected from newborn camel calves and adult camels was analysed by flow cytometry. In comparison to the cells collected from adult camels, newborn calf neutrophils and monocytes showed lower percentages of phagocytosis positive cells. The analysis of phagocytosis capacity (number of bacteria ingested by each cell) as measured by the mean fluorescence intensity (MIF) of phagocytosis positive cells revealed reduced phagocytosis capacity of newborn calf monocytes in comparison to adult monocytes. Together, these results show impaired antimicrobial functions of neutrophils and monocytes from newborn camel calves.

Key words: Flow cytometry, monocyte, neutrophil, newborn camel, phagocytosis

After birth, newborns leave the sterile uterine environment and become exposed to huge amount of microorganisms (Bandrick *et al,* 2014). At this stage, protective mechanisms are immature and their immune response is characterised by low concentrations of immunoglobulins (Kamber *et al,* 2000). Neutrophils and monocytes are key innate immune cells with central roles in antimicrobial defense mainly by phagocytosis and subsequent killing of bacteria during the early phase of infection (Hussen *et al,* 2016; Hussen and Schuberth, 2017; Adrover *et al,* 2019). Neutrophil and monocyte anti-microbial activity is mainly mediated by phagocytosing bacteria and killing the ingested microbes by means of oxygen-dependent and -independent mechanisms (Mantovani *et al,* 2011). In other veterinary species, neutrophils and monocytes phagocytosis activity has been shown to be influenced by age. For bovine calves, antimicrobial functions of neutrophils and monocytes is impaired during early phase after birth (Batista *et al,* 2015).

Age-related changes in phagocytosis capacity of camel neutrophils and monocytes are not investigated. The objective of the current study was therefore to analyse the ability of neutrophils and monocytes collected from peripheral blood of newborn dromedary camel calves and adult camels to phagocytose bacteria *in vitro*.

Materials and Methods

Blood samples were collected from fifteen newborn camel calves (aged < one month) and 35 adult camels aged between 6 and 12 years at Camel Research Centre, King Faisal University, Al-Ahsa, Saudi Arabia. Blood was obtained by venipuncture of the vena jugularis externa into vacutainer tubes containing EDTA (Becton Dickinson, Heidelberg, Germany).

Cell separation

Separation of whole camel leukocytes was done after hypotonic lysis of blood erythrocytes (Hussen *et al,* 2017). Briefly, blood was suspended in distilled water for 20 sec and double concentrated PBS was added to restore tonicity. This was repeated (usually twice) until complete erythrolysis. Separated cells were finally suspended in RPMI medium at 5×10^6 cells/ml. The mean viability of separated cells was evaluated by dye exclusion (propidium iodide; 2 µg/ml, Calbiochem, Germany) and it was above 92%.

SEND REPRINT REQUEST TO JAMAL HUSSEN email: jhussen@kfu.edu.sa

Phagocytosis Assay

Heat killed *Staphylococcus aureus* (*S. aureus*) bacteria (Pansorbin, Calbiochem, Merck, Nottingham, UK) were labeled with fluoresceinisothiocyanate (FITC, Sigma-Aldrich, St. Louis, Missouri, USA). Separated leukocytes were plated in 96 well plates (1×10^6/well) and incubated with FITC-conjugated *S. aureus* (50 bacteria/cell) for 30 minutes (37°C, 5% CO_2). Control samples were incubated without bacteria. After incubation, samples were analysed by flow cytometry after addition of propidium iodide (PI, 2 µg/ml final) to exclude dead cells. Phagocytic activity of monocytes and neutrophils was defined as the percentage of green fluorescing cells among viable cells. Mean green fluorescence intensity (MFI) of phagocytosis-positive cells was measured as indicator for the number of bacteria phagocytosed by each cell.

Statistical Analysis

Statistical analysis was performed with Prism (GraphPad). Results are presented as means ± S.E. of the mean (SEM). Differences between means were tested with t test and results were considered significant at a p-value of less than 0.05.

Results and Discussion

The present study analysed the impact of age on the capacity of camel blood neutrophils and monocytes to phagocytose bacteria *in vitro*.

Newborn camel calves show higher mortality rates in comparison to adult camels. The higher mortality is often a result of recurrent bacterial infections (Chaffee, 1968; Wernery *et al*, 1992; Kamber *et al*, 2000; Bornstein *et al*, 2008; Rhouma *et al*, 2018). Phagocytosis represents a key antimicrobial mechanism used by the innate immune cells neutrophils and monocytes to ingest and kill bacteria (Soehnlein and Lindbom, 2010). In order to see whether animal's age affects antimicrobial functions of these camel innate immune cells, the capacity of neutrophils and monocyte, collected from 15 newborn camel calves (aged < four weeks) and 35 adult camels, to phagocytose *S. aureus* was analysed by flow cytometry (Fig 1 A).
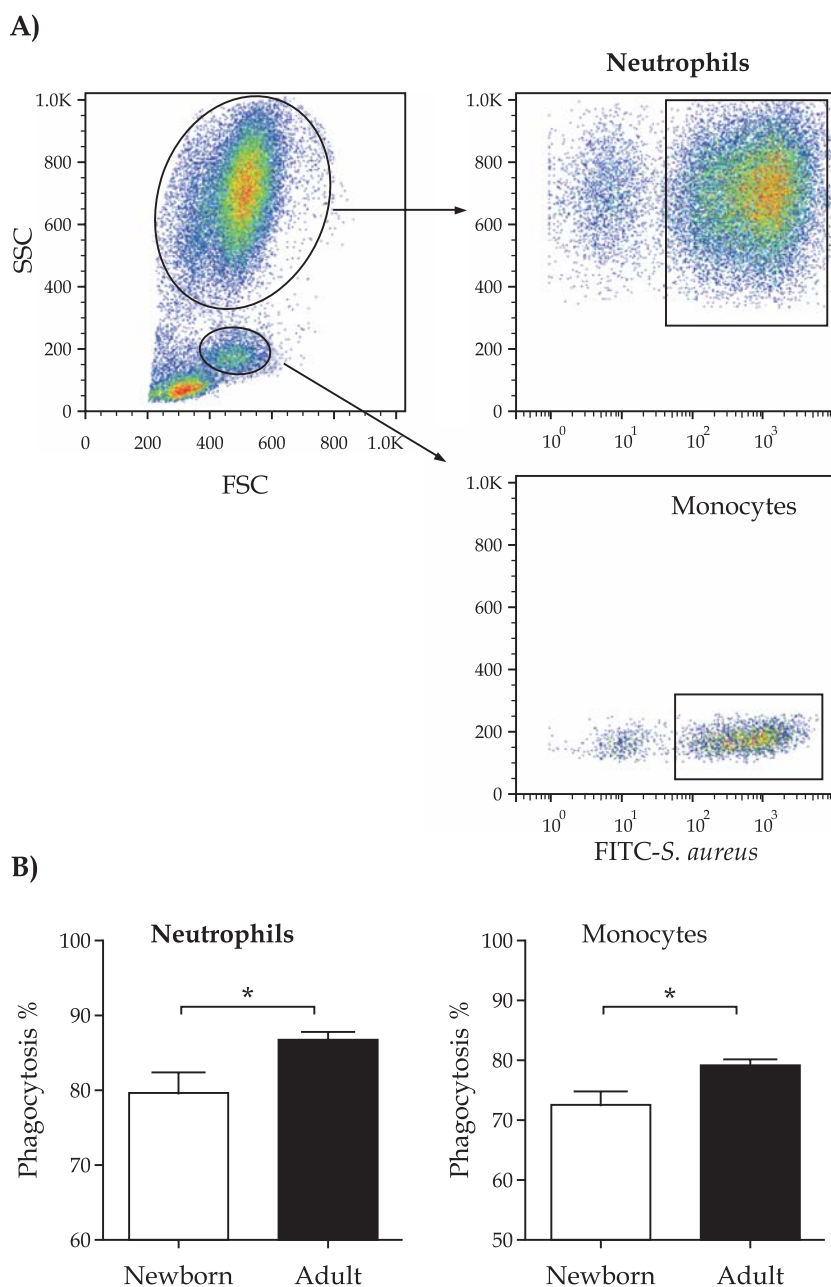

Fig 1. Flow cytometric analysis of phagocytosis of bacteria by camel neutrophils and monocytes. A) Separated camel leukocytes were incubated with FITC-labelled heat inactivated *S. aureus* and analysed by flow cytometry. After setting agates on granulocytes and monocytes according to their FSC and SSC properties, phagocytosis-positive cells were defined based on their higher green fluorescence (representative results are shown). B). The percentage of phagocytosis-positive neutrophils and monocytes were calculated and presented graphically (means ±SEM). (* = p<0.05).

A)
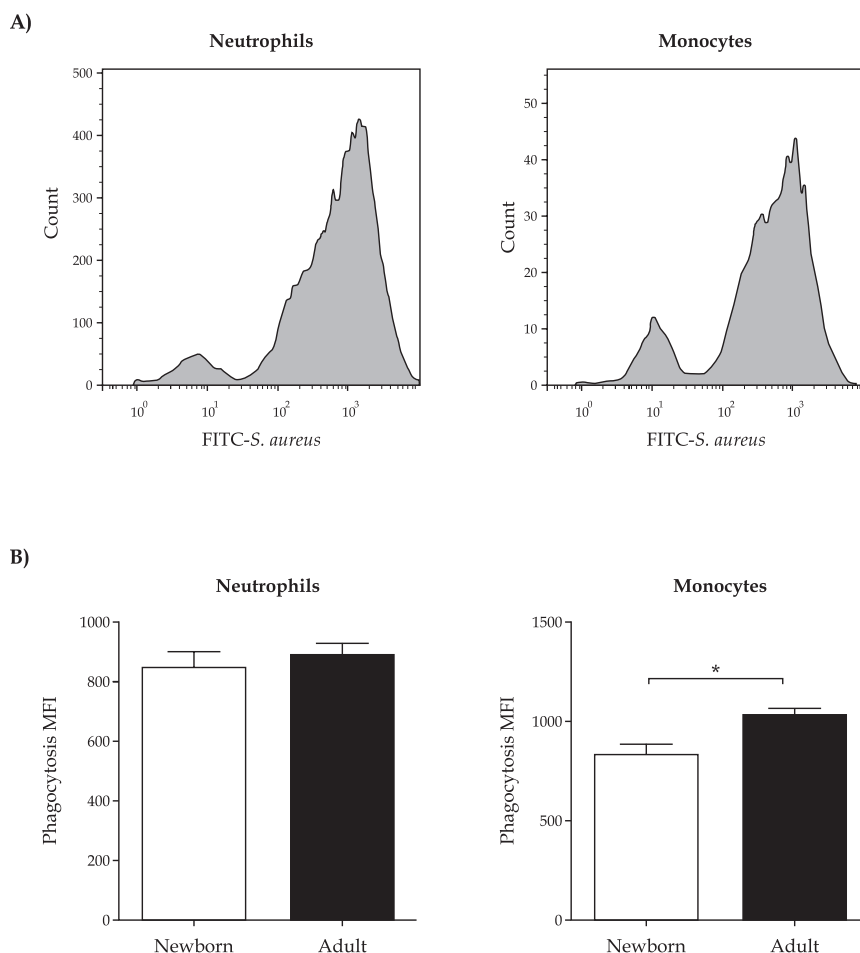

Neutrophils

Monocytes

B)

Neutrophils

Monocytes

Fig 2. Phagocytosis capacity (number of bacteria ingested by each cell).of camel neutrophils and monocytes. A) Separated camel leukocytes were incubated with FITC-labelled heat inactivated *S. aureus* and analysed by flow cytometry. After setting agates on granulocytes and monocytes according to their FSC and SSC properties, phagocytosis capacity were identified using histograms. B). The mean fluorescence intensities of green fluorescence-positive neutrophils and monocytes were calculated and presented graphically (means ±SEM). (* = p<0.05).

In comparison to cells collected from adult camels, newborn calf neutrophils and monocytes showed lower percentages of phagocytosis positive cells (Fig 1 B). The percentage of phagocytosis-positive cells was however, higher for neutrophils than monocytes (Fig 1 B).

The analysis of phagocytosis capacity (number of bacteria ingested by each cell) as measured by the mean fluorescence intensity (MIF) of phagocytosis positive cells revealed reduced phagocytosis capacity of newborn calf monocytes in comparison to adult monocytes. However, the number of bacteria ingested by each neutrophil did not differ between newborn and adult animals (Fig 2 A and B).

The reduced ability of blood neutrophils and monocytes to ingest bacteria may be due to reduced expression of phagocytosis receptors like complement receptor 3 (CR3), which is mainly expressed on granulocytes and monocytes and mediates the phagocytosis of complement-opsonised targets (Ley *et al*, 2007). Similar results were reported for bovine calves with reduced antimicrobial functions of their neutrophils and monocytes (Batista *et al*, 2015). The reduced phagocytosis ability of blood neutrophils and monocytes in newborn camels may therefore contribute to the higher susceptibility of these animals to bacterial infections during their early life postpartum.

In summary, the current study shows that phagocytosis of bacteria by neutrophils and monocytes, as a key antimicrobial function, is reduced in newborn camel calves. Further studies are needed for the analysis of mechanisms responsible for the reduced phagocytosis function of camel neutrophils and monocytes.

Acknowledgements

References

Adrover JM, Del Fresno C, Crainiciuc G, Cuartero MI, Casanova-Acebes M, Weiss LA, Huerga-Encabo H, Silvestre-Roig C, Rossaint J, Cossío I, Lechuga-Vieco AV, García-Prieto J, Gómez-Parrizas M, Quintana JA, Ballesteros I, Martin-Salamanca S, Aroca-Crevillen A, Chong SZ, Evrard M, Balabanian K, López J, Bidzhekov K, Bachelerie F, Abad-Santos F, Muñoz-Calleja C, Zarbock A, Soehnlein O, Weber C, Ng LG, Lopez-Rodriguez C, Sancho D, Moro MA, Ibáñez B and Hidalgo A (2019). A neutrophil timer coordinates immune defense and vascular protection. Immunity. 50(2):390-402.

Bandrick M, Ariza-Nieto C, Baidoo SK and Molitor TW (2014). Colostral antibody-mediated and cell-mediated

immunity contributes to innate and antigen-specific immunity in piglets. Developmental and Comparative Immunology 43(1):114-20.

Batista CF, Blagitz MG, Bertagnon HG, Gomes RC, Santos KR and Della Libera AM (2015). Evolution of phagocytic function in monocytes and neutrophils blood cells of healthy calves. Journal of Dairy Science 98(12):8882-8.

Bornstein S, Gluecks IV, Younan M, Thebo P and Mattsson JG (2008). *Isospora orlovi* infection in suckling dromedary camel calves (*Camelus dromedarius*) in Kenya. Veterinary Parasitology 152(3-4):194-201.

Chaffee PS (1968). Infection in a newborn camel. Journal of Small Animal Practice 93:134-6.

Hussen J, Koy M, Petzl W and Schuberth HJ (2016). Neutrophil degranulation differentially modulates phenotype and function of bovine monocyte subsets. Innate Immunity 22(2):124-137.

Hussen J and Schuberth HJ (2017). Heterogeneity of Bovine Peripheral Blood Monocytes. Frontiers in Immunology 8:1875.

Hussen J, Shawaf T, Al-Herz AI, Alturaifi HR and Alluwaimi AM (2017). Reactivity of commercially available monoclonal antibodies to human CD antigens with peripheral blood leucocytes of dromedary camels (*Camelus dromedarius*). Open Veterinary Journal 7(2):150-53.

Kamber R, Farah Z, Rüsch P and Hässig M (2000). The supply of newborn camel foals (*Camelus dromedarius*) with immunoglobulin G. Schweiz Arch Tierheilkd 142(10): 581-8.

Ley K, Laudanna C, Cybulsky MI and Nourshargh S (2007). Getting to the site of inflammation: the leukocyte adhesion cascade updated. Nature Reviews Immunology 7(9):678-89.

Mantovani A, Cassatella MA, Costantini C and Jaillon S (2011). Neutrophils in the activation and regulation of innate and adaptive immunity. Nature Reviews Immunology 11(8):519-31.

Rhouma M, Bessalah S, Salhi I, Thériault W, Fairbrother JM, and Fravalo P (2018). Screening for faecal presence of colistin-resistant *Escherichia coli* and mcr-1 and mcr-2 genes in camel-calves in southern Tunisia. Acta Veterinaria Scandinavica 60(1):35.

Soehnlein O and Lindbom L (2010). Phagocyte partnership during the onset and resolution of inflammation. Nature Reviews Immunology 10(6):427-39.

Wernery U, Ali M, Wernery R and Seifert HS (1992). Severe heart muscle degeneration caused by *Clostridium perfringens* type A in camel calves (*Camelus dromedarius*). Revue D'élevage et de Médecine Vétérinaire des Pays Tropicaux 45(3-4):255-9.

ASSESSMENT OF GENETIC VARIABILITY IN *Kappa* CASEIN GENE IN INDIAN DROMEDARY

Yamini, G.C. Gahlot, Urmila Pannu, Mohammed Ashraf and Sanjay Choudhary[1]

Department of Animal Genetics and Breeding College of Veterinary and Animal Sciences, RAJUVAS, Bikaner 334001, Rajasthan
[1]Livestock Production Management Division, ICAR-National Dairy Research Institute, Karnal, Haryana

ABSTRACT

The present study was undertaken to explore the genetic variability in *kappa* casein gene in Bikaneri camel. DNA from camel were extracted through spin column method. PCR was carried out in a final reaction volume of 50 µl and the reaction mixture was subjected to standard PCR protocol. PCR products (488 bp) were digested with *Alu*I. The RFLP analysis of *kappa* casein gene through *Alu*I restriction enzyme detected 2 genotypic pattern in all the studied animals in a genotypic frequency of 0.41 and 0.59 for CT and TT genotype and gene frequency 0.79 (T allele) and 0.21 (C allele). In conclusion, the genetic polymorphism in *kappa* casein gene which is detected first time in Indian camel is considered the best way for enhancing milk composition by selection of animals with superior traits.

Key words: Genetic polymorphism, *Kappa* casein, Polymerase chain reaction

Camel milk becomes an important source of protein for many nomadic communities of all over the world, where other sources of proteins are scarce (Kappeler *et al,* 1998 and Konuspayeva *et al,* 2009). Recently, there has been an increasing trend in consumption of non-bovine milk as an alternative protein source for humans, and is being promoted as healthy food due to its therapeutic value such as antioxidant activity (Hinz *et al,* 2012). Camel milk is rich in insulin and insulin like proteins and it has higher antimicrobial, anti-inflammatory, antiviral, antifungal and anti-cancerous properties (Konuspayeva *et al,* 2007; Alhaider *et al,* 2013; Ismael *et al,* 2013; Kanwar *et al,* 2015). Camel milk is almost similar to goat milk in composition and contains less short-chain fatty acids than cow, sheep and buffalo milk. Its milk contains 2.4 to 5.3 per cent total protein (Konuspayeva *et al,* 2009; Nikkah, 2011a, 2011b) which is divided into caseins (CN ~80%) and whey proteins (Giambra *et al,* 2013). Milk Caseins proteins are further categorised into 4 main types such as αs1-casein, αs2-casein, β-casein, and κ-casein, encoded by single autosomal four genes CSN1S1, CSN2, CSN1S2 and CSN3, respectively (Ikonen *et al,* 2008 and Ereifej *et al,* 2011). Despite of less fraction of *Kappa* casein (3.5 %) in camel milk, it plays an important role in stabilising casein micelles and causes cleavage of phenylalanine-methionine bond and results in initiation of micelle aggregation for curd formation (El-Agamy, 2006; Lutfuaalah

et al, 2011). Genetic polymorphisms in casein gene are important due to their effects on quantitative traits and technological properties of milk (Frajman and Dovc, 2004). Previously, various workers have studied the characterisation of candidate gene and genetic polymorphism in camels (Pauciullo *et al,* 2013; Othman *et al,* 2016; Tanegonbadi *et al,* 2016), bovine (Lucy *et al,* 1991; Schlee *et al,* 1994; Geet *et al,* 2003), ovine (Wallis *et al,* 1998; Bastos *et al,* 2001) and caprine (Wallis *et al,* 1998; Gupta *et al,* 2007).

Studies on analysis of genetic polymorphism on κ-casein gene in Indian camels are lacking. Therefore, the aim of present study was to investigate genetic polymorphism in *kappa* casein gene in Indian camels.

Materials and Methods

Animals and DNA isolation

The blood samples of 70 Bikaneri camels were collected from Bikaner region which is in grid position of 28.02°N and 73.31°E with mean annual rainfall of 277. 55mm. Blood samples (10mL) were obtained and stored at -20°C temperature until DNA extraction was carried out. Genomic DNA was extracted from blood sample through spin column method as per standard method (Sambrook and Russell, 2001) under manufacturer's protocols through Genomic DNA Purification Kit supplied by HIMEDIA Pvt. Ltd. Horizontal agarose gel electrophoresis was carried out to check the quality of genomic DNA using 0.8% w/v agarose.

Polymerase chain reaction

For amplification of 488bp of *kappa* casein gene, the specific forward (CSN3F- 5'CAC AAA GAT GAC TCT GCT ATC G 3') and reverse (CSN3R - 5' GCC CTC CAC ATA TGT CTG 3') primers which were designed by using Primer 3 plus software according to available sequence on NCBI GenBank database. The PCR reaction was carried out for making final volume 50 µl containing GeneTaq PCR Master Mix 25µl, Forward primer 0.5µl, Reverse primer 0.5 µl, template DNA 4 and Nuclease free water 20 µl. The PCR was carried out in Master cycler Gradient Eppendorf (Germany) thermal cycler. PCR program was set up as follows in table 1. PCR amplified DNA product were analysed by analytical agarose gel electrophoresis as per the procedure described by Sambrook *et al* (2001).

Endonuclease digestion

Restriction Fragment Length Polymorphism (RFLP) method with *Alu*I restriction enzyme was applied for genotyping analysis of *kappa*-casein gene (Othman *et al,* 2016). Total 15 µl of the amplified products were digested with 1.5 µl of *Alu*I in a final volume of 45 µl (Nuclease free water 13 µl, 10X Buffer 2 µl, *Alu*I RE 1.5 µl, PCR product 15 µl) at 37°C overnight for digestion in incubator.

Electrophoresis

The restriction fragments were resolved by polyacrylamide gel electrophoresis on 12% gel in 0.5X TBE buffer at 110V for 2 Hrs. As a DNA size marker, low molecular weight ladder (50 bp ladder, NEB) was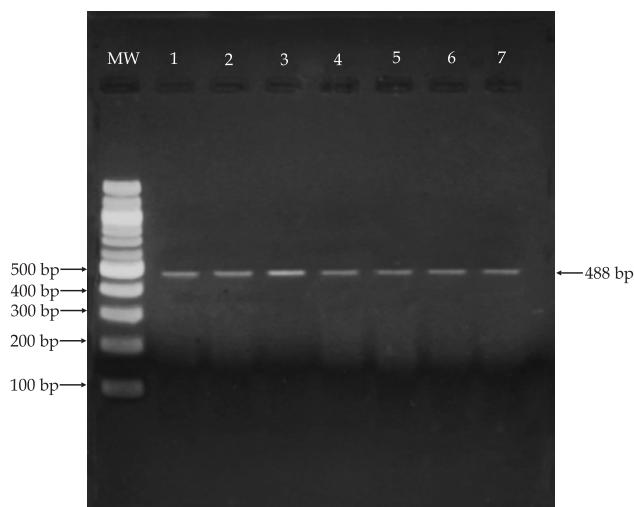 run parallel in the gel. After staining with Ethidium bromide, the fragments were visualised by UV transilluminator and documented by photography.

Table 1. PCR Conditions of *kappa* casein (CSN3) Gene

Steps	Temperature	Time	No. of Cycle
I. Initial Denaturation	95°C	5 min.	1
II. Cycle (i) Denaturation (ii) Annealing (iii) Synthesis	94°C 57.2°C 72°C	45 secs. 1 min. 1 min.	Over all total 36 cycles
III. Final extension	72°C	10 min.	1
IV. Hold	4°C	5 min	1

Statistical Analysis

Estimation of Gene and Genotype frequencies

The data was generated by estimating frequency of restriction digestion patterns of the PCR products. The allele and genotype frequencies were calculated by using standard formula (Falconer and Mackay, 1996).

$$\text{Genotype frequency} = \frac{\text{Number of individuals of a particular genotype}}{\text{Total number of animals of all genotypes}}$$

Results and Discussion

DNA was extracted from all blood samples. All the samples employed in the present investigation were found to be devoid of fragmentation as evidenced by the absence of smearing on gel and presence of intact bright genomic DNA band. The PCR products were assessed by electrophoresis on 1.5% agarose gel and visualised under UV light. A clear cut amplified band of 488 bp with no smearing was obtained in all studied animals (Fig 1). The restriction digestion of 488 bp fragment of *kappa* casein gene indicated the presence of 2 types of restriction patterns in indian dromedary. The first pattern was assigned as genotype CC was not detected, whereas second pattern TT produced 3 fragments 203-bp, 158-bp and 127-bp and the third pattern CT was identified by presence of 4 separate intact fragments of 203-bp, 146-bp,127-bp and 12-bp (Fig 2). Two types of genotype CT and TT was detected having 2 alleles C and T. Scrutiny of table 2 shows the distribution of gene and genotypic frequency for *kappa* casein gene. The genotypic frequency of observed genotype TT and CT were distributed in frequency of 0.59 and 0.41, respectively. An excess of homozygote over heterozygote is
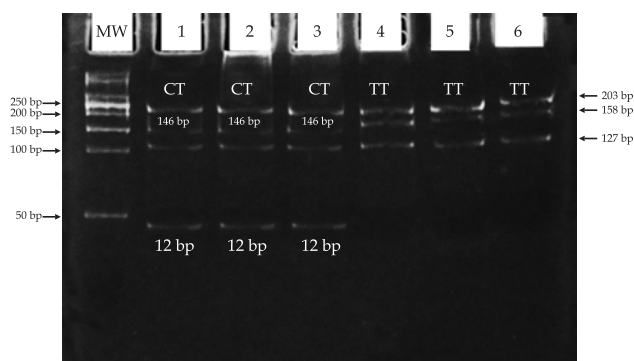

Fig 1. PCR amplicons of *kappa* casein gene of dromedary camel.
Lane 1-7: PCR amplicons of 488 bp
MW : Molecular weight marker (100 bp ladder)

Fig 2. Restriction fragment analysis of *kappa* casein gene in dromedary camel.
MW: Molecular weight marker
Lane 1-3: Genotype CT
Lane 4-6: Genotype TT

preferred in camel which could be the effect of natural selection over years of evolution. The estimated allele frequency of T and C allele as observed is 0.79 and 0.21, respectively. The allele C is found to be less frequent in comparison to T.

Table 2. Genotypic and allele frequency of *kappa* casein gene.

Kappa casein gene	Number of animals 70	Genotypic frequency			Allele frequency	
		CC	CT	TT	C	T
		—	0.41 (29)	0.59 (41)	0.21	0.79

Polymorphism in *kappa* casein gene is identified in different breeds of Sudanese camel showed 3 genotypes CC, CT and TT and allelic frequency of T allele was more as compared with C allele (Pauciullo *et al*, 2013). Othman *et al* (2016) who reported that restriction digestion of 488 bp PCR product with *Alu*I yielded 3 restriction patterns with CC genotype yielded 203,127,120 and 38 bp, CT genotype yielding 4 fragments 203,158,127,120 and 38 bp and TT genotype yielded 203,158 and 127 bp for Maghrabi camel but only one type of genotype TT was found in strong agreement with our study. All 3 genotypes CC, CT and TT were detected in all 3 previous studies and CC genotype having lowest frequency (Pauciullo *et al*, 2013; Othman *et al*, 2016; Tanegonbadi *et al*, 2016). In our study CC genotype was not detected. On comparison of the results of the present study with those by Othman *et al* (2016) and Tanegonbadi *et al* (2016) it can be observed that TT genotype had higher frequency. While Rachagani *et al* (2008) concluded that the frequency of genotype BB allele is less in Tharparkar breed as compared to AA and AB. Genotype BB of *kappa* casein gene had more influence on the monthly milk yield, monthly SNF

yield and protein yield in Sahiwal cattle. However, reports by Mitra *et al* (1998) presented lower (0.12) gene frequency of CSN3 B allele in Murrah, Nili-Ravi and Egyptian buffaloes. Singh *et al* (2005) observed lower frequency of the CSN3 B allele in Murrah (0.10) and Bhadawari (0.08) which is contrary to our finding in camel.

The polymorphism on *kappa* casein gene was first time detected in any Indian camel breed. It can be a starting point for further characterisation of *kappa* casein gene. The different regions of *kappa* casein gene could be further studied with large number of animals.

References

Alhaider A, Abdelgader AG, Turjoman AA, Newell K, Hunsucker SW, Shan, B, Ma, Gibson DS and Duncan MW (2013). Through the eye of an electrospray needle: mass spectrometric identification of the major peptides and proteins in the milk of the one humped camel (*Camelus dromedarius*). Journal of Mass Spectrometry 48:779-794.

Azevedo ALS, Nascimento CS, Steinberg RS, Carvalho MRS, Peixoto MGCD, Teodoro RL, Verneque RS, Guimaraes SEF and Machado MA (2008). Genetic polymorphism of the kappa Casein gene in Brazilian cattle. Genetics and Molecular Research 7:623-630.

Bastos E, Cravador A, Azevedo J and Guedes- Pinto H (2001). Single strand conformation polymorphism (SSCP) detection in six genes in Portuguese indigenous sheep breed "Churra da Terra Quente". Biotechnology, Agronomy, Society and Environment 5:7-15.

Ereifej KI, Alu'datt MH, AlKhalidy HA, Alli I and Rababah T (2011). Comparison and characterisation of fat and protein composition for camel milk from 8 Jordanian locations. Food Chemistrys 127:282-289.

El-Agamy EI (2006). Camel milk. In: Handbook of Milk of Non-Bovine Mammals. Park YW, Haenlein GF (Eds), Blackwell Publishing, Iowa, USA. pp 297-344.

Falconer DS and Mackay TFC (1996). Genotypic frequencies. Introduction to quantitative Genetics (4th Edition). pp 51-55.

Frajman P and Dovc P (2004). Milk production in the post-genomic era. Acta agriculturaeslovenica 84:109-119.

Geet W, Davis ME, Hlines HC, Irvin KM and Simmen RCM (2003). Association of single nucleotide polymorphisms in the growth hormone and growth hormone receptor genes with blood serum insulin-like growth factor I concentration and growth traits in Angus cattle. Journal of Animal Science 81:641-648.

Giambra IJ, El Zubeir IEYM and Erhardt G (2013). Biochemical and molecular characterization of polymorphisms of α s1-casein in Sudanese camel (*Camelus dromedarius*) milk. International Dairy Journal 28: 88-93.

Gupta N, Ahlawat SPS, Kumar D and Malik G (2007). Single nucleotide polymorphism in growth hormone gene exon-4 and exon-5 using PCR SSCP in Black Bengal

goats - A prolific meat breed of India. Meat Science, 76:658-665.

Hinz K, O'Connor P, Huppertz T, Ross R and Kelly A (2012). Comparison of the principal protein in bovine caprine, buffalo, equine, and camel milk. The Journal of Dairy Research 79:185-91

Ikonen T, Ojala M and Syväoja EL (2008). Effects of composite casein and beta-lactoglobulin genotypes on renneting properties and composition of bovine milk by assuming an animal model. Journal of Dairy Science 71:188-195.

Ismael AB, Hafez SMAE, Mahmoud MB, Elaraby A-KA and Hassan HM (2013). Development of new strategy for non-antibiotic therapy: Dromedary camel lactoferrin has a potent antimicrobial and immunomodulator effects. Advances in Infectious Diseases 3:231-237.

Kanwar J, Roy K, Patel Y, Zhou S-F, Singh M, Singh D, Nasir M, Sehgal R, Sehgal A, Singh R, Garg S and Kanwar R (2015). Multifunctional iron bound lactoferrin and nanomedicinal approaches to enhance its bioactive functions. Molecules 20:9703-9731.

Kappeler S, Farah Z and Puhan Z (1998). Sequence analysis of *Camelus dromedarius* milk caseins. Journal of Dairy Research 65:209-222.

Konuspayeva G, Faye B, Loiseau G and Levieux D (2007). Lactoferrin and immunoglobulin contents in camel's milk (*Camelus bactrianus, Camelus dromedarius,* and hybrids) from Kazakhstan. Journal of Dairy Science 90:38-46.

Konuspayeva G, Faye B and Loiseau G (2009). The composition of camel milk meta-analysis of the literature data. Journal of Food Composition and Analysis 22:95-101.

Lucy MH, Hauser SD, Eppard PJ, Krivi GG and Collier RJ (1991). Genetic polymorphism within the bovine somatotropin (bST) gene detected by polymerase chain reaction and endonuclease digestion. Journal of Dairy Science 74 (Suppl. 1), 284.

Lutfuaalah G, Amjad A, Amin F and Ahmad A (2011). Homology modeling of bovine *kappa*-casein. Journal-Chemical Society of Pakistan 33:433-438.

Mitra A, Schlee P, Krause I, Blusch J, Werner T, Balakrishnan and Pirchner F (1998). Kappa-casein polymorphism in Indian dairy cattle and buffalo: A new genetic variant in buffalo. Animal Biotechnology 9:2:81-87.

Nikkah A (2011a). Equidae, camel, and yak milks as functional foods: a review. Journal of Nutrition and Food Sciences 1, 1000116.

Nikkah A (2011b). Science of camel and yak milks: human nutrition and health perspectives. Food and Nutrition Sciences 2:667-673.

Othman E, Amira M, Nowier and Medhat E (2016). Genetic Variations in 2 casein genes among maghrabi camels reared in Egypt. Biosciences Biotechnology Research Asia 13:473-480.

Pauciullo A, Shuiep ES, Cosenza G, Ramunno L and Erhardt G (2013). Molecular characterisation and genetic variability at κ-casein gene (CSN3) in camels. Gene 513: 22-30.

Rachagani S and Gupta ID (2008). Bovine kappa-casein gene polymorphism and its association with milk production trait. Genetic and Molecular Biology 31(4):893-897.

Sambrook J and Russell D (2001). Cold Spring Harbor, NY: Cold Spring Harbour Laboratory. Molecular Cloning: a Laboratory Manual, 3rd edn.

Schlee P, Graml R, Rottmann O and Pirchner F (1994). Influence of growth hormone genotypes on breeding values of Simmental bulls. Journal of Animal Breeding and Genetics 111:253-256.

Singh S, Pushpendra K and Bhattacharya (2005). DNA polymorphism of K-CN and ß-CN gene and its association with milk production and quality traits in buffaloes (*B. bubalis*). Proceedings of National Symposium on Domestic Animals Diversity: Status Opportunity and Challenges, Karnal, India.

Tanegonbady R, Ahani Azari M, Zerehdaran S, Khanahmadi A and Toghdori A (2016). Study of *kappa*-casein gene polymorphism association with milk production and composition in golestan province camels. Genetic Engineering and Biosafety Journal 5:61-66.

Wallis M, Lioupis A and Wallis OC (1998). Duplicate growth hormone genes in sheep and goat. Journal of Molecular Endocrinology 21:1-5.

Short communication

MOLECULAR IDENTIFICATION OF 20 *Escherichia coli* ISOLATES FROM DEAD NEONATAL CAMEL CALVES (*Camelus dromedarius*) IN THE UNITED ARAB EMIRATES

F.A. Hassan[1,2], U. Wernery[3], M. Joseph[3], A. Anouassi[1], K. Mariena[2] and P. Rangsun[2]

[1]Advanced Scientific Group, Abu Dhabi, UAE
[2]Suraneree University of Technology, Thailand
[3]Central Veterinary Research Laboratory, Dubai, UAE

ABSTRACT

Escherichia coli causes major neonatal diarrhoea resulting in a high camel calf mortality. In this study, we concentrated on the gut microbiota of dead 1 to 2 week-old camel calves. Faecal samples were collected during necropsy from small intestines of calves which had died from colibacillosis. Twenty *E. coli* strains were isolated and all of them were successfully amplified by conventional PCR of the 16S rRNA *E. coli* gene. The strains were further tested using the commercially made real-time kits PowerChek Diarrhoeal *E. coli* 4-plex Real-time PCR Kit I and II (Kogenebiotech, Seoul, Korea) that target 8 pathogenic *E. coli* genes. All 20 samples analysed showed negative results. Even after sequencing and blasting against the GenBank database, all six pathotype strains were excluded and all GenBank data were matched with commensal flora of *E. coli*. Since the immune system of newly born camels is weak and their immune response is immature, infection might result from unsanitary conditions in breeding herds, ingestion of contaminated mother's milk or unhygienic food. Other virulence factors of *E. coli* could also be responsible for these calf fatalities.

Key words: Camel, *E. coli* strains, molecular identification

Colibacillosis and colisepticaemia have been reported in Old World Camels (OWCs) and New World Camels (NWCs) and an overview of the current situation is presented by Wernery *et al* (2014). Colibacillosis or colisepticaemia occur mainly in young camelids with considerable economic losses. Morbidity can reach 30% and without immediate veterinary intervention mortality can reach 100%.

The objective of this study was to test 20 *E. coli* strains isolated from dromedary camel calves during necropsy molecular biologically for the presence of pathogenic genes.

Materials and Methods

Sample collection

All 20 *E. coli* samples were isolated from the small intestines of 1 or 2 week-old necropsied calves which showed *E. coli* septicaemia. Bacterial cultural and biochemical analysis were performed at 3 veterinary centres: Advanced Scientific Group breeding centre, Abu Dhabi, Al Wathba veterinary clinic, Abu Dhabi and Central Veterinary Research Laboratory, Dubai. PCR was carried out with primers for the 16s rRNA gene of *E. coli* genera.

DNA Extraction

DNA were extracted using 2 different methods: boiling method and G-spin™ Genomic DNA Extraction Kit (iNtRON Biotechnology Korea). DNA was extracted according to the iNtRON G-spin™ Extraction Kit protocol.

PCR Primer

Twenty *E. coli* samples were identified using the 16S rRNA gene with the E.coli primer pair where the forward primer is 5'CCC CCT GGA CGA AGA CTG A3' and the reverse is 5'ACC GCT GGC AAC AAA GGA3' (Wang *et al*, 2002; Brandal *et al*, 2007).

Conventional PCR

The 16S rRNA gene of the *E. coli* primer pair were used in this study. The forward primer is 5'CCC CCT GGA CGA AGA CTG A3' and the reverse is 5'ACC GCT GGC AAC AAA GGA3'. The PCR assay was carried out in 25 µL of reaction mixture consisting of PCR buffer (20 mM Trisp-HCl, 50 mM

KCl, and 1.5 mM MgCl$_2$), 0.4 mM of dNTPs (Promega, Madison, USA), 0.2 µM of each primer (Alpha DNA Canada), 1 unit of hot start Taq polymerase (Promega USA), and 2 µL of the DNA template. The reaction mixture was run on a thermal cycler (Veriti Thermal Cycle Applied Biosystems, CA USA) with an initial denaturation of 95°C for 5 minutes, then 30 cycles of 95°C for 1 minute, 55°C for 30 seconds, and 72°C for 40 seconds. The final extension was performed at 72°C for 5 minutes.

Gel Electrophoresis

The PCR products were analysed by gel electrophoresis with 10 µL of sample applied to a 2% agarose gel prepared with 5 µL of 20.000X RedSafe nucleic acid staining solution (iNtRON Biotechnolgy, Korea) and electrophoresed at 90 V for 40 minutes in 1X TAE buffer (0.04 M Tris/acetate, EDTA 1 mM). A 100 bp ladder (Promega, Madison, USA) was used as a standard marker. Then, the gel was visualised with a UV transilluminator and photographed.

Realtime PCR

Multiplex real-time PCR were carried out using PowerChek Diarrhoeal *E. coli* 4-plex Real-time PCR Kits I (VT1, VT2, LT, ST) and II (eaeA, aggR, bfpA, and ipaH) (Kogenebiotech, Seoul, Korea) according to the manufacturer's protocol. Assay was performed on a Rotor-Gene Q Real-time PCR (QIAGEN, Hilden Germany) with initial denaturation of 95°C for 10 minutes, then 40 cycles of 95°C for 15 seconds and 60°C for 1 minute where fluorescent detection was carried out at the end of the second step of each cycle with appropriate probe dyes according to the kit protocol.

Sequencing 16S rRNA gene

The PCR product for the 16S rRNA gene primers were purified with a QIAquick PCR purification kit (QIAGEN, CA, USA) and directly sequenced with PCR primers, forward and reverse, separately. Sequencing was carried out with Bigdye Terminators on an ABI 3730 genetic analyser (Applied Biosystems, CA, USA) according to the manufacturer's protocol.

Results and Discussion

DNA was extracted from subcultures of 20 *E. coli* samples isolated from dead camel calves and amplified successfully with the 16S rRNA *E. coli* gene. All samples were PCR positive giving a single band of 400 bp on a 2% agarose gel by electrophoresis. *E. coli* strain JM109 competent cells (Promega, Madison, USA) were used as a positive PCR control which also gave a clear 400 bp band. Three known *Salmonella* strains were also used as a negative control which gave no band. A 100 bp ladder (iNtRON Biotechnolgy, Korea) was used as a molecular weight marker.

In this study, we ran commercial made real-time kits that target 8 genes, namely VT1(stx1), VT2(stx2), LT, ST, eaeA, aggR, bfpA, and ipaH. PowerChek Diarrheal *E. coli* 4-plex Real-time PCR Kits I and II (Kogenebiotech, Seoul, Korea) with 2 multiplex real-time PCRs. All 20 *E. coli* DNA samples were run on a Rotor-Gene Q Real-time PCR (QIAGEN, Hilden, Germany) according to the manufactures protocol. All 20 samples showed no amplification whereas the fluorescent curve of the positive control threshold after 17 cycles and the negative control showed no amplification.

This study demonstrated that all 20 *E. coli* isolates that killed neonatal camels were non-pathogen using normal routine molecular biological tools. However, other virulence factors could be responsible for these calf mortalities.

References

Brandal LT, Lindstedt BA, Aas L, Stavnes TL, Lassen J and Kapperud G (2007). Octaplex PCR and fluorescence-based capillary electrophoresis for identification of human diarrheagenic *Escherichia coli* and Shigella spp. Journal of Microbiological Methods 68:331-341. https://doi.org/10.1016/j.mimet.2006.09.013

Wang G, Clark C and Rodgers F (2002). Detection in escherichia coli of the genes encoding the major virulence factors, the genes defining the O157 : H7 Serotype and components of the type 2 shiga toxin family by multiplex PCR. Journal of Clinical Microbiology 40:3613-3619. https://doi.org/10.1128/JCM.40.10.3613

Wernery U, Kinne J and Schuster RK (2014). Camelid Infectious Disorders, 1st. Ed. OIE, Paris. pp 100-104.

EFFECT OF ITRACONAZOLE ON THE PHARMACOKINETICS OF MIDAZOLAM IN BACTRIAN CAMELS

Weidong Yue[1], Ren San[1] and Surong Hasi[1,2]

[1]College of Veterinary Medicine, Inner Mongolia Agricultural University/Key Laboratory of Clinical Diagnosis and Treatment Technology in Animal Disease, Ministry of Agriculture and Rural Affairs, Hohhot 010018
[2]Inner Mongolia Institute of Camel Research, Badain Jaran, 750300, China

ABSTRACT

The objective of this study was to investigate the effect of the CYP3A enzyme specific inhibitor Itraconazole on the pharmacokinetics of midazolam in Bactrian camels. The camels were allocated randomly into 2 groups of 5 animal each. Camels in group 1 were given a single dose of midazolam only, and camels in group 2 were administered 4 consecutive days of Itraconazole and a single dose of Midazolam. Blood samples were collected from the jugular vein at different times. Midazolam concentration in plasma was determined by high-performance liquid chromatography-ultraviolet detection. The pharmacokinetic parameters of Midazolam were analysed by Phoenix WinNonLin v7.0. There were no significant differences in the clearance or mean residence time of midazolam between the two groups. However, substantial differences were observed in $T_{1/2}$, T_{max}, C_{max}, AUC_{0-t} and V_d between them. $T_{1/2}$, C_{max} and AUC_{0-t} in group 2 were higher than that in group 1, whereas T_{max} and V_d in group 2 were significantly lower than that in group 1. Therefore, midazolam was metabolised mainly by CYP3A in Bactrian camels, and Itraconazole, a specific inhibitor of CYP3A enzyme, could inhibit CYP3A activity significantly and affect the pharmacokinetics of midazolam in Bactrian camels.

Key words: Bactrian camel, CYP3A enzyme, itraconazole, midazolam, pharmacokinetics

Midazolam is a water-soluble benzodiazepine sedative-hypnotic (Paulson *et al*, 2017). It can relieve headaches and moderate ataxia and, at physiologic pH, the drug becomes much more lipid-soluble (Dundee *et al*, 1984). Midazolam is also considered to be a "model" substrate drug for CYP3A enzyme in animals. It has been used widely to evaluate CYP3A activity and, through finite sampling, has been employed to evaluate CYP3A activity *in vivo* (Lee *et al*, 2002; Katzenmaier *et al*, 2011; Halama *et al*, 2013). Itraconazole is a broad-spectrum triazole used to treat infections caused by dermatophytes, yeasts, dimorphic and dematiaceous fungi and molds (Haria *et al*, 1996). Itraconazole is also a competitive inhibitor of CYP3A, causing significant drug–drug interactions if co-administered with other CYP3A substrates (Neuvonen *et al*, 1998; Olkkola *et al*, 1996; Templeton *et al*, 2008). Itraconazole is eliminated by CYP3A oxidation to hydroxyitraconazole and N-desalkyl-itraconazole. After multiple doses, 40–50% of total CYP3A inhibition is attributed to hydroxyitraconazole and N-desalkyl-itraconazole (Ke *et al*, 2014). Some investigators recommended

Itraconazole as an alternative strong CYP3A inhibitor for use in clinical studies, but noted that the other investigators could suggest other CYP3A inhibitors (Ke *et al*, 2014; Vermeer *et al*, 2016).

The pharmacokinetic characteristics of drugs (including midazolam) are affected significantly by Itraconazole (Olkkola *et al*, 1996; Isoherranen *et al*, 2004). The area under the curve (AUC) of midazolam was increased by 1.45- or 1.44-fold after single or repeated Itraconazole treatment in rats, respectively (Sawada *et al*, 2002). Therefore, midazolam and itraconazole can be used as a specific probe substrate and inhibitor for CYP3A, respectively, to study the effect of the CYP3A-enzyme specific inhibitor itraconazole on the pharmacokinetics of midazolam in Bactrian camels.

Materials and Methods

Experimental Camels

All study procedures and animal care activities were conducted in accordance with the Bioethics Committee of the College of Veterinary Medicine in Inner Mongolia Agricultural University

(12150000460029509N) and the Camel Protection Association of Inner Mongolia (5115000050270530X9). Ten 3-year-old healthy Bactrian camels (380–450 kg), 6 male and 4 female, were kept in a herd under ambient conditions. All were from private farmer of West Alxa in Inner Mongolia, China, and were considered to be clinically healthy following a physical examination. None of these experimental animals had received any drugs for ~6 months before study commencement. During the study, food was not allowed, water was supplied *ad libitum*.

Drug administration

The camels were allocated randomly into 2 groups of 5 each according to weight and sex. Camels in group 1 were given a single dose of Midazolam (0.1 mg/kg, i.m.) only; camels in group 2 were given a single dose of Itraconazole (0.1 mg/kg, i.m.) for 4 consecutive days and, 2 h after final injection, administered a single dose of midazolam (0.1 mg/kg, i.m.) again. 5 mL of blood samples were collected from the jugular vein at 0, 5, 15, and 30 min as well as 1, 2, 4, 6, 12, 24, and 36 h following drug administration. All of experimental camels were returned back to the owner when we finished sample collection. The midazolam concentration in plasma was determined by HPLC-UV detection. The pharmacokinetic parameters of Midazolam were analysed using Phoenix WinNonLin v7.0 (Certara, Saint Louis, MO, USA).

Sample analyses

A plasma sample (200 μL) was placed in a 1.5-mL Eppendorf tube, and 600 μL of acetonitrile (Sigma–Aldrich, Saint Louis, MO, USA) added. The mixture was vortex-mixed for 3 min, and then centrifuged at 12000 × g for 10 min to precipitate proteins. The supernatant was transferred to a new 1.5-mL Eppendorf tube and evaporated to dryness at 40°C under a low stream of nitrogen. The residue was re-dissolved in 400 μL of 0.01 mol/mL phosphate-buffered saline:acetonitrile (60:40 v/v) and passed through an organic membrane microporous filter (0.22 μm). Then, 10 μL of the filtrate was analysed immediately by HPLC using a LC-2010 AHT system (Shimadzu, Kyoto, Japan) fitted with a C18 column (4.6 mm × 150 mm, 5 μm, Sigma–Aldrich) with a UV detector (SPD-10A; Shimadzu). The detection wavelength was 254 nm, mobile phase was acetonitrile: phosphate-buffered saline (40:60 v/v), flow rate was 0.5 mL/min, and the column temperature was 30°C. The standard curves for midazolam was linear from 0.19 to 25 μg/mL and the lower limit of detection was 0.1μg/mL,

the lower limit of quantification 0.19μg/mL. The within-day and between-day variability measured for low, medium and high concentrations of the quality control samples were<2% and <7%, respectively.

Pharmacokinetic and data analyses

Non-compartmental analyses of the plasma concentration–time data of midazolam were undertaken for each camel using Phoenix WinNonLin v7.0. C_{max} was the maximum observed concentration occurring at T_{max} (the time of the maximum observed concentration). The maximum plasma concentration (C_{max}) and the time required to reach C_{max} (T_{max}) were calculated directly from the data by Phoenix WinNonLin v7.0. The elimination rate constant was estimated by log-linear regression of the concentrations observed during the linear phase of elimination. The area under the plasma concentration–time curve (AUC) was calculated by the trapezoidal method with extrapolation to infinite time. The $AUC_{0-\infty}$ was the AUC from dosing time extrapolated to infinity based on the final observed concentration. The mean residence time (MRT) was calculated by the linear trapezoidal rule with extrapolation to infinity.

Statistical analyses

Data are the mean ± standard deviation (SD). Plasma concentration–time data are presented in a semi-logarithmic graph. Single-factor analysis of variance with repeated experiments was used to evaluate data to account for the experimental design. Significance was set at $p < 0.05$. Prism v5.0 (GraphPad, San Diego, CA, USA) was used for graph drawing.

Results and Discussion

The pharmacokinetic parameters of midazolam in plasma following administration of a single dose (0.1 mg/kg, i.m.) are given in table 1. Group 1 presentation of the pharmacokinetic parameters of midazolam after administration (0.1 mg/kg) only, whereas group 2 presentation of the pharmacokinetic parameters of midazolam administration of (0.1 mg/kg) following administration for 4 consecutive days of itraconazole (0.1 mg/kg). The mean plasma concentration–time curves are shown in Fig 1. Comparisons of the main pharmacokinetic parameters for group 1 and group 2 are shown in Fig 2.

Fig 2 reveals the statistical analyses of the main pharmacokinetic parameters of Midazolam in the two groups. The main pharmacokinetic parameters of Midazolam were influenced significantly by the CYP3A enzyme specific inhibitor Itraconazole.

Compared with group 1, the T_{max}, clearance (CL) and Vd of Midazolam were decreased significantly (p<0.05), whereas Cmax, AUC and $T_{1/2}$ were increased significantly (p<0.05) in group 2. There was an increasing trend of MRT in group 2, however, did not reach a statistically significant level (p>0.05).

The C_{max} of Midazolam in group 1 and group 2 was 0.62±0.12 µg/mL and 0.79±0.06 µg/mL at a T_{max} of 0.85±0.09 h and 0.54±0.06 h, respectively (Table 1). The $AUC_{0-\infty}$, half-life ($T_{1/2}$), volume of distribution (Vd) and $MRT_{0-\infty}$ of Midazolam in group 1 and group 2 was 2.03±0.56 h.µg/mL, 2.50±0.07 h, 259.17±41.30 mL/kg, 3.71±0.16 h, and 3.00±0.21 h.µg/mL, 3.67±0.23 h, 152.02±22.50 mL/kg, 4.60±0.52 h, respectively. The main pharmacokinetic parameters of Midazolam were influenced significantly by the CYP3A enzyme specific inhibitor itraconazole. Compared with group 1, the T_{max}, clearance (CL) and V_d of midazolam were decreased significantly (p<0.05), whereas C_{max}, AUC and $T_{1/2}$ were increased significantly (p<0.05) in group 2.

Table 1. Pharmacokinetic parameters of midazolam after a single intramuscular administration in camels (n = 5).

PK	Unit	Group 1	Group 2
T_{max}	h	0.85±0.09	0.54±0.06*
C_{max}	µg/mL	0.62±0.12	0.79±0.06*
AUC_{0-t}	h.µg/mL	1.47±0.34	2.16±0.15*
$AUC_{0-\infty}$	h.µg/mL	2.03±0.56	3.00±0.21*
$T_{1/2}$	h	2.50±0.07	3.67±0.23*
CL	mL/h/kg	53.46±14.25	34.38±5.13*
V_d	mL/kg	259.17±41.30	152.02±22.50*
MRT_{0-t}	h	3.71±0.16	4.60±0.52*

T_{max}, time to reach the maximum plasma concentration; C_{max}, maximum plasma concentration; AUC_{0-t}, area under the curve from the time of dosing to the final measurable (positive) concentration; $AUC_{0-\infty}$, AUC from the time of dosing to the time extrapolated to infinity based on the final observed concentration; $T_{1/2}$, Terminal half-life; CL, Total body clearance for extravascular administration; V_d, apparent volume of distribution; MRT_{0-t}, mean residence time from the time of dosing to the final measurable (positive) concentration. Data are the arithmetic mean ± SD. *indicate significant difference.

CYP enzymes are superfamily enzymes responsible for metabolism of many endogenous and exogenous substances and drugs. Among them, CYP3A plays an important part in metabolism of ~50% of drugs and its metabolic activity was affected by many other drugs (Shirasaka *et al*, 2013; Kanazawa *et al*, 2004). Itraconazole, a CYP3A enzyme-specific inhibitor, can significantly influence the pharmacokinetic profile of midazolam in different animals (Vossen *et al*, 2007; Reves *et al*, 1983).

Midazolam is a specific substrate of CYP3A enzyme, and was completely eliminated through biotransformation, the $T_{1/2}$ of midazolam is usually 1.5–3.5 h (Yu *et al*, 2004). The main metabolite is α-hydroxy Midazolam. Itraconazole is a potent specific inhibitor of CYP3A enzyme, and causes significant drug–drug interactions if co-administered with CYP3A substrates. To investigate the activity of CYP3A enzyme in Bactrian camels, the pharmacokinetic characteristics of Midazolam (a CYP3A-specific substrate) in Bactrian camels were studied. The main pharmacokinetic parameters of Midazolam in two groups of camels were compared and analysed to evaluate the inhibitory effect of Itraconazole on CYP3A enzyme activity.

Schwartz and colleagues reported the pharmacokinetic parameters of midazolam given as a single dose of 0.2 mg/kg to dogs. The C_{max} of midazolam was 0.86±0.36 µg/mL and 0.20±0.06 µg/mL following intravenous and intramuscular administration, respectively; the T_{max} after intramuscular administration was 7.8±2.4 min with a bioavailability of 50 ± 16% (Schwartz *et al*, 2013). Simon and co-workers focused on Midazolam use in sheep. Midazolam was distributed rapidly and extensively, and eliminated rapidly following administration (0.5 mg/kg, i.m). Also, the V_d, $T_{1/2}$, CL, and AUC of Midazolam were 838±330 mL/kg, 0.79±0.44 h, 1272±310 mL/h/kg, and 423±143 h·ng/mL, respectively. In addition, the C_{max}, T_{max}, AUC were 820±268 ng/mL, 0.46±0.26 h, 1396±463 h·ng/mL, respectively. In the present study, the pharmacokinetic parameters of midazolam in Bactrian camels was similar to those of dogs and sheep, except
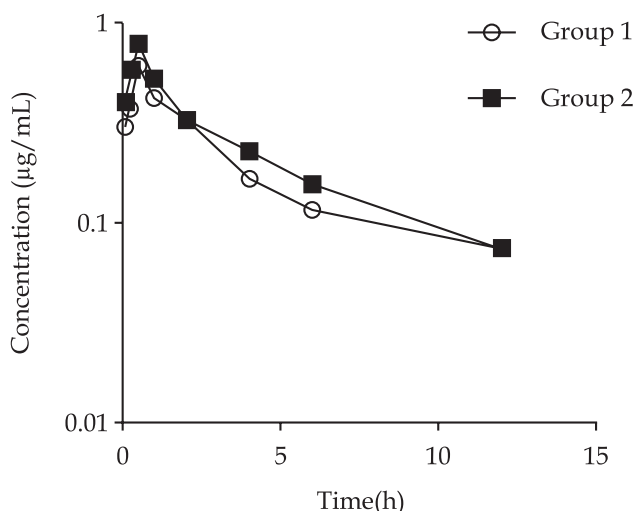

Fig 1. Semi-logarithmic plot of serum Midazolam concentration vs time in two groups of Bactrian camels.
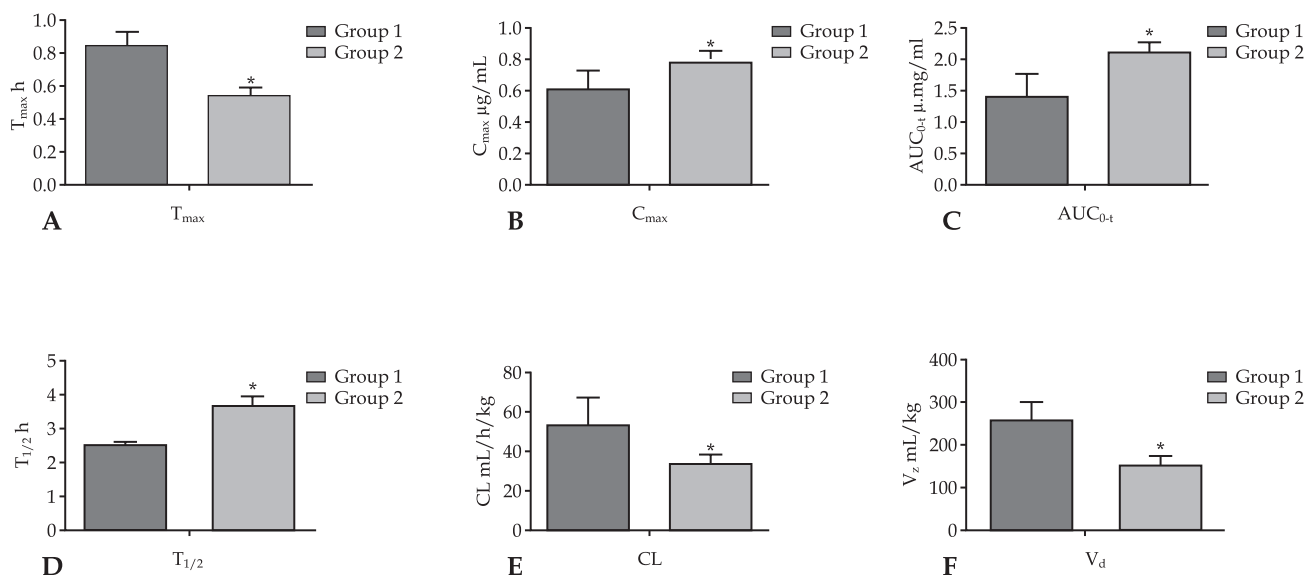
Fig 2. Comparative analyses of the main pharmacokinetic parameters of MDZ in two groups of Bactrian camels. The bar charts A, B, C, D, E and F indicate the comparison of T_{max}, C_{max}, AUC_{0-t}, $T_{1/2}$, CL and V_d on MDZ in group 1 and group 2, respectively; *$p < 0.05$.

that the $T_{1/2}$ and AUC of midazolam in Bactrian camels were lower than those in sheep.

Compared with group 1, the $T_{1/2}$, Cmax, and AUC_{0-t} of Midazolam in group 2 were increased significantly ($p < 0.05$) by 46.8%, 27.4%, and 46.9%, respectively, whereas the T_{max}, V_d and CL were decreased significantly ($p < 0.05$) by 36.5%, 41.3% and 35.7%, respectively. These data showed that the enzyme inhibitor itraconazole could inhibit CYP3A activity significantly in Bactrian camels.

As expected, midazolam elimination was decreased upon itraconazole administration. Hence, our results suggest that inhibition of CYP3A enzyme by the potent specific inhibitor of itraconazole resulted in a substantial pharmacokinetic interaction with midazolam. These data emphasise that it is through the appropriate trial designs to evaluate the plausibility of pharmacokinetic interactions in development of drugs to treat diseases in Bactrian camels.

Therefore, the itraconazole, a specific inhibitor of CYP3A enzyme, could inhibit the activity CYP3A enzyme significantly and affect the pharmacokinetic characteristics of Midazolam in Bactrian camels.

References

Dundee JW, Halliday NJ, Harper KW and Brogden RN (1984). Midazolam, a review of its pharmacological properties and therapeutic use. Drugs 28:519-543.

Halama B, Hohmann N, Burhenne J, Weiss J, Mikus G and Haefeli WE (2013). A nanogram dose of the CYP3A probe substrate midazolam to evaluate drug interactions. Clinical Pharmacology and Therapeutics 93:564-571.

Haria M, Bryson HM and Goa KL (1996). Itraconazole, a reappraisal of its pharmacological properties and therapeutic use in the management of superficial fungal infections. Drugs 51:585-620.

Isoherranen N, Kunze KL, Allen KE, Nelson WL and Thummel KE (2004). Role of Itraconazole metabolites in CYP3A4 inhibition. Drug Metabolism and Disposition 32:1121-1131.

Kanazawa H, Okada A, Igarashi E, Higaki M, Miyabe T, Sano T and Nishimura R (2004). Determination of midazolam and its metabolite as a probe for cytochrome P450 3A4 phenotype by liquid chromatography–mass spectrometry. Journal of Chromatography A 1031(1-2): 213–218.

Katzenmaier S, Markert C, Riedel KD, Burhenne J, Haefeli WE and Mikus G (2011). Determining the time course of CYP3A inhibition by potent reversible and irreversible CYP3A inhibitors using a limited sampling strategy. Clinical Pharmacology and Therapeutics 90:666-673.

Ke AB, Zamek-Gliszczynski MJ, Higgins JW and Hall SD (2014). Itraconazole and clarithromycin as ketoconazole alternatives for clinical CYP3A inhibition studies. Clinical Pharmacology and Therapeutics 95:473-476.

Lee JI, Chavesgnecco D, Amico JA, Kroboth PD, Wilson JW and Frye RF (2002). Application of semisimultaneous midazolam administration for hepatic and intestinal cytochrome p450 3A phenotyping. Clinical Pharmacology and Therapeutics 72:718-728.

Neuvonen PJ, Kantola T and Kivistö KT (1998). Simvastatin but not pravastatin is very susceptible to interaction with the cyp3a4 inhibitor Itraconazole. Clinical Pharmacology and Therapeutics 63:332-341.

Olkkola KT, Ahonen J and Neuvonen PJ (1996). The effects of the systemic antimycotics, itraconazole and fluconazole, on the pharmacokinetics and pharmacodynamics of intravenous and oral midazolam. Anaesthesia and Analgesia 82:511-516.

Paulson SK, Wood-Horrall RN, Hoover R, Quintas M, Lawrence LE and Cammarata SK (2017). The pharmacokinetics of the CYP3A substrate midazolam after steady-state dosing of delafloxacin. Clinical Therapeutics 39:1182-1190.

Reves JG, Samuelson PN and Vinik HR (1983). Midazolam. Contemporary Anaesthesia Practice 7:147.

Sawada Y, Takedomi S, Matsuo H, Yamano K, Iga T and Ohtani H (2002). Effects of single and repeated treatment with itraconazole on the pharmacokinetics of midazolam in rats. Drug Metabolism and Pharmacokinetics 17:275-283.

Schwartz M, Muñana KR, Nettifee-Osborne JA, Messenger KM and Papich MG (2013). The pharmacokinetics of midazolam after intravenous, intramuscular, and rectal administration in healthy dogs. Journal of Veterinary Pharmacology and Therapeutics 36:471-477.

Shirasaka Y, Chang SY, Grubb MF, Peng CC, Thummel KE, Isoherranen N and Rodrigues AD (2013). Effect of CYP3A5 expression on the inhibition of CYP3A-catalyzed drug metabolism: impact on modeling CYP3A-mediated drug-drug interactions. Drug Metabolism and Disposition 41:1566-1574.

Templeton IE, Thummel KE, Kharasch ED, Kunze KL, Hoffer C, Nelson WL and Isoherranen N (2008). Contribution of Itraconazole metabolites to inhibition of CYP3A4 *in vivo*. Clinical Pharmacology and Therapeutics 83:77-85.

Vermeer LM, Isringhausen CD, Ogilvie BW and Buckley DB (2016). Evaluation of Ketoconazole and Its Alternative Clinical CYP3A4/5 inhibitors as inhibitors of drug transporters: The in vitro effects of ketoconazole, ritonavir, clarithromycin, and itraconazole on 13 clinically-relevant drug transporters. Drug Metabolism and Disposition 44:453-459.

Vossen M, Sevestre M, Niederalt C and Jang IJ (2007). Dynamically simulating the interaction of midazolam and the CYP3A4 inhibitor itraconazole using individual coupled whole-body physiologically-based pharmacokinetic (WB-PBPK) models. Theoretical Biology and Medical Modelling 4:13.

Yu KS, Cho JY, Jang IJ, Hong KS, Chung JY, Kim JR, Lim HS, Oh DS, Yi SY, Liu KH, Shin JG and Shin SG (2004). Effect of the CYP3A5 genotype on the pharmacokinetics of intravenous midazolam during inhibited and induced metabolic states. Clinical Pharmacology and Therapeutics 76:104-112.

DR GAHLOT WAS INVITED TO
INTERNATIONAL CAMEL CONFERENCE, CHINA

Dr. T.K. Gahlot, Editor, Journal of Camel Practice and Research was invited to People's Republic of China for attending 7th China Camel Industry Development Conference (2019) organised by China Animal Husbandry Association, Co-Organised by Alxa League Administrative Office and hosted by Ejina Banner, Alxa League, Inner Mongolia, China from 25 to 27 November 2019. He delivered a lead paper entitled, "Camel Surgery- an overview of current and futuristic approaches and challenges". Organisers have also requested Dr.Gahlot to deliver a presentation on "Camel Science and Industry- An Overview" to the faculty and students of Inner Mongolia Agricultural University, Hohhot, Inner Mongolia during this visit. Delegates of the conference were also taken to Bactrian Camel Festival organised on 26th November. The purpose of this conference was to promote the sustainable development of camel science, industry and culture and accelerate the development and strengthen the cooperation between the domestic and foreign scholars. Dr Gahlot was earlier invited to China in 2017 alongwith two more faulty members.

NEW BOOK: HANDBOOK OF RESEARCH ON HEALTH AND
ENVIRONMENTAL BENEFITS OF CAMEL PRODUCTS

The new book entitled, "Handbook of Research on Health and Environmental Benefits of Camel Products" is authored by Omar Amin Alhaj, Jordan, Bernard Faye, France and Rajendra Prasad Agrawal, India. It is published in the United States of America by IGI Global (ISSN: 2330-3271; eISSN: 2330-328X). The various chapter of book are contributed by 37 authors from 16 countries. This book has 17 chapters spread in 477 pages. Eleven chapters are based on different facets of camel milk which are very interesting. These chapters describe camel milk composition and nutritional value, strategies and technologies for camel milk preservation, microbial aspect of lactic acid bacteria isolated from camel milk, manufacture of dairy and non-dairy camel milk products, manufacture and challenges of camel milk cheese, exploring potential therapeutic properties of camel milk, health-improving and disease-preventing potential of camel milk against chronic diseases and autism: camel milk and chronic diseases, potential anti-diabetic effect of camel milk, effects of industrial processing methods on camel milk composition, nutritional value, and health properties, camel colostrums composition, nutritional value, and nutraceuticals and camel milk disguised cosmeceutical. Chapters also contain information about the recent introduction of the CHY-Max–M1000®,on market solved the problem of clotting. Obtained by genetic engineering, this camel rennet allows high cheese yield. Scientists from India have investigated and assessed the effect of regular camel milk consumption on glycaemic status of diabetic patients and animal models. All the experiments' results concluded to the reduction of blood glucose and glycosylated haemoglobin. One chapter is based on Interaction between camel farming and environment. Chinese authors have contributed one chapter on camel hair structure, properties, and commercial products. The chapter on camel meat is contributed by a group of scientists from Oman and Sudan led by Isam Tawfik Kadim. The scientists from Saudi Arabia and Malaysia have contributed a chapter on camel gelatin composition, properties, production, and applications. This chapter discusses the processing of camel gelatin extraction. Gelatine has an ability to form a thermo reversible gel at normal body temperature and high water content make it an exceptional food ingredient.

HISTOLOGY OF ATRIOVENTRICULAR NODE AND ATRIOVENTRICULAR BUNDLE IN THE DROMEDARY CAMEL FOETUS

Marwa-Babiker A.M.[1,4], Hassan A. Ali[2], Zarroug H. Ibrahim[2,3] and Haider Ismail[1]

[1]Department of Anatomy, College of Veterinary Medicine, University of Bahri, Khartoum-North, Sudan
[2]Department of Biomedical Science, College of Veterinary Medicine, Sudan University of Science and Technology, P.O. Box. 204, Khartoum-North, Sudan
[3]College of Agriculture and Veterinary Medicine, Qassim University, Buraidah, Saudi Arabia
[4]Department of Anatomy, College of Veterinary Medicine and Animal Resources, King Faisal University, Saudi Arabia

ABSTRACT

Atrioventricular node (AVN) and Atrioventricular bundle (AVB) development in the camel heart was studied during the 1st, 2nd and 3rd trimesters of gestation using histological techniques. Thirty hearts of camel foetuses were used in this study. Specimens were collected from Tamboul and Al-Salam slaughterhouses, Sudan. The samples were prepared by routine histological procedures and stained by the general histological stain (H&E) and some other special stains. AVN was found close to the atrioventricular opening in the 1st trimester and close to the opening of the coronary sinus in the 2nd and 3rd trimesters. It generally appeared as a group of large-sized and lightly stained cardiac muscle cells. AVB was embedded in myocardium in the 2nd trimester as a bundle of lightly stained fibres either located between the endocardium and myocardium or within the myocardium; in the early stages of the 3rd trimester they appeared as groups of fibres which were covered by connective tissue between the endocardium and myocardium. It was concluded that the AVN and AVB showed very important histological developmental changes throughout the 3 gestational stages.

Key words: Atrioventricular bundle, atrioventricular node, camel, foetus, histology

Atrioventricular node is in contact with atrial myocardium. The bundle of His penetrates the right fibrous trigone, then divides into two specialised ventricular branches (right and left), which are also surrounded by a fibrous sheath that separates the specialised myocytes from the ordinary myocardium.

The anatomy and histology of the atrioventricular bundle (AVB) and sinus node was studied in the heart of the dromedary camel (Ghazi and Tadjalli, 1993; 1996). They stated that the trunk of the atrioventricular bundle (Bundle of His) was a direct continuation of the atrioventricular (AV) node with no sharp line of demarcation between the node and the bundle. The atrioventricular bundle ran through the fibrous trigone and entered the lower part of the interventricular membranous septum beneath the right endocardium. They then lay over or slightly to the side of the centre of the muscular interventricular crest.

Histologically, the AVB in the heart of camels comprised multiple strands of Purkinje cells separated by collagen fibres and surrounded by connective tissue. It resembled that in humans and dogs except

that, in camels, intercalated discs were present at the intercellular connections in the AVB (Ghazi and Tadjalli, 1996).

The development of the atrioventricular bundle (AVB) and ventricular Purkinje system and their innervation has been studied in sheep foetuses from 27 to 140 days of gestation (Canale *et al,* 1987).

Morphological developmental changes in the dromedary camel heart foetus have recently been studied (Marwa-Babiker *et al*, 2015; 2016a,b; 2017). However, the reviewed literature lacks investigation on the development of AVN and AVB in dromedary camels. The present work was therefore aimed to investigate the development of AVN and AVB of the camel heart during the 1st, 2nd and 3rd trimesters of gestation using histological techniques.

Materials and Methods

Thirty hearts of camel foetuses obtained from Al-Salam and Tamboul slaughter houses, Sudan, were used in this study. Depending on the age, the foetuses were divided into 3 equal groups: 1st trimester 0.1-23.5 cm CVRL (65-130 days), 2nd trimester 24-71 cm CVRL

(131-260 days) and 3rd trimester 71.5-132 cm CVRL (261-426 days). The age of foetus was determined by using the equation of Crown Vertebral-Rump Length (CVRL) GA= (CVRL+23.99)/0.366] GA (Gestational Age) in days as described by Elwishy *et al* (1981).

The histological samples which were fixed in 10% buffered formalin included the entire hearts from the 1st and early 2nd trimesters and 1cm³ thick specimens from the late 2nd and 3rd trimesters.

Specimens were taken from atrioventricular node and atrioventricular bundle and were prepared for routine histological procedures (Bancroft and Stevens, 2008). General histological stains (H&E) and some special stains including Van Geison's and Masson's Trichrome for collagenous fibres, Verhoff's and Gomori's Aldehyde fuchsin for elastic fibres, Gordon and Sweet for reticular fibres were used in this study (Bancroft and Stevens, 2008).

Results and Discussion

The atrioventricular node (AVN) was 1st observed at the stage of 13 cm CVRL (101 days of gestation) as a group of large-sized and lightly stained cardiac muscle cells which were located between the right atrium and right ventricle (Figs 1 A and B). The node was close to the right atrioventricular opening and it was surrounded by an accumulation of fibroblasts and separated from the surrounding ordinary cardiac muscles by a loose connective tissue which contained reticular fibres (Fig 1 B). The cells possessed large, oval or spherical, centrally located nuclei and they were located in rich connective tissue. In one section at this stage (17 cm CVRL; 112 days of gestation) the AVN appeared as scattered 3 groups of cells separated from each other by connective tissue rich in fibroblasts (Fig 2).

At the early stage of the 2nd trimester 38 cm CVRL (169 days of gestation), the AVN consisted of a group of spherical cells which had oval and central nuclei. These cells were surrounded by cardiac muscle fibres which were followed by connective tissue formed mainly of elastic fibres (Fig 3, A and B). At the late stage of the 2nd trimester the AVN appeared as a group of cells with the same structure but they were embedded in rich amounts of connective tissue (Fig 4 A and B).

The atrioventricular Bundle (AVB) appeared at the stage of 61 cm CVRL (232 days of gestation) as a bundle of lightly stained fibres that were embedded in the myocardium (Fig 5, A). At the stage of 68 cm CVRL (251 days of gestation) AVB was in the form of a group of lightly stained fibres which were covered by connective tissue. The fibres were spherical or oval and they had spherical and central nuclei and their cytoplasm was dark peripherally and light centrally and it had clear striation (Fig 5 B and C).

At the early stages of the 3rd trimester 76 cm CVRL, 273 days of gestation AVN consisted of a group of dark stained cells (modified cardiac muscle cells). These cells had oval and central nuclei and were surrounded by connective tissue that consisted of a large amount of fibroblasts followed by cardiac muscle fibres (Fig 6 A and B). At the middle and late stages of the 3rd trimester, AVN was embedded in connective tissue containing large amounts of adipose tissue (Fig 7 A, B and C).

At the early stages of the 3rd trimester of gestation represented by 76 cm CVRL (273 days of gestation), AVB appeared as groups of fibres which were covered by connective tissue between the endocardium and myocardium. The fibres nuclei were lightly stained centrally and darkly stained peripherally (Fig 8 A). They were also observed as bundles of lightly stained fibres with spindle shaped and oval pale nuclei in the epicardium and between the myocardial muscles (Fig 8 B).

At 89 cm CVRL (309 days of gestation) and 91 cm CVRL (314 days of gestation) AVB appeared as bundles of spindle shaped fibres with oval central nuclei. The bundles were separated by connective tissue (Fig 9). At the stage of 97 cm CVRL (331 days of gestation), the AVB appeared as bundles of fibres between the myocardial muscles near the endocardium (Figs 10 A, B and C). They had a light cytoplasm and pale central nuclei and were either separated from the myocardium by loose connective tissue or directly attached to it. AVB fibres at this stage possessed clear striation (Fig 10 C).

Anatomists who seek to demonstrate the location of the components of cardiac conduction system must be contented with the fact that the components of the system cannot be distinguished from the working myocardial elements by gross dissection (Anderson *et al,* 2009). It has been stated that AVB and lower nodal cells were derived from ventricular myocardium (Aanhaanen *et al,* 2010). According to Virágh and Challice (1977) AVN originated from the cells at the distal end of specialised tissue and proliferated into the loose mesenchyme of the dorsal AV cushion. The proliferation took place proximal to the developing interventricular septum with which the specialised inner layer of the AV canal was interconnected. The
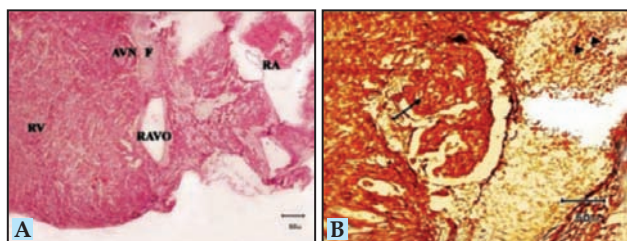
Fig 1. A: A photomicrograph showing atrioventricular node (AVN) of 13 cm CVRL camel foetus surrounded by a large amount of connective tissue, F, fibroblasts, RA, right atrium, RV, right ventricle, RAVO, right atrioventricular opining. H&E (X4). **B:** A photomicrograph showing reticular fibres (arrowheads), surrounding AVN (arrow). Gordon and Sweet stain (X10).
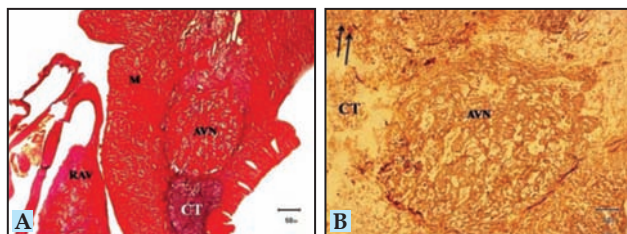

Fig 2. A photomicrograph showing scattered AVN (arrowheads) of 17 cm CVRL camel foetus, connective tissue CT, myocardium M. H&E (X10).

Fig 3. A: A photomicrograph showing atrioventricular node AVN of 38 cm CVRL camel foetus close to cardiac muscle (M), surrounded by connective tissue (CT) and situated close to the right atrioventricular valve (RAV). Aldehyde fuchsin (X10). B: The same section in A showing a few amount of reticular fibres (arrows). Gordon and Sweet (X40).
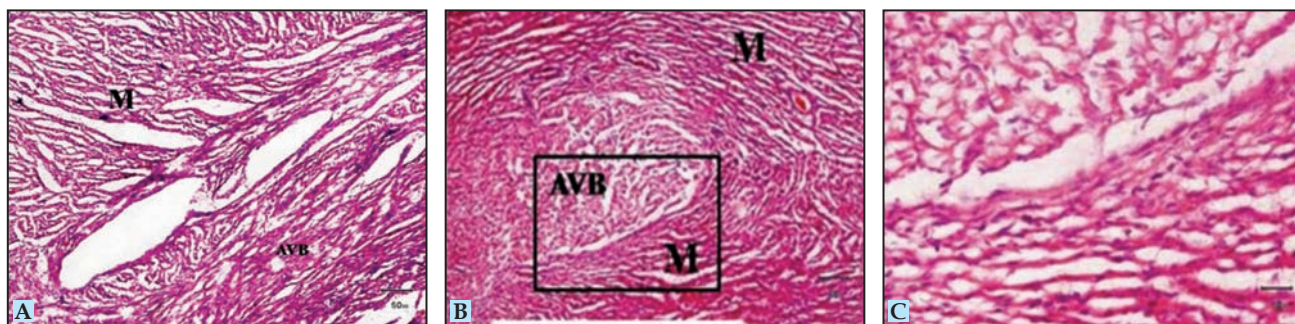
Fig 4. A: A photomicrograph showing AVN of 71 cm CVRL camel foetus, near to the cardiac muscle (M), surrounded by a large amount of connective tissue (CT). H&E (X4). **B:** a magnification of the rectangle in A (X40).
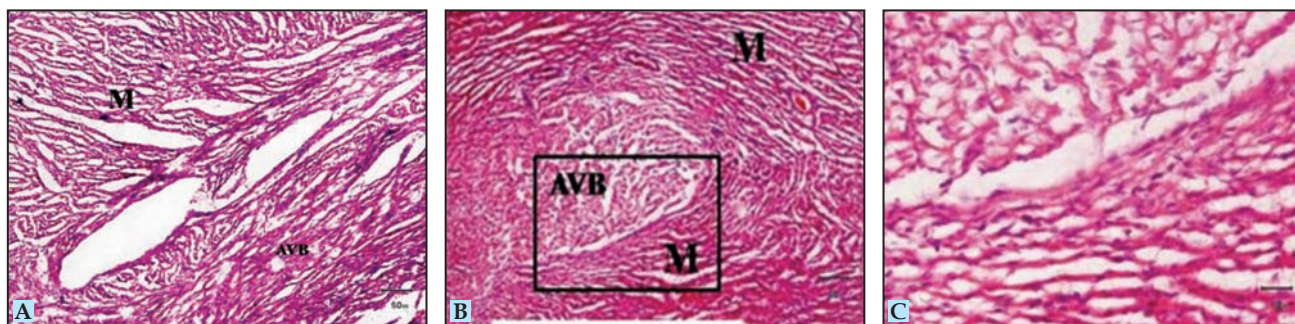
Fig 5. A: A photomicrograph showing atrioventricular bundle (AVB) of 61 cm CVRL camel foetus embedded in cardiac muscle (M). H&E (X10). **B:** AVB embedded in myocardium of 68 cm CVRL. H&E (X10). **C:** magnification of the rectangle in B showing the cytoplasm of AVB fibres as light centrally and dark peripherally (X40).

AVN and AVB originate as separate structures that united together very early in foetal development (James, 1970). This is generally in accordance with the current study in which the AVN was observed early at the 1st trimester of gestation located between the right atrium and right ventricle close to the opening of coronary sinus and the AVB appeared in the 2nd trimester as a bundle of lightly stained fibres in the myocardium. However, unusually, in one section at (17 cm CVRL; 112 days of gestation) AVN appeared as scattered 3 groups of cells separated from each other by connective tissue rich in fibroblasts.

As mentioned by Virágh and Challice (1977) who studied the histogenesis of the AVN and AVB in mouse embryos, in younger embryos the inner cell layer of the dorsal wall of the AV canal formed a specialised interconnecting tissue between the atrial and ventricular muscles. In this study, AVN was also observed close to the right atrioventricular opening and it was surrounded by an accumulation of fibroblasts and separated from the surrounding ordinary cardiac muscles by loose connective tissue containing reticular fibres. The primordia of AVN and AVB of 11- and 12-days mouse embryo according to
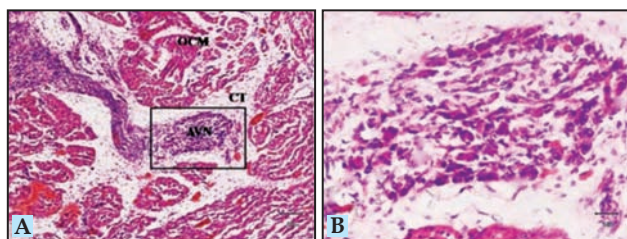
Fig 6. A: A photomicrograph showing atrioventricular node (AVN) of a camel foetus at 76 cm CVRL. It is located between ordinary cardiac muscles (OCM) surrounded by connective tissue (CT). H&E (X10). **B:** is a magnification of a rectangle in (A) showing AVN cells (X40).
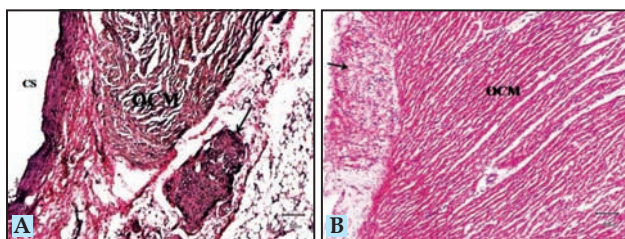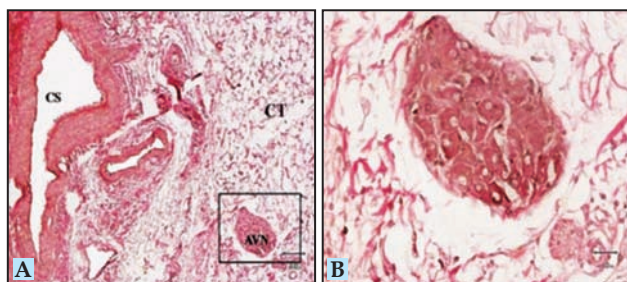

Fig 7. A: A photomicrograph showing atrioventricular node (AVN) in camel foetus at 89 cm CVRL. It is surrounded by connective tissue (CT) separating the node from coronary sinus (CS). Van Gieson's. (X10). **B:** magnification of the rectangle in A showing AVN (X40). **C:** A photomicrograph showing atrioventricular node (arrow) near the ordinary cardiac muscle OCM and coronary sinus (CS) in camel foetus at 92 cm CVRL. Verhoff's (X10).

Fig 8. A: A photomicrograph showing the atrioventricular bundle (AVB) (arrow) at 76 cm CVRL camel foetus. It is located between endocardium and myocardium. H and E (X10). **B:** 79.5 cm CVRL camel foetus showing AVB (arrows) between endocardium and myocardium and in between ordinary cardiac muscles (OCM). H&E (X10).
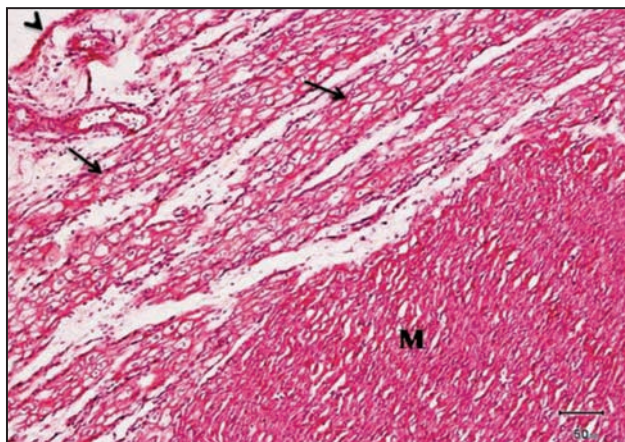
Fig 9. A photomicrograph of 91 cm CVRL camel foetus showing atrioventricular bundle AVB, (arrows) located between endocardium (arrowhead) and myocardium (M). H&E (X10).
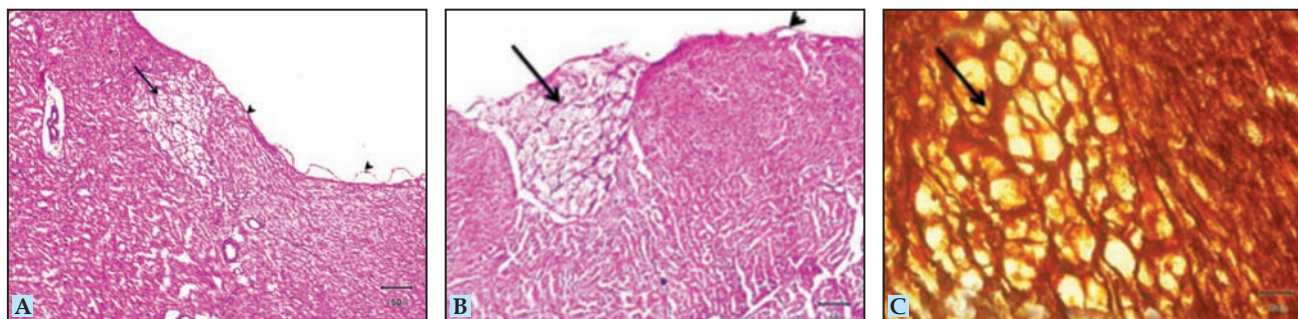
Fig 10. A and **B:** Photomicrographs showing atrioventricular bundle (arrows) of camel foetus at 97 cm CVRL. It is located between the myocardial fibres or beneath endocardium (arrowheads). H&E (X10). **C:** showing AVB (arrow) with striation. Gordon and Sweet (X40).

Virágh and Challice (1977) were interconnected with the ventricular trabeculae and were in contact with the myocardium of the interventricular septum. In the 12-days embryos blood capillaries and connective tissue cells began to isolate the primordium of the conducting system from the force producing myocardium.

Arguello *et al* (1988) studied the development of the AVN and AVB of embryonic chick hearts by using electrophysiological and morphological techniques. They claimed that the earliest identification of the AVN and upper AVB group of cells was achieved at 5-6 days of development and the earlier AVN and AVB responses had similar characteristics to those of the adult heart. They concluded that the AVN and upper AVB cells were derived from the low interatrial septum and the possibility that AV canal cells contribute to this event was discarded.

Nabipour (2004) stated that in the guinea pig the cells of the AVB appeared to be organised into fascicles separated by fine fibrous septa and the majority of them were ovoid in shape with light cytoplasm and central nuclei. He also described intercalated discs at the AVN intercellular junctions. This study agreed with the previous study regarding the shape and organisation of AVB but disagreed with it regarding the presence of intercalated discs at the AVN intercellular junctions.

In the persent study, no ganglia were seen associated with the AVB. This was in agreement with the findings of Nabipour (2004) in the guinea pig who stated that the innervation of AVB was poor and no ganglia were present within or around the AVB and its branches.

Nabipour and Shahabodini (2007) studied the histological structure of the AVN and AVB in 4 months-old ovine foetuses. They reported that the AVN was caudally located and adjacent to the root of the aorta and it was almost spherical in shape and consisted of spiral cells. The node was mainly composed of perinuclear clear zone cells (P cells). In contrast, in the early stages of the 3rd trimester in this study, the AVN consisted of a group of darkly stained cells with oval and central nuclei. These cells were surrounded by connective tissue that consisted of a large amount of fibroblasts.

The AVB was a direct continuation of the AVN and passed through the fibrous ring toward the apex of the interventricular septum where the right branch of the bundle was detached. The cells of the AVB were wider, shorter and lighter than normal myocardial cells. Some of the bundle cells had been changed to Purkinje cells, whereas some others remained unchanged (Nabipour and Shahabodini, 2007). In this study the AVB appeared in the 2nd trimester as a bundle of lightly stained fibres that were embedded in the myocardium, or as fibres lightly stained centrally and darkly stained peripherally with clear peripheral striations. In the 3rd trimester the bundles consisted of lightly stained fibres with spindle-shaped and oval pale nuclei which were located in the subendocardial region and between the myocardial fibres, or separated from the myocardium by loose connective tissue or directly attached to it.

References

Aanhaanen WTJ, Mommersteeg MTM and Norden J (2010). Developmental origin, growth and 3-dimensional architecture of the atrioventricular conduction axis of the mouse heart. Circulation Research 107:728-736.

Anderson RH, Yanni J, Boyett MR, Chandler NJ and Dobrzynski H (2009). The anatomy of the cardiac conduction system. Clinical Anatomy 22(1):99-113.

Arguello C, Alanis J and Valenzuela B (1988). The early development of the atrioventricular node and bundle of His in the embryonic chick heart. An electrophysiological and morphological study. Development 102:623-637.

Bancroft DG and Stevens A (2008). Theory and Practice of Histological Techniques. 6th ed. Bath press, Avan. Churchill Livingston. Edinburgh. London and New York.

Canale E, Smolich JJ and Campbell GR (1987). Differentiation and innervation of the atrioventricular bundle and ventricular Purkinje system in sheep heart. Development 100(4):641-651.

Elwishy AB, Hemeida NA, Omer MA, Mobarak AM and El Sayed MAI (1981). Functional changes in the pregnant camel with special reference to foetal growth. British Veterinary Journal 137:527-537.

Ghazi SR and Tadjalli M (1993). The anatomy of the atrioventricular bundle in the heart of camels (*Camelus dromedarius*). Veterinary Research Communications 17 (6): 411-416.

Ghazi SR and Tadjalli M (1996). Anatomy of the sinus node of camels (*Camelus dromedarius*). Anatomia Histologia Embryologia 25(1):37-41.

James TN (1970). Cardiac conduction system: foetal and postnatal development. American Journal of Cardiology 25(2):213-226.

Marwa-Babiker AM, Ali HA, Ibrahim ZH and Ismail HI (2015). Ultrastructure of prenatal heart of dromedary camel during 1st trimester. Nova Journal of Medical and Biological Sciences 4(3):1-6.

Marwa-Babiker AM, Ali HA, Ibrahim ZH and Ismail HI (2016a). Histology of sinoatrial node in the dromedary camel foetus. International Journal of Advanced Veterinary Science and Technology 5:226-231.

Marwa-Babiker AM, Ali HA, Ibrahim ZH and Ismail HI (2016b). A morphological study on myocardial bridges of the dromedary camel heart during prenatal development. International Journal of Advanced Research 4(1):1358-1365.

Marwa-Babiker AM, Ali HA, Ibrahim ZH and Ismail HI (2017). Histological study on prenatal purkinje fibres (PF) development in dromedary camel. Journal of Camel Research and Production.1:1-9.

Nabipour A (2004). Histology of the atrioventricular bundle in the heart of Guinea pig (*Cavia percellus*). Iranian Journal of Veterinary Research, University of Shiraz 5(2):7-13.

Nabipour A and Shahabodini MR (2007). Histological study of the atrioventricular node and bundle in the heart of ovine foetus. Iranian Journal of Veterinary Research, University of Shiraz 18(1):64-70.

Virágh S and Challice CE (1977). The development of the conduction system in the mouse embryo heart: II. Histogenesis of the atrioventricular node and bundle. Developmental Biology 56(2):397-411.

SOUTH AUSTRALIA TO CULL 10,000 CAMELS

Thousands of camels in South Australia will be shot dead from helicopters as a result of extreme heat and drought. The marksmen who will shoot the animals come from Australia's department for environment and water. A five-day cull started on Wednesday, as Aboriginal communities in the region have reported large groups of camels damaging towns and buildings. Some complain that they are roaming the streets looking for water and we are worried about the safety of the young children and others say that we have been stuck in stinking hot and uncomfortable conditions, feeling unwell, because all the camels are coming in and knocking down fences, getting in around the houses and trying to get water through air-conditioners. The slaughter will take place in the area of Anangu Pitjantjatjara Yankunytjatjara (APY) - a sparsely-populated part of South Australia which is home to a number of indigenous groups. Some feral horses will also be killed. The camel cull is not directly linked to the fires crisis but owing to ongoing dry conditions and the large camel congregations threatening all of the main APY communities and infrastructure, immediate camel control was needed.

SIX NEW SAUDI MERS CASES AS STUDY SHOWS VIRUS INFECTING BACTRIAN CAMELS

Saudi Arabia's Ministry of Health (MOH) announced 6 new MERS-CoV cases over the past 3 days, including 3 in Riyadh and 3 fatalities, and in a new research development, experimental infection tests on Bactrian camels found that they are susceptible to the virus.

To explore susceptibility in Bactrian camels, a research team based at the National Institute of Allergy and Infectious Diseases (NIAID), Rocky Mountain Laboratories in Hamilton, Montana, experimentally infected two male camels that were housed in an animal biosafety level 3 facility. They reported their findings on May 23 in Emerging Microbes and Infection.

After intranasal inoculation with MERS-CoV, the investigators collected nasal swabs from both animals on the first 5 day after inoculation, and from one of the camels at weekly intervals through the 28th day after inoculation. Both camels were euthanised, one 5 days after and one 28 days after inoculation, and the researchers examined and tested their tissues.

The animals developed mainly an upper respiratory illness, and though clinical signs were benign, the Bactrian camels shed large quantities of MERS-CoV, similar to what scientists have observed with dromedary camels, suggesting that the Bactrians are susceptible to the virus. Moreover, the virus shedding kinetics of MERS-CoV in Bactrian camels was virtually identical to previous experimental studies in dromedary camels.

(CIDRAP News | May 28, 2019)

EVIDENCE OF PESTE DES PETITS RUMINANTS' VIRUS IN DROMEDARY CAMELS IN THE KINGDOM OF SAUDI ARABIA

Infection with the Peste des petits ruminants virus (PPRV) is a highly devastating viral infection of small ruminants. Dromedary camels live in close proximity of small ruminants in Arabian Peninsula (AP) and many other regions in the world. Little is known about the reasons behind continuous PPRV emergence in Saudi Arabia (KSA). Some dromedary camel population were tested across the kingdom for the presence of specific PPRV antibodies. Our results showed detection of specific PPRV antibodies (2.92%) in sera of tested dromedary camels from the eastern and south regions of the KSA. Results suggested the exposure of dromedary camels to PPRV infection. Thus, dromedary camels may play some important roles in the sustainability of PPRV in the small ruminants across the AP.

(Veterinary Medicine International, Volume 2019, Article ID 4756404, 4 pages)

MULTIPLE SPLENIC ABSCESSATIONS IN A CAMEL: CASE REPORT

Mohamed Tharwat[1,2]

[1]Department of Veterinary Medicine, College of Agriculture and Veterinary Medicine,
Qassim University, P.O. Box 6622, Buraidah, 51452, Saudi Arabia
[2]Department of Animal Medicine, Faculty of Veterinary Medicine, Zagazig University, Zagazig, Egypt

ABSTRACT

This report describes the clinical, haematobiochemical, ultrasonographic and pathologic findings in a male Arabian camel with multiple splenic abscesses. The camel had a history of 15 days decreased appetite, weight loss and complete absence of faeces. On admission, the camel was dull and depressed, and the abdomen was mildly distended. Rectal examination revealed clean rectum and only mucous was found. Haematobiochemical abnormalities included neutrophilic leukocytosis and hyperproteinemia. Transcutaneous abdominal ultrasonography revealed distended intestines without observable gut movement. Spleen was imaged in the caudal left flank where multiple anechoic splenic masses, initially thought to be abscesses or tumours, were imaged. Transcutaneous aspiration of the masses revealed thick yellowish pus. The camel was hospitalised and scheduled for abdominal exploration and splenectomy but unfortunately, it collapsed next morning. Postmortem examination showed distended intestines but with no external or internal obstructing causes. No volvolous or intussusception was detected. The most important finding was the enlarged spleen with multiple abscesses containing thick yellowish pus. The spleen was also adhered intensively to first gastric compartment and large intestines. In the present case, clinical diagnosis was based on ultrasound examination with ultrasound-guided aspiration. It is a rare report on multifocal splenic abscessation in dromedary camels.

Key words: Abscess, camel, spleen, ultrasonography

Splenic abscesses as well as splenomegaly are the primary causes in cattle for splenic and carcass condemnations in abattoirs (Jajaa *et al*, 2018). In cattle, traumatic reticuloperitonitis caused by penetrating foreign body is the primary cause for splenic abscessation (Radostits *et al*, 2010). However, in horses, splenic abscesses are uncommon (Spier *et al*, 1986; Dart *et al*, 1987; Steel *et al*, 1998). Similarly, splenic abscesses are very rare in dogs, cats and humans (Chang *et al*, 2006; Richter, 2012; Abdellatif *et al*, 2014).

Splenic abscesses are more likely occurring secondary to conditions that compromise the spleen, such as splenic torsion and thrombosis (Tillson, 2003). An additional predisposing factor is abdominal trauma, and splenic abscess has been reported to develop weeks after the trauma event (Chun *et al*, 1980).

This report describes the clinical, hematobiochemical, ultrasonographic and pathologic findings in a male Arabian camel with multiple splenic abscesses.

Materials and Methods

A male Arabian camel was presented at the Veterinary Teaching Hospital, Qassim University, Saudi Arabia, with a history of decreased appetite, weight loss and complete absence of faeces. The camel was treated previously by different veterinarians with mineral oils, nerve and muscle tonics for possible obstruction in gastro-intestinal obstruction but with no improvement. Camel underwent a thorough clinical examination.

A complete blood count was carried out through VetScan HM5, Abaxis, California, USA. An automated biochemical analyser (VetScan VS2, Abaxis, California, USA) was used to determine the serum concentrations of total protein, albumin, globulin, calcium, creatine kinase (CK), aspartate aminotransferase (AST), and γ-glutamyl transferase (GGT).

Ultrasonographic examination was carried out in sternal recumbency using a 3.5 MHz sector transducer (SSD-500, Aloka, Tokyo, Japan). The camel was sedated using xylazine 2% (0.3 mg/kg BW IV, Alcomed, Holland). Hairs were clipped and shaved on both sides of the abdomen from the dorsal midline to *linea alba*. After the application of transmission gel to the transducer, the camel was examined starting from the caudal abdomen and extending forward on both sides of the abdomen. The

abdominal viscera including the compartment 1, 2, 3, peritoneum, small and large intestines, kidneys and spleen were imaged (Tharwat *et al*, 2012a,b,c; Tharwat *et al*, 2013; 2018a,b). The camel collapsed 12h after admission and thorough postmortem examination was then carried out.

Results

On clinical examination the camel was dull and depressed, and the abdomen was mildly distended (Fig 1). Rectal examination revealed mucous in the rectum.

Haematological examination revealed haematocrit 24.9% (reference range 28.9±2.7%), RBCs 10.34×10^6/μL (reference range 11.3±1.4×10^6/μL), haemoglobin 15.9 g/dL (reference range 16.0±2.3 g/dL), MCV 24 fl (reference range 25.5±1.5 fl), MCH 15.2 pg (reference range 14.7±2.4 pg), MCHC 63.8 g/dL (reference range 57.6±9.0 g/dL),

Fig 1. A male dromedary camel with splenic abscessation showed dullness, depression and complete absence of faeces for the past 15 days.
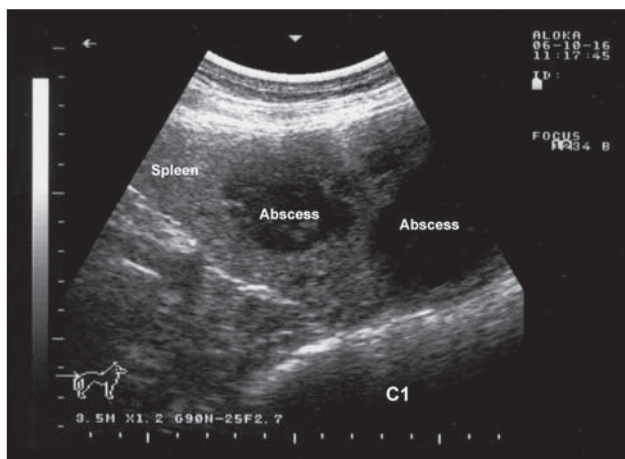
Fig 2. Ultrasonographic findings in a male camel with splenic abscesses. Images were taken from the left caudal flank showing multiple anechoic masses within the splenic parenchyma. C1; compartment 1.

white blood cell count 46570/μL (reference range 16.9±2.7×10^9/L), neutrophils 42950 /μL (reference range 9.8±3.0×109/L), and lymphocytes 2700 /μL (reference range 5.9±2.4×10^9/L). Blood chemistry profile showed total protein 9.4 g/dL (reference range 7.9±0.4 g/dL), albumin 4.6 g/dL (reference range 4.2±0.4 g/dL), globulin 4.8 g/dL (reference range 3.7±0.5 g/dL), CK 413 U/L (reference range 139±22 U/L), calcium 10.4 mg/dL (reference range 8.6±0.7 mg/dL), AST 272 U/L (reference range 69±44 U/L), GGT 149 U/L (reference range 12±5.0 U/L). Reference haematological and serum chemistry values were taken from Tharwat *et al* (2013) and Tharwat (2015).

Transcutaneous abdominal ultrasonographic examination showed distended intestines (right lower abdomen) with no observable gut movement. Spleen was imaged in the caudal left flank where multiple anechoic splenic nodules were detected (Fig 2). Splenic nodules were thought to be abscesses or tumours. Transcutaneous aspiration of the masses using a 14 gauge 15 cm length needle revealed thick yellowish pus.

Postmortem examination showed enlarged spleen with multiple abscesses containing thick yellowish pus (Fig 3). The spleen was also adhered intensively to the impacted compartment 1 and large intestines.

Discussion

Reports of splenic abscesses are very rare in the veterinary literature. In humans, splenic abscesses are uncommon with a reported frequency of 0.14– 0.7% in post-mortem studies (Chun *et al*, 1980). However, this uncommon disease has been recently reported more frequently because of advances in imaging modalities
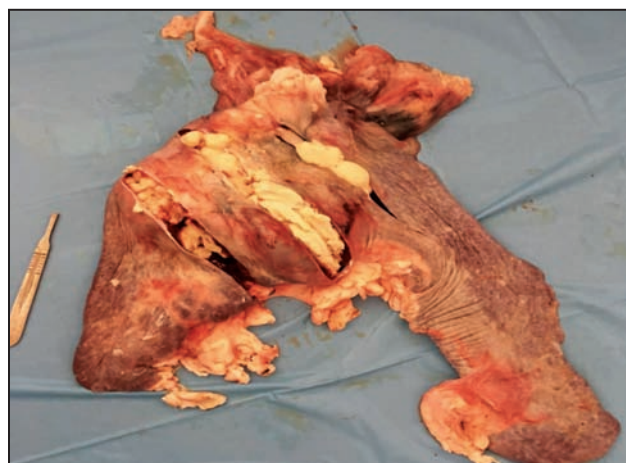
Fig 3. Post mortem findings revealed multifocal splenic abscesses which contained thick pus.

and increasing numbers of immunocompromised and cancer patients (Chang *et al,* 2006).

Clinical signs in the camel were observed 15 days earlier, and included depression, decreased appetite, weight loss, mild abdominal distension and complete absence of faeces. Fever, anorexia, and lethargy were observed in a dog with splenic abscess and septic peritonitis (Abdellatif *et al,* 2014); while in a horse the clinical signs observed were lethargy, weight loss and intermittent pyrexia and animal was treated successfully (Steel *et al,* 1998).

The blood picture and serum chemistry panel in the present case provided little aid in obtaining a diagnosis of splenic abscesses. Leukocytosis, as found in our case, is the most frequently observed laboratory finding in patients with splenic abscess (Faught *et al,* 1989; Kumar *et al,* 2011).

The clinical presentation of splenic abscess is nonspecific (Chun *et al,* 1980). The vague symptoms of this disease make diagnostic imaging studies very useful (Chiang *et al,* 2003). Splenic ultrasonography of the present case report showed multiple anechoic masses suggestive of abscesses or tumours. Lymphosarcoma or haematomas have a similar ultrasonographic appearance in horses (Spier *et al,* 1986; Chaffin *et al,* 1992).

References

Abdellatif A, Günther C, Peppler C and Kramer M (2014). A rare case of splenic abscess with septic peritonitis in a German shepherd dog. BMC Veterinary Research 10:201

Chaffin MK, Schmitz DG, Brumbaugh GW and Hall DG (1992). Ultrasonographic characteristics of splenic and hepatic lymphosarcoma in three horses. Journal of the American Veterinary Medical Association 201:743-747.

Chang KC, Chuah SK, Changchien CS, Tsai TL, Lu SN, Chiu YC, Chen YS, Wang CC, Lin JW, Lee CM and Hu TH (2006). Clinical characteristics and prognostic factors of splenic abscess: a review of 67 cases in a single medical center of Taiwan. World Journal of Gastroenterology 12:460-464.

Chiang IS, Lin T-J, Chiang IC and Tsai M-S (2003). Splenic abscesses: review of 29 cases. The Kaohsiung Journal of Medical Sciences 19:510–514.

Chun CHRM, Contreras L, Varghese R, Waterman N, Daffner R and Melo JC (1980). Splenic abscess. Medicine (Baltimore) 59:50-56.

Dart AJ, Hutchins DR and Begg AP (1987). Suppurative splenitis and peritonitis in a horse after gastric ulceration caused by larvae of *Gasterophilus intestinalis.* Australian Veterinary Journal 64:155-158.

Faught WE, Gilbertson JJ and Nelson EW (1989). Splenic abscess: presentation, treatment options, and results. American Journal of Surgery 158(6):612-614.

Ginel P, Lucena R, Arola J, Martin M and Mozos E (2001). Diffuse splenomegaly caused by splenic abscessation in a dog. Veterinary Record 149:327-329.

Jajaa Ishmael Festus, Mushongab Borden, Greencd Ezekiel and Muchenjea Voster (2018).Factors responsible for the post-slaughter loss of carcass and offal's in abattoirs in South Africa. Acta Tropica 178:303-310.

Köhler-Rollefson, I, Mundy, P and Mathias, E (2001). Managing and treating camels. In; A Field Manual of Camel Diseases: Traditional and Modern Healthcare for the Dromedary. ITDG publishing, London. pp 1-67.

Kumar A, Kashyap B and Gupta P (2011). Staphylococcal splenic abscess in a septicaemic pediatric patient. Annals of Tropical Medicine and Public Health 4:116-118.

Ooi LL and Leong SS (1997). Splenic abscesses from 1987 to 1995. American Journal of Surgery 174:87–93.

Radostits OM, Gay CC, Hinchcliff KW and Constable PD (2010). Veterinary Medicine. A Textbook of the Diseases of Cattle, Horses, Sheep, Pigs, and Goats, 10th ed. Saunders Elsevier, Philadelphia.

Richter MC (2012). Spleen. In Veterinary Surgery: Small Animal. 2nd edition. Edited by Tobias KM, Johnston SA. Canada: Elsevier Science and Saunders. pp 1341-1352.

Sangchan A, Mootsikapun P and Mairiang P (2003). Splenic abscess: clinical features, microbiologic finding, treatment and outcome. Journal of the Medical Association of Thailand 86:436-441.

Schulz B, Hrovat A, Neuerer F, Murgia D, Boos H, Hirschberger J and Hartmann K (2006). Splenic abscess in a dog. A case report. Tierärztliche Praxis Ausgabe G Grosstiere Nutztiere 34:260.

Spier S, Carlson GP, Nyland TG, Snyder JR and Fischer PE (1986). Splenic haematoma and abscess as a cause of chronic weight loss in a horse. Journal of the American Veterinary Medical Association 189:557-559.

Steel CM, Lonsdale RA and Bolton JR (1998). Successful medical treatment of splenic abscesses in a horse. Australian Veterinary Journal 76:541-542.

Tharwat M, Al-Sobayil F, Ali A and Buczinski S (2012a). Transabdominal ultrasonographic appearance of the gastrointestinal viscera of healthy camels (*Camelus dromedarius*). Research in Veterinary Science 93:1015–1020.

Tharwat M, Al-Sobayil F, Ali A and Buczinski S (2012b). Ultrasonographic evaluation of abdominal distension in 52 camels (*Camelus dromedarius*). Research in Veterinary Science 93:448-456.

Tharwat M, Al-Sobayil F, Ali A and Buczinski S (2012c). Ultrasonography of the liver and kidneys of healthy camels (*Camelus dromedarius*). Canadian Veterinary Journal 53:1273–1278.

Tharwat M, Al-Sobayil F and El-Magawry S (2013). Clinicobiochemical and postmortem investigations in 60 Camels (*Camelus dromedarius*) with Johne's disease. Journal of Camel Practice and Research 20:145-149.

Tharwat M (2015). Hematology, biochemistry and blood gas analysis in healthy female dromedary camels, their calves and umbilical cord blood at spontaneous parturition. Journal of Camel Practice and Research 22:239-245.

Tharwat M, Sadan M, El-shafaey, El-hassan saeed E and Al-hawas A (2018a) Bilateral renal abscessation and chronic active pyelonephritis in a male camel (*Camelus dromedarius*) caused by *Escherichia coli*. Journal of Veterinary Medical Science 80:778-783.

Tharwat M, Sadan M, El-Shafaey E, Al-Hawas A and Saeed EMA (2018b) Unilateral nephrectomy in a female dromedary camel with pyelonephritis caused by *Staphylococcus lugdunensis*. Pakistan Veterinary Journal. 38:116-118.

Tillson DM (2003). Spleen. In (Slatter DH) Textbook of Small Animal Surgery. Volume 2. 1st ed USA: Elsevier Health Sciences. pp 1051.

Tung CC, Chen FC and Lo CJ (2006). Splenic abscess: an easily overlooked disease? The American Surgeon 72:322–325.

OVARIAN NEOPLASMS IN DROMEDARY CAMEL: PREVALENCE, TYPES AND PATHOLOGY

M.O. Elshazly, Sahar S. Abd El-Rahman, Dalia A Hamza[1] and Merhan E. Ali

Department of Pathology, Faculty of Veterinary Medicine, Cairo University, Egypt
[1]Department of Zoonosis, Faculty of Veterinary Medicine, Cairo University, Egypt

ABSTRACT

The objective of this study was to investigate the incidence of ovarian tumours in camels and to identify their common types. A total of 500 non-pregnant dromedary camels' ovaries aged between 6-15 years old were collected from Giza abattoirs during the period of January 2016 to January 2018 and were examined for the presence of any neoplasm. Tissue specimens were taken from all of the collected ovaries for histopathological examination. A total of 34 (6.8%) camels were found with neoplastic lesions included; papillary cystadenoma (0.6%), fibroadenoma (0.2%), granulosa cell tumour (1.2 %), luteoma (0.8%), thecoma and luteinised thecoma (0.4%), fibrothecoma (0.4%), teratoma (2%), fibroma (1.6%), cavernous haemangioma (0.4%) and mixed tumours (0.6%). In conclusion, teratoma was the most common type of ovarian tumour followed by granulosa cell tumour, luteoma, fibroma, cavernous haemangioma, fibrothecoma, thecoma and luteinised thecoma, while fibroadenoma was the least observed neoplasm.

Key words: Dromedary camel, histopathology, neoplasms, ovary

The ovaries in dromedary camels are paired sex glands or gonads in female and are important organs concerned with germ cell maturation, storage and its release. The ovaries are also concerned with steroidogenesis which is very rigorous for normal ovarian processes, such as follicle growth, maturation of oocyte, and ovulation. In contrast, altered steroidogenesis as a result of any neoplastic reaction can lead to profound ovarian pathology. Ovarian tumours are a group of neoplasms affecting the ovary and having a diverse spectrum of features according to the particular tumour entity. Ovarian tumours are subdivided into three main categories; epithelial tumours, sex cord stromal tumours and germ cell tumours (Moulton, 1978; Kennedy *et al*, 1998). Teratomas considered the most reported type of ovarian tumours (Tibary and Anouassi, 2000). Dysgerminoma has been reported, but it is extremely rare (El-Khouly *et al*, 1990). Granulosa cell tumours (GCTs) were also recognised in camel (Ali *et al*, 2013). Hence, the purpose of the present study was to findout prevalence, types and histopathological details of ovarian neoplasms.

Materials and Methods

Examination procedures and sampling

The ovaries of 500 adult non-pregnant she-camels aged between 6- 15 years old slaughtered in different abattoirs in Egypt (El-Monib, Kerdasa and El-basateen) were collected during the period from January 2016 to January 2018 and examined. Previous reproductive history of these slaughtered animals was not available. Thorough macroscopic examination was carried out to all of the collected ovaries and any abnormal swelling was recorded.

Histopathological examination

Part of each ovarian tissue as well as any suspected neoplastic swelling was fixed in 10% buffered neutral formalin for histopathological examination. A routine processing for the formalin fixed specimens was carried out. Sections of 3µm thickness were stained with haematoxylin and eosin (H&E) according to Bancroft and Gamble (2008). The obtained sections were examined using electric light microscope, Olympus BH2 (Tokyo, Japan). Special stains were used i.e., Massons' Trichrome and Von Kossa stains where ever required (Bancroft and Gamble, 2008).

Results and Discussion

The overall incidence of ovarian tumours observed in she-camels was (34/500; 6.8 %) (Table 1). The most prevalent neoplasm was teratoma and the least observed one was adenofibroma (Fig 1).

Gross and histopathological findings:

According to the histopathological criteria, ovarian tumours were classified into 4 broad

categories, i.e. surface epithelial tumours, sex cord-stromal tumours, tumours of germ cells and tumours developed from non-gonadal supporting tissue of the ovary (mesenchymal and mixed tumours) (Table 1).

Papillary cystadenoma

Unilateral papillary cystadenoma was diagnosed microscopically in ovaries of 3 camels (0.6%), grossly one of them had small ovoid mass with cystic appearance on cut section, while the other showed the usual irregular appearance of the ovary. However, the 3rd one was accompanied with fibroma and teratoma. It was characterised by presence of papillary protrusions extended from the ovarian surface into the lumen; those protrusions were covered by low cuboidal to columnar ciliated epithelium, with stratification in some areas (Fig 2a), rested on vascular fibrous stroma. Adenomatous arrangement with cyst formation was a conspicuous finding (Fig 2b). Focal areas of calcification were noticed in one case of mucinous type.

Fibroadenoma

It was observed in one case (0.2%) and was detected only on microscopic examination. The neoplastic mass was composed of glandular structures of variable shapes and sizes surrounded by proliferated fibrous stroma that stained positively with Massons' Trichrome stain (Fig 2c).

Granulosa cell tumour

It was observed in 6 cases (1.2%). Grossly, unilateral swellings were observed in the affected ovaries, 4 of which were on the right and 2 were on the left ovary. The largest tumour mass measured was 5.8 cm in length× 3.1 cm in width (Fig 2d), while the smallest one was 2.6 cm in length and 1.6 cm in width. The cut section of the neoplastic masses in 2 cases appeared cystic. Microscopically, the neoplastic mass consisted of marked proliferation of granulosa cells that appeared with scant cytoplasm, round to oval hyperchromatic nuclei and irregular nuclear contour. Mitotic figures were common finding in one case. The neoplastic cells attempted to mimic the normal Graafian follicles but with variable histological arrangements, either as single or multiple rows of round to columnar cells lining fluid filled spaces. Sometimes, they tended to form nests with cystic Call-Exner bodies which appeared gland-like or rosette patterns of abortive follicles, few of which contained secretory globule resembling an ovum (Fig 2e). Juvenile type of granulosa cell tumour (Fig 2f) was observed in two cases, it was characterised

Table 1. The types and percentage of the detected ovarian tumours of camels.

Type of ovarian tumour	Number of lesions	Percentage from examined cases (500)	Percentage from neoplastic cases (34)
Surface epithelial tumour			
Papillary cystadenoma	3	0.6%	8.88%
Fibroadenoma	1	0.2%	2.94%
Sex cord stromal tumour (SCST)			
Granulosa cell tumour	6	1.2%	17.64%
Luteoma	4	0.8%	11.76%
Typical thecoma and Luteinised thecoma	2	0.4%	5.88%
Ovarian fibrothecoma	2	0.4%	5..88%
Germ cell tumour			
Ovarian teratoma	10	2%	29.41%
Mesenchymal tumour			
Ovarian fibroma	8	1.6%	23.52%
Ovarian haemangioma	2	0.4%	5.88 %
Mixed tumour			
Papillary cystadenoma, fibroma and teratoma	1	0.2%	2.94%
Fibroma and granulosea cell tumour.	2	0.4%	5.88%
Total number of lesions	41	8.2	120.58%
Total number of cases	34	6.8	100%

N.B: more than one lesion may be found in one case
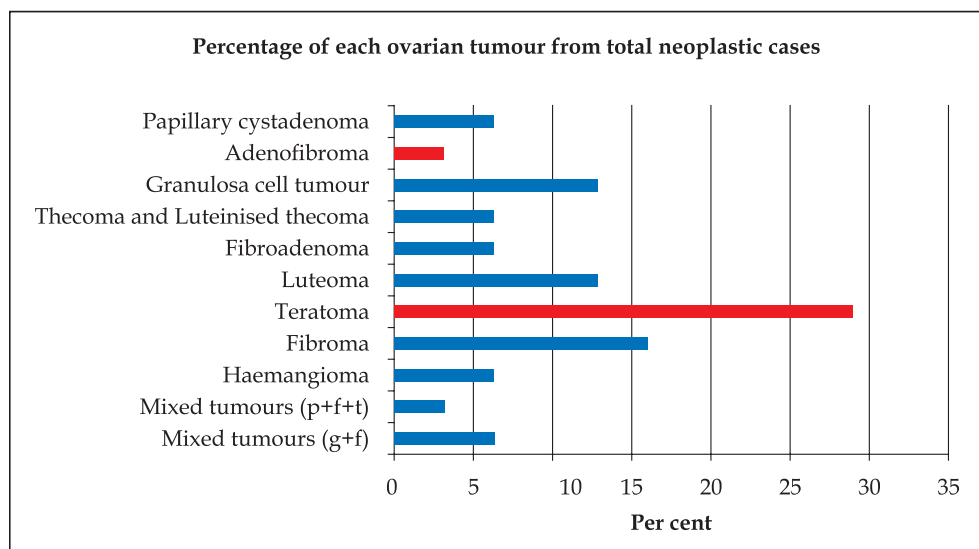
Fig 1. The percentage of each ovarian tumour in relation to the other detected ones (p: papillary cystadenoma, f: fibroma, t:teratoma, g:granulosa cell tumour).

by appearance of diffuse or macrofollicular patterns (Fig 3a) with microcysts formation containing eosinophilic secretions, where tumour cells either had scant cytoplasm or were luteinised. Two cases were accompanied by fibroma.

Ovarian luteoma

It was observed in 4 ovaries (0.8%). Stromal luteomas appeared unilateral, well circumscribed solid masses, and gray-white or a bit yellowish, about 1-3 cm in diameter (Fig 3b). Histologically, it consisted of sharply circumscribed round masses of polygonal cells with vacuolar cytoplasm (granulosa lutein cells) (Fig 3c), round vesicular nuclei, variably prominent nucleoli with mild nuclear atypia. In 1 case the neoplastic cells showed marked pleomorphism and cellular atypia (Fig 3d). An increased vascularisation was apparent with presence of newly formed blood capillaries and haemolysed blood. Areas of cellular degeneration and necrosis were apparent.

Typical thecoma and luteinised thecoma

It was observed in 2 cases (0.4%). The tumour appeared small having a firm encapsulated mass 1-2 cm in diameter which was yellowish on cut section. Microscopically, Thecoma composed of spindle cells with oval or spindle nuclei and abundant pale vacuolated cytoplasm, while luteinised thecoma, revealed nests of lutein cells on a background of spindle cells (Figs 3e and f).

Fibrothecoma

It was noticed in 2 cases (0.4%), the tumour mass was unilateral solid, mostly rounded and surrounded by thick firm consistent wall with a size of 1cm in diameter. Microscopically, the tumour mass showed hypercellularity with an obvious two cellular patterns (Fig 4a); one belongs to fibroma that consisted of spindle-shaped cells with elongated nuclei in a fibro-collagenous stroma, while the other was for thecoma and was composed of round to oval and spindle shaped cells without any features of atypia or myxoid change. No mitotic figures were observed.

Benign mature cystic teratoma (Dermoid cyst)

It was observed in 10 cases (2%). Grossly, most of these cysts were rounded to ovoid, ranged from 2-5 cm in diameter, one of them was irregular of 4.8 cm in length × 1.9 cm in width (Fig 4b), another one appeared doubled on two sides and separated by a septum (Fig 4c). All of them were surrounded by thick firm wall that enclosing a cavity filled with totipotential tissues such as hair and bone admixed with viscous material (Fig 4d). Histologically, the cavity of the teratoma was lined by keratinised stratified squamous epithelium (Fig 4e), under which there was a fibrous connective tissue containing hair follicles (Fig 4f), sweat and sebaceous glands in 4 cases. In the 5th case, the cyst cavity contained nervous tissue (Fig 5a) associated with osteoid tissue while in the 6th case glandular tissue was detected (Fig 5b), and in another two cases, myxomatous and hyalinised stroma were associated with osteoid tissue, bone marrow, cartilage, muscles and fat (Figs 5c and d), areas of calcification were noticed in one of them, which stained positive with Von Kossa stain (Fig 5e). Ganglionic tissue (Fig 5f) was
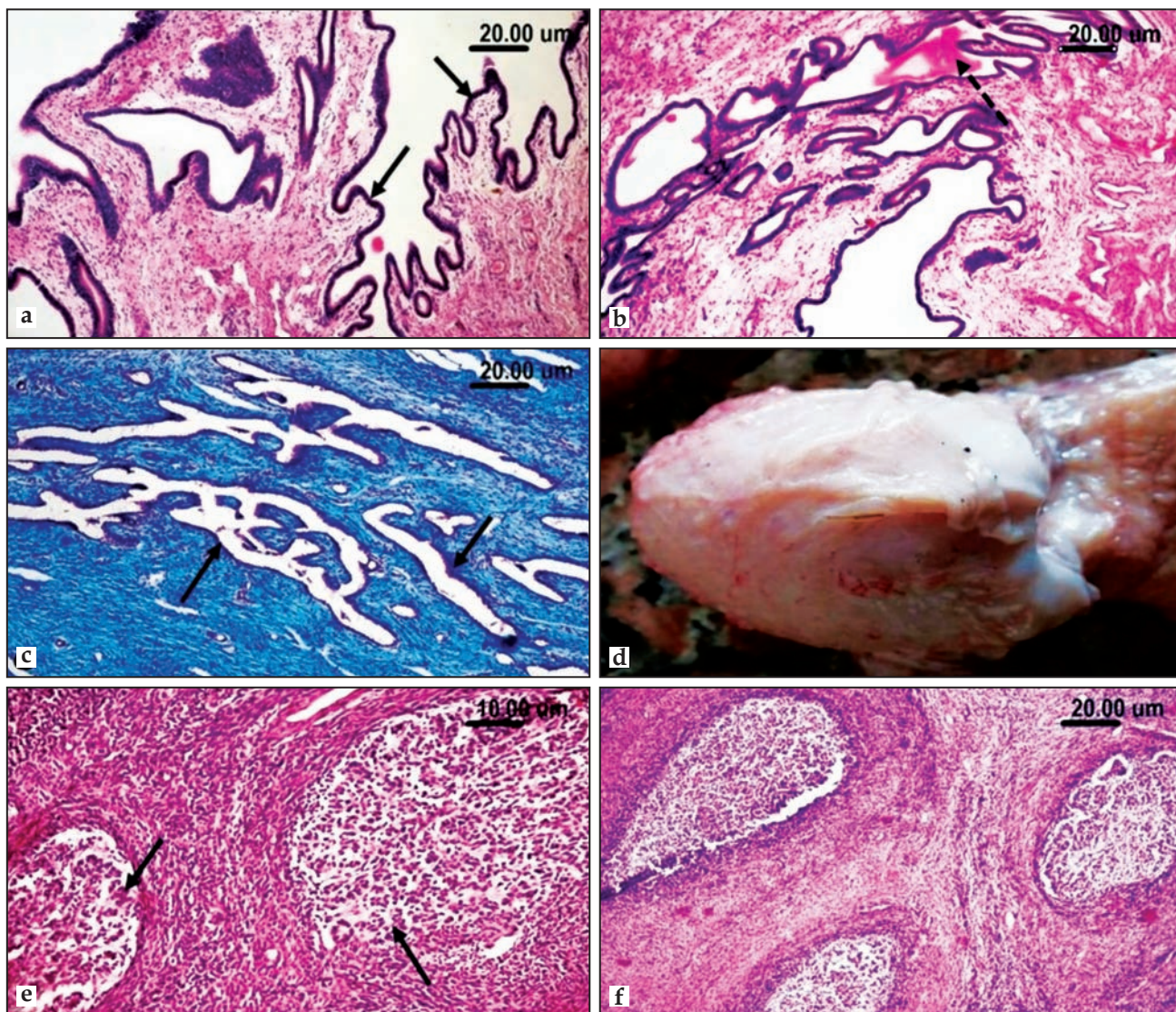
Fig 2. Ovarian sections of she-camels showing; (**a**) Papillary cyst adenoma revealing irregular papillary protrusions (arrow) extended from the ovarian surface into the lumen and (**b**) adenomatous arrangement with cyst formation (dashed arrow). (**c**) Fibroadenoma composed of glandular structures (arrow) of variable shapes and sizes surrounded by proliferated fibrous stroma (MTC stain). (**d**) Gross mass of granulosa cell tumour, (**e**) Call-Exner bodies (arrow) in the granulosa cell tumour appearing gland-like or rosette patterns of abortive follicles. (**f**) Juvenile type of granulose cell tumour. (H&E)

observed in 1 case in association with osteoid tissue while the last case was accompanied with fibroma and papillary cystadenoma.

Ovarian fibroma

It was observed in 8 cases (1.6%). The ovarian fibromas appeared as hard, whitish rounded to slightly ovoid masses ranged from 1 to 3 cm in diameter (Fig 6a). Histologically, the neoplasms consisted of bundles of fibroblasts and collagen running in different directions but usually form whorls around the blood vessels in the vicinity. In 2 cases, it was more collagenous. All fibromas reacted positively with Massons' Trichrome stain (Figs 6b and

c). Three cases of them were accompanied by other types of tumour, one was associated with teratoma and papillary cystadenoma and the others were associated with granulosa cell tumour.

Cavernous haemangioma

Two cases of cavernous haemangioma (0.4%) were noticed among the examined she-camels' ovaries. The neoplasm was mushy brown mass on the surface of the affected ovary, one was about 1 cm in diameter and the other was about 2.3 cm. Microscopic examination revealed numerous thin-walled blood-filled spaces of different sizes, separated by fibrous connective tissue septa (Fig 6d).
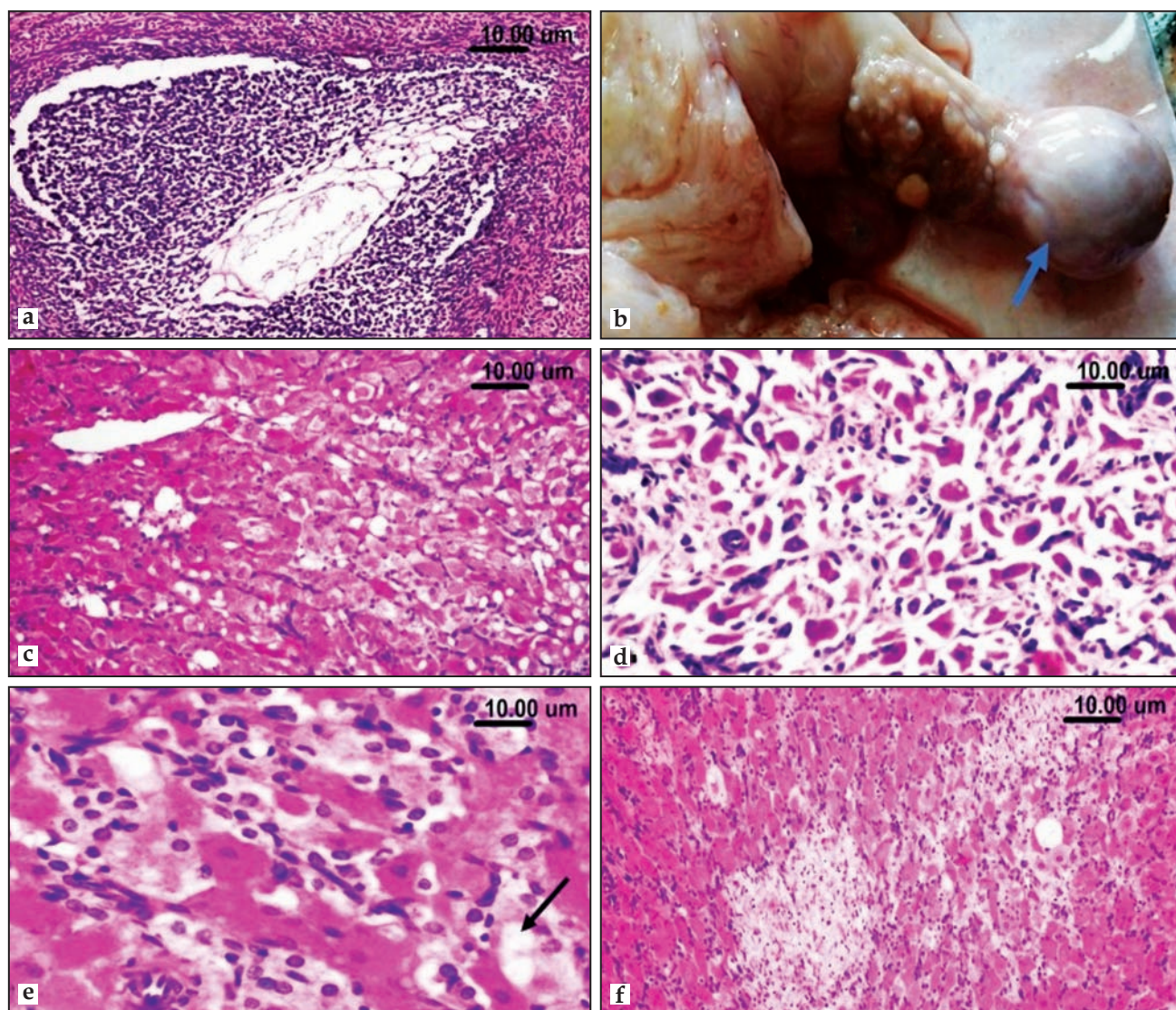
Fig 3. Ovaries of she-camels showing; (**a**) Granulosa cell tumour with diffuse or macrofollicular patterns. (**b-d**) Luteoma; rounded well circumscribed solid grayish white mass (arrow) composed of masses of polygonal cells with vacuolar cytoplasm (**c**) and sometimes marked pleomorphism with cellular atypia of the neoplastic cells (**d**). (**e**) Thecoma; tumour cells have abundant dense vacoulated cytoplasm (arrow). (**f**) Luteinised thecoma showing cluster of luteinised cells is present with in fibromatous tissue. (H&E).

Mixed tumours

Three cases showed presence of more than one type of the previously mentioned tumours in the same ovary; one of them revealed presence of papillary cystadenoma, fibroma and teratoma (Fig 6e), while the other 2 cases revealed presence of fibroma and granulose cell tumour (Fig 6f).

Reproductive disorders in she-camel are rapidly becoming a major part of the veterinary care provided to the Camelidae especially when dealing with genetically superior animals. The incidence and pathology of the genital tract affections of she-camel could provide valuable information which can be used in evaluation of animal reproductivity. In the persent study, ovarian tumours represented (6.8%) A lower percent (0.87%) was noticed by Simenew *et al* (2015) and included; papillary cystadenoma (0.6%), fibroadenoma (0.2%), granulosa cell tumour (1.2%), luteoma (0.8%), thecoma and luteinised thecoma (0.4%), fibrothecoma (0.4%), teratoma (2%), fibroma (1.6%), cavernous haemangioma (0.4%) and mixed tumours (0.6%).

Papillary cystadenoma was observed in 3 cases (0.6%), which agreed with Wajid (2015) who recorded (1.25%) in one case. While, granulosa cell tumour (GCT) was observed in 6 cases (1.2%). It
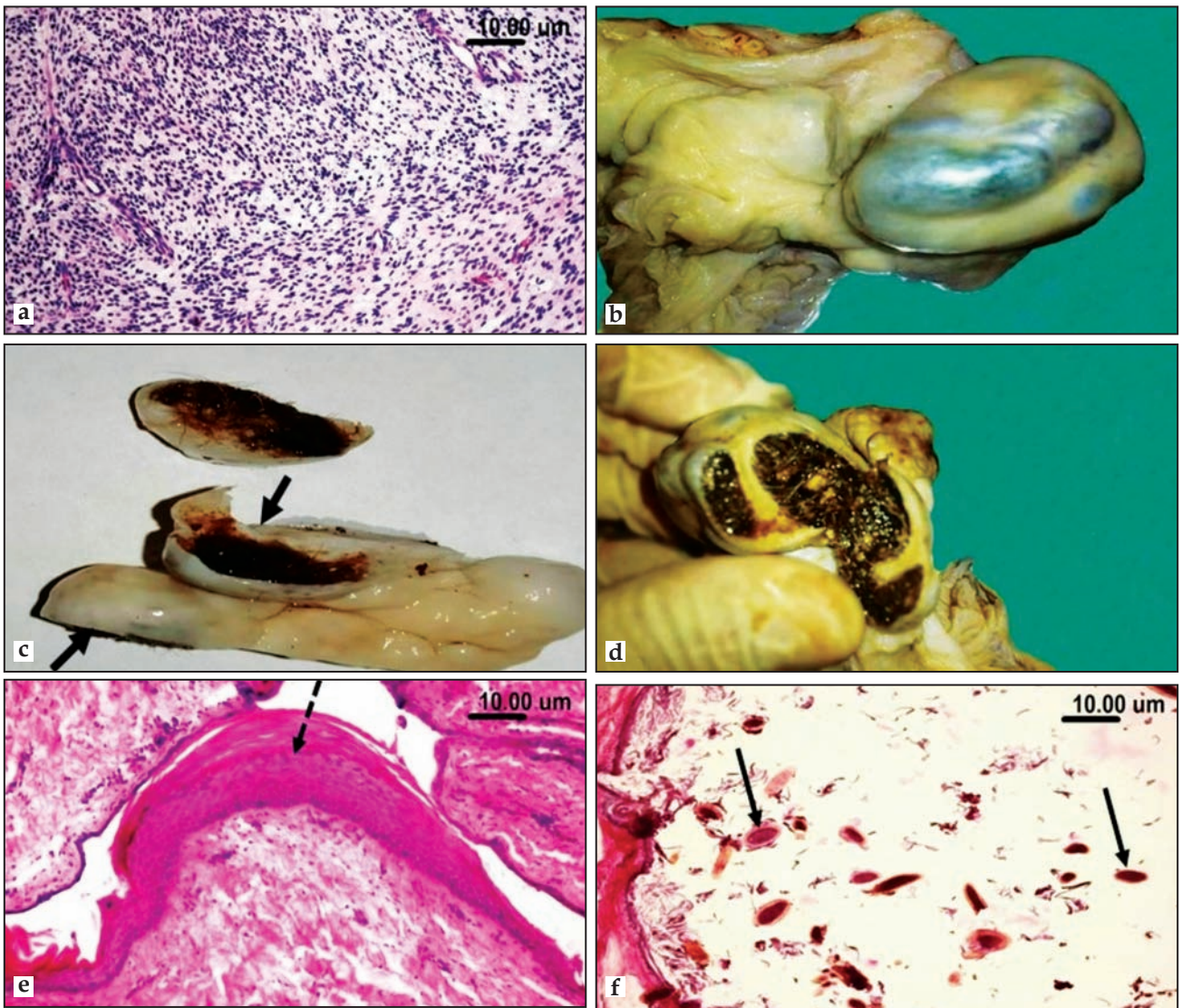
Fig 4. Ovary of she camels showing; (**a**) Fibrothecoma composed of two cellular patterns belongs to both fibroma and thecoma. (**b-f**) Teratoma; large irregular mass on the ovarian surface (**b**), Doubled cysts separated by a septum containing hair and bone (**c**), Totipotential tissues such as hair and bone admixed with viscous material (**d**), Stratified squamous epithelium (dashed arrow) (**e**) and Hair follicles (arrow) underlying the fibrous connective tissue (**f**).

was firstly described in she-camels by Ali *et al* (2013) and Alsobayil *et al* 2018. Fibroadenoma was noted only in one case (0.2%). Granulosa cell tumours are considered as sex cord-gonadal stromal tumours or the non-epithelial tumour group, arise from granulosa cells. Adult granulosa cell tumours are well known as hormonally active (Koukourakis *et al,* 2008; Schumer and Cannistra, 2003). GCTs have occasionally occurred in horses and cattle but are rarely malignant (Crabtree, 2011; Pérez-Martínez *et al,* 2004).

The ovarian luteoma was detected in 4 cases (0.8%), firstly reported in camels in the persent study. Luteoma was previously recorded in cow, bitch and cat (McEntee, 1990). Young (2011)

stated that stromal luteomas occur mostly (80%) in postmenopausal women. Numanoglu *et al* (2014) added that it was also accompanied with hyperestrogenic state and was confirmed with hyperplasia of endometrium. Concerning thecoma and luteinised thecoma, both were observed 0.4% in our study. Thecoma have also been reported in cow, bitch and sow (McEntee, 1990).

Fibrothecoma was detected in present study (0.4%), it was reported in cow (Soleimanzadeh *et al,* 2017). Based on an ultrastructural study, Amin *et al* (1971) reported that the ovarian fibroma and thecoma are variants of single neoplasm with a common origin from the ovarian stroma.
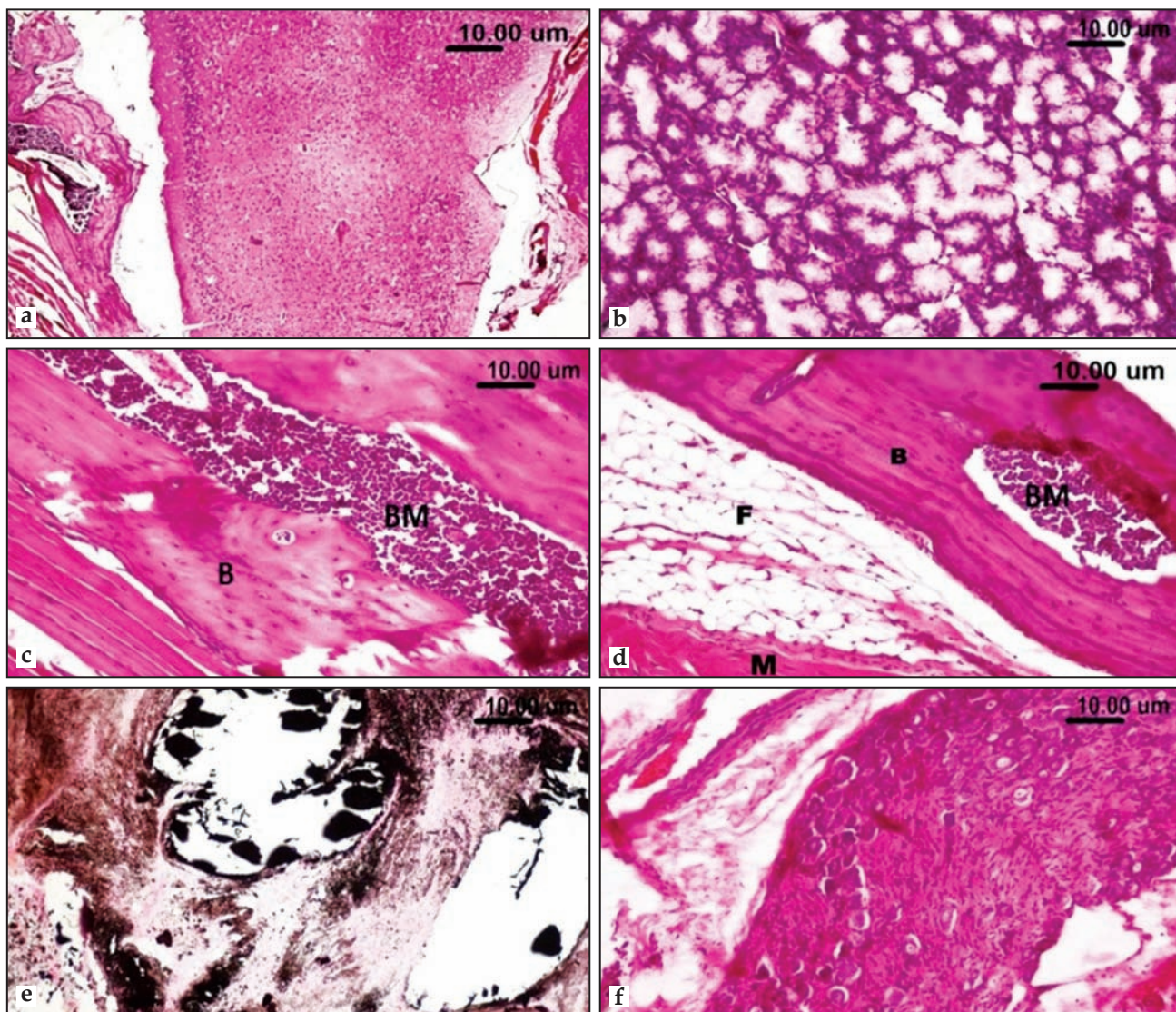
Fig 5. Ovary teratomas of different she-camels showing; (**a**) Nervous tissue, (**b**) Glandular tissue, (**c** and **d**) Bony tissue (B) Admixed with bone marrow (BM), Cartilage, muscles (M) and Fat (F), (**e**) Areas of calcification stained positive with Von Kossa stain, and ganglionic tissue (**f**).

It has been documented that germ cell tumour (teratoma) are the most common camel tumour (Tibary and Anouassi, 2000). As judged by our work, Benign cystic ovarian teratomas were detected with an incidence of 2 % of all cases examined. These are believed to originate as congenital developmental anomalies involving a single somatic cell layer (AL-Afaleq *et al*, 2012). The incidence of teratomas in camels was found to be 0.99, 0.29, 0.4, 0.67, 0.16, 0.17 and 1.4% in the previous investigations (Nawito *et al*, 1967; Omar *et al*, 1984, El-Wishy, 1989; Fetaih, 1991; Heikal, 1999; Hamouda *et al*, 2011; Benaissa *et al,* 2015, respectively).

The histopathological findings of the examined dermoid cysts in this investigation were similar to those described in other animal species (Jubb *et al*, 1993). The observed teratomas were of a dermoid cyst type with more or less the same histological structure reported by El-Khouly *et al* (1991) and Mesbah *et al* (2002) in camel's ovary. It was benign and didn't have any effect on follicular activity on the contralateral ovary. In present investigation, occurrence of ovarian fibroma was 1.6%. The result was in agreement with Al-Afaleq *et al* (2012) who found fibroma in she-camel (0.71%) in Saudi Arabia.

Two cases of cavernous haemangioma (0.4%) were detected in present study, which is nearly similar to Al-Afaleq *et al* (2012) (0.18%) in Saudi Arabia. Histogenesis of haemangioma remains obscure but it is suggested to arise from the blood
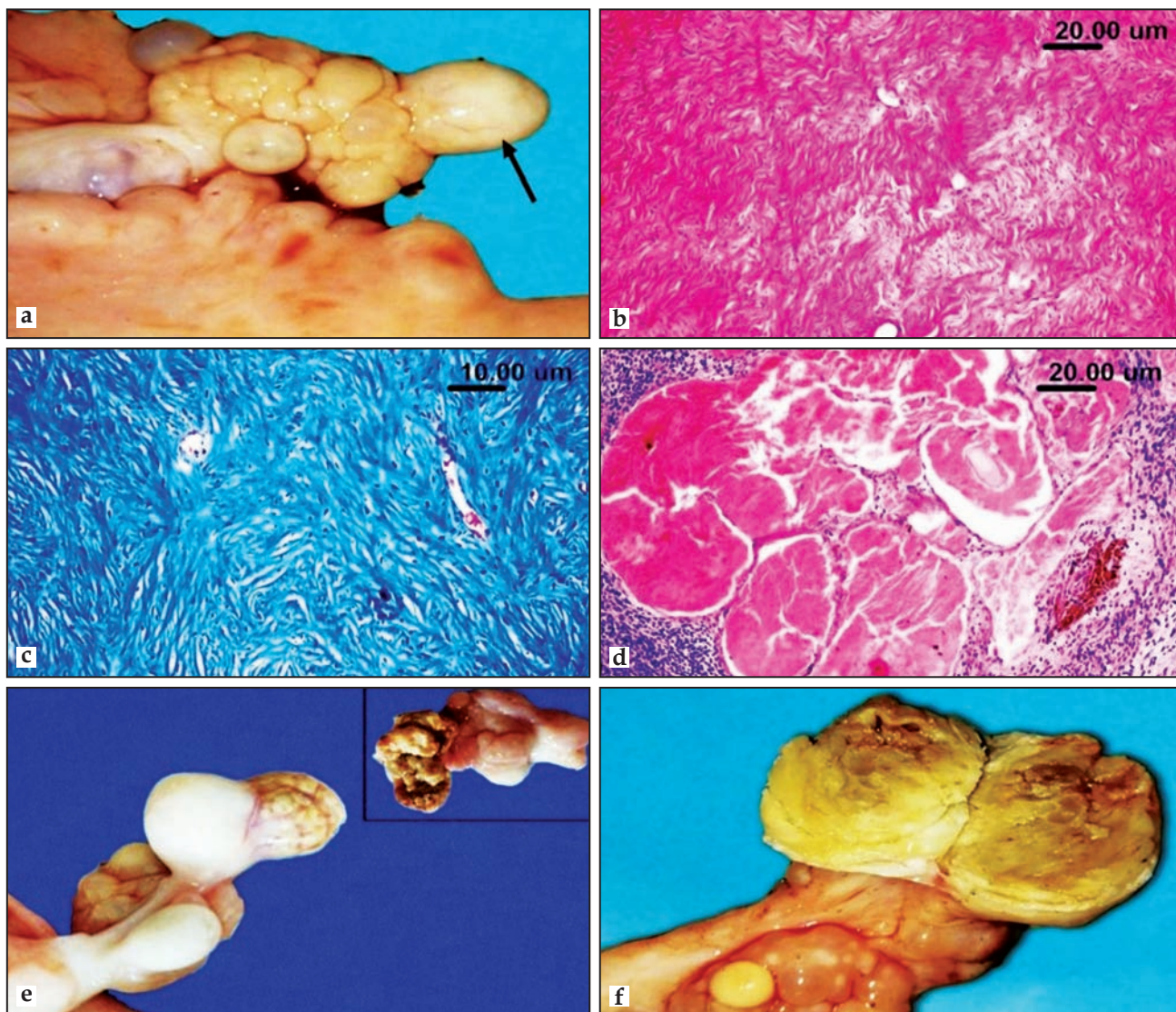
Fig 6. Ovaries of she camels showing; (**a-c**) Fibroma; hard, whitish ovoid mass on the ovarian surface, that is formed of wavy bundles of fibroblasts and collagen running in different directions (**b**) and Positively stained with Massons' Trichrome stain (**c**). (**d**) Cavernous haemangioma showing numerous thin-walled blood-filled spaces of various sizes and separated by fibrous septa. (**e**) Mixed tumour of papillary cystadenoma, fibroma and teratoma. (**f**) Mixed tumour of fibroma and granulosa cell tumour.

vessels of the corpus luteum (Hsu, 1983). Some authors believed that it was a true primary pure ovarian mesenchymal neoplasm or a part of mature teratoma. Others stated that the haemangiomas were hamartomatous malformation but not neoplastic lesions. The formation of this lesion may be stimulated by some factors, such as hormones, pregnancy, or infection (Bolat *et al,* 2010).

In conclusion, the persent study demonstrated the usefulness of morpho-pathological examination to determine the characteristics of each tumour. Additionally, ovarian tumours originating from germ cell are the most common variant represented by ovarian teratoma followed by ovarian fibroma,

granulosa cell tumour and luteoma followed by papillary cystadenoma then cavernous haemangioma, fibrothecoma, thecoma and luteinised thecoma and finally adenofibroma.

References

Al-Afaleq AI, Hegazy AA, Hussein MF *et al,* (2012). Pathological disorders of the female reproductive system in slaughtered camels (*Camelus dromedarius*) in Saudi Arabia. Comparative Clinical Pathology 21:245-251.

Alsobayil FA, Ali A, Derar DR, Tharwat M, Ahmed AF and Khodeir M (2018). Tumours in dromedary camels: prevalence, types and locations. Journal of Camel Practice and Research 25(2):189-197.

Ali A, Al-Sobayil FA, Tharwat M, Mehana EE and Al-Hawas

A (2013). Granulosa cell tumour in a female dromedary camel. Comparative Clinical Pathology 22:1251-1254.

Amin HK, Okagaki T and Richart RM (1971). Classification of fibroma and thecoma of the ovary. Cancer (Philadelphia) 27:438-446.

Bancroft JD and Gamble M (2008). Theory and Practice of Histological Techniques. 6th ed. Churchill Livingstone, China: Elsevier.

Benaissa MH, Faye B and Kaidi R (2015). Reproductive abnormalities in female camel (*Camelus dromedarius*) in Algeria: Relationship with age, season, breed and body condition score. Journal of Camel Practice and Research 22(1):67-73.

Bolat F, Erkanli S and Kocer NE (2010). Ovarian haemangioma: Report of 2 cases and review of the literature. Turk PatolojiDerg 26(3):264-266.

Crabtree J (2011). Review of 7 cases of granulosa cell tumour of the equine ovary. Veterinary Record 169(10):251.

El Khouly AA, Gadar FA and Tawfic MS (1991). Histological and histochemical studies on ovarian congenital anatomical defects and some ovarian tumours in camels. Zagazig Veterinary Journal 19(2):558-572.

El-Khouly AA, El-Nasr A, Ontabli A and Gadir FA (1990). Some pathologic affections of camel ovaries in U.A.E. Zagazig Veterinary Journal 18:210-217.

El-Wishy AB (1989). Genital abnormalities of the female dromedary (*Camelus dromedarius*). An abattoir survey Zuchthygiene 24(2):84-87.

Fetaih H (1991). Some pathological studies on the affections of genital system of she-camel. Ph. D. Thesis, Faculty of Veterinary Medicine, Suez Canal University.

Hamouda MM, Al-Hizab FA and Hasseeb MM (2011). Pathologic studies on ovarian abnormalities in nagas (*Camelus dromedarius*) in Al–ahsa, Saudi Arabia. Scientific Journal of King Faisal University (Basic and Applied Sciences). 12(1)265-276.

Heikal RN (1999). Studies on the incidence of reproductive affections in she-camel in relation to slaughter house materials. M.V. Sc. Thesis, Faculty of Veterinary Medicine - Alexandria University.

Hsu FS (1983). Ovarian haemangioma in swine. Veterinary Pathology 20:401-409.

Jubb KVF, Kennedy PC and Palmer N (1993). Pathology of Domestic Animals. 4th edn, Academic press, Inc., San Diego, California, London.

Kennedy PC, Cullen JM, Edwards JF, Goldschmidt MH, Larsen S, Munson L and Nielsen S (1998). Histological classification of tumours of the genital system of domestic animals, second series. VI. WHO, Armed Forces Institute of Pathology, Washington.

Koukourakis GV, Kouloulias VE, Koukourakis MJ, Zacharias GA, Papadimitriou C, Mystakidou K, Pistevou-Gompaki K, Kouvaris J and Gouliamos A (2008). Granulosa cell tumour of the ovary: Tumour review. Integrative Cancer Therapies 7(3):204-215.

McEntee K (1990). Reproductive Pathology of Domestic Mammals, 1st edn, Academic press, Inc., San Diego, California, London.

Mesbah SF, Kafi IM and Nili H (2002). Ovarian teratoma in a camel (*Camelus dromedarius*). Veterinary Record 151(25):776.

Moulton JE (1978). Tumours of the Genital System. Moulton JE (ed).Tumours of Domestic Animals, 2nd edn. University of California Press, Berkeley. pp 309-345.

Nawito MF, Shalash MR and Hoppe R (1967). Reproduction in the female camel. Bull. 2, 82, Anim, Sci. Res. Cent., Cairo.

Numanoglu C, Guler S, Ozaydin I, Han A, Ulker V and Akbayir O (2014). Stromal luteoma of the ovary: A rare ovarian pathology. Journal of Obstetrics and Gynaecology 35(4):1-2.

Omar MA, Ismail EM and Elhariri MN (1984). Seasonal variations of sexual disorders in the she-camel "*Camelus dromedarius*". Journal of the Egyptian Veterinary Medical Association 44:51-59.

Pérez-Martínez C, Durán-Navarrete AJ, García-Fernández RA, Espinosa-Alvarez J, Escudero Diez A and García-Iglesias MJ (2004). Biological characterisation of ovarian granulosa cell tumours of slaughtered cattle: Assessment of cell proliferation and oestrogen receptors. Journal of Comparative Pathology 130(2-3):117-123.

Schumer ST and Cannistra SA (2003). Granulosa cell tumour of the ovary. Journal of Clinical Oncology 21:1180-1189.

Simenew Keskes Melaku, Moa Melaku, Ashenafi Feyisa, Tilaye Demissie, Fekadu Regassa, Getnet Abie Mekonnen, Gizat Almaw, Tesfaye Sisay Tessema, Tesfu Kassa and Fufa Dawo (2015). Pathological and Bacteriological Study on Abnormalities of Female Internal Reproductive Organ of *Camelus dromedarius* Slaughtered at Akaki Abattoir, Ethiopia. American-Eurasian Journal of Scientific Research 10(4):193-202.

Soleimanzadeh A, Batavani R, Nourian A and Pashaie B (2017). Ovarian fibrothecoma in a holstein cow: A Case report. Iranian Journal of Veterinary Science and Technology IJVST. 9(2):70-74.

Tibary A and Anouassi A (2000). Reproductive disorders in the female camelid. In: Recent Advances in Camelid Reproduction, Skidmore J.A. and Adams G.P. (Eds). International Veterinary Information Service.

Wajid SJ (2015). A Pathological abattoir survey of the reproductive tracts of non-pregnant camels (*Camelus dromedarius*) in Iraq. OSR Journal of Pharmacy and Biological Sciences (IOSR-JPBS). 10(3):84-90.

Young, KM (2011). Sex Cord-Stromal, Steroid Cell and Other Ovarian Tumours With Endocrine, Paraendocrine and Paraneoplastic Manifestations. In: Kurman RJ, Ellenson LH, Ronnett BM, (eds). Blaustein's Pathology of the Female Genital Tract. 6th ed. New York: Springer. pp 826-846.

BOOK REVIEW

Book   : **Handbook of Research on Health and Environmental Benefits of Camel Products**

Authors : Omar Amin Alhaj University of Petra, Jordan
            Bernard Faye Independent Researcher, France
            Rajendra Prasad Agrawal Independent Researcher, India

Publisher : IGI Global, United States of America

ISSN   : 2330-3271; eISSN: 2330-328X

Edition   : First 2019

     The various chapter of book are contributed by 37 authors from 16 countries. This book has 17 chapters spread in 477 pages. The opening chapter is based on historical background and population of camels. This is good for all those writing introduction of their camel based research. This chapter introduces some essential figures on the economic value of camels based on the most recent statistics of the Food and Agricultural Organisation(FAO). Eleven chapters are based on different facets of camel milk which are very interesting. These chapters describe camel milk composition and nutritional value, strategies and technologies for camel milk preservation, microbial aspect of lactic acid bacteria isolated from camel milk, manufacture of dairy and non-dairy camel milk products, manufacture and challenges of camel milk cheese, exploring potential therapeutic properties of camel milk, health-improving and disease-preventing potential of camel milk against chronic diseases and autism: camel milk and chronic diseases, potential anti-diabetic effect of camel milk, effects of industrial processing methods on camel milk composition, nutritional value, and health properties, camel colostrums composition, nutritional value, and nutraceuticals and camel milk disguised cosmeceutical. While few chapters highlight the medicinal or therapeutic, nutraceuticals and cosmeceutical properties of camel milk, the others point out about camel milk products and their industrial processing methods. These chapters highlight many value-added products which are produced like yoghurt, cheese, ice cream, snacks, and camel milk protein hydrolysates, which are used in the field of functional food and nutraceuticals. Chapters also contain information about the recent introduction of the chy-max–m1000®,on market solved the problem of clotting. Obtained by genetic engineering, this camel rennet allows high cheese yield. Another chapter highlights the potential health benefits of camel milk including antioxidant, anti-cancer activity, antihypertensive properties, ant diabetic activity, antimicrobial activity, hypoallergenicity activity, and anti-crohn's disease. Scientists from india have investigated and assessed the effect of regular camel milk consumption on glycaemic status of diabetic patients and animal models. All the experiments' results concluded to the reduction of blood glucose and glycosylated haemoglobin. One chapter is based on interactionbetweencamelfarming andenvironment. Chinese authors have contributed one chapter on camel hairs tructure, properties, and commercial products. The chapter on camel meat is contributed by a group of scientists from Oman and Sudan led by Isam Tawfik Kadim. These chapters describe camel meat production, structure, and quality and camel meat nutrient content and potential health benefits. Authors pointed out an important feature that characterises camelid meat products is the low level of intramuscular and subcutaneous fat compared to red meat sources. The scientists from Saudi Arabia and Malaysia have contributed a chapter on camel gelatin composition, properties, production, and applications. This chapter discusses the processing of camel gelatin extraction. Gelatine has an ability to form a thermo reversible gel at normal body temperature and high water content make it an exceptional food ingredient.

     I congratulate the editors and authors of this unique book which provides volumes of information regarding the camel products.

Dr. T.K. Gahlot
Editor
Journal of Camel Practice and Research

SERTOLI-LEYDIG CELL TUMOUR IN A FEMALE DROMEDARY CAMEL

Ahmed Ali[1,2], Derar Derar[1,2], Khaled M.A. Hassanein[3,4], Abdella Al-Howas[1], Madeh Sadan[1], El-Sayed El-Shafaey[1] and Fahd A. Al-Sobyil[1]

[1]Department of Veterinary Medicine, College of Agriculture and
Veterinary Medicine, Qassim University, P.O. Box 6622 - Buraidah 51452, Saudi Arabia
[2]Faculty of Veterinary Medicine, Department of Theriogenology, Assiut University, Egypt
[3]Department of Pathology and Clinical Pathology, Faculty of Veterinary Medicine, Assiut University, Egypt
[4]Medical Research Centre, Jazan University, Saudi Arabia

ABSTRACT

The present study described the first case of Sertoli-Leydig cell tumour in dromedary camel. An 8-year-old, primiparous, female dromedary was presented with a history of failure of conception. The camel had normal calving since 1.5 years. The animal was in good health condition. Trans-rectally, a firm, round, smooth, mass (~9 cm in diameter) was palpated bulging out of the surface of the right ovary. Ultrasonographically, the right ovary was enlarged, homogenous, but with some cystic areas. Unilateral ovarioectomy was performed. Microscopically, the ovarian cortex was composed of tubules of immature Sertoli cells. There were large leydig cells. Alpha-inhibin was expressed uniformly within the cytoplasm of the majority of cells lining tubules, thus confirming classification of the lesions as Sertoli-Leydig cell tumour.

Key words: Dromedary, ovary, Sertoli-Leydig cell, tumour

Ovarian tumours are uncommon in dromedary camels. Most of the reported ovarian tumours were teratomas, dysgerminoma and granulosa cell tumours (Elwishy, 1990; El-Khouly *et al*, 1990; Ali *et al*, 2013). Sertoli-Leydig cell tumour, arises from the sex cord cells present in the ovary (Young and Scully, 1985; Sachdeva *et al*, 2008). Morphologically, cells of testis looks like at different phases of development, but ultrastructurally, it is similar to ovarian granulosa cell tumours and comprises female sex chromatin (Patnaik *et al*, 1988). These tumours produce androgens and rarely estrogen hormones (Young, 1993). Sertoli-Leydig cell tumours are often detected in bitches than in other animal species or in women (Patnaik *et al*, 1988; Young, 1993; Vissiennon *et al*, 2010). Of 71 ovarian tumours in dogs, sex cord stromal constituted about one-third of cases, which were equally divided between Sertoli-Leydig and granulosa cell tumours (Patnaik and Greenlee, 1987).

Sertoli-Leydig cell tumour is not previously reported in camels. Persent study reports this tumour with its clinical and histopathological details.

Materials and Methods

An 8-year-old primiparous, non-lactating, female dromedary camel was presented for failure of conception for 4 months. The animal had normal calving since 1.5 years. At admission, the animal was evaluated for the body condition score (BCS, 1–5; Sghiri and Driancourt, 1999) and examined for rectal temperature, heart and respiratory rates, and rumen contraction. The reproductive tract was examined by transrectal palpation ultrasonographically (Aloka SSD-500, equipped with a 5 MHz linear array transducer; Aloka Co., Ltd., Tokyo, Japan) and through exploration of the vagina. A unilateral ovariectomy was performed in sternal recumbency. Food and water were withheld for 24 h. The camel was sedated by xylazine HCl (0.3 mg/kg body weight, Bomazine 10%, iv, BOMAC Laboratories Ltd, New Zealand). The left flank region was prepared for aseptic surgery. Anaesthesia of the flank area was achieved with inverted "L" infiltration using 2% lidocaine (Norbrook Laboratories, UK). An oblique cranio–caudal linear skin incision was performed at the lower flank. Blunt dissection was performed in the muscles of the flank and haemostasis was carried out. The parietal peritoneum was opened and the affected ovary was identified and then exteriorised. The mass was removed after double ligation of the ovarian pedicle using number 1 Polydiaxanone (Ethicon, USA). The uterine horn was then reduced

back to the peritoneal cavity. The flank incision was sutured routinely in 5 layers (Tibary and Anouassi, 1997). Postoperatively, systemic antibiotics (procaine penicillin 30,000 IU/kg and dihydrostreptomycin 10 mg/kg, Pen Sterpt®, Norbrook, Northem, Ireland) and an anti-inflammatory (phenylbutazone 4.4 mg/kg, Phenylarthrite®, Vetoquinol, Lure-France) were administered in for 5 and 3 days, respectively. Skin sutures were removed 14 days, post-surgery.

Ovarian samples were fixed in buffered formalin and routine processing by alcohol, xylol then blocked in paraffin. The tissue was sectioned at 4 μm and stained with haematoxylin and eosin for histopathological examination (Bancroft and Stevens, 2008).

The immunophenotyping of the tumour cells was analysed by immunohistochemistry. Inhibin alpha polyclonal antibody (#MBS9127039) provided by MyBioSource, Inc. USA was used. Immunohistochemical staining was performed as described previously (Mousa and Mousa, 2003). In brief, sections were incubated with the primary antibodies against inhibin (diluted at 1:1000) overnight at 4°C. Thereafter, the sections were incubated with the biotinylated secondary antibody for 1 h and with avidin biotin conjugated peroxidase for 45 min. Finally, the sections were washed and stained with 30 3' -diaminobenzidine tetrahydrochloride (DAB), including 0.01% H_2O_2 in 0.05 M Tris-buffered saline (pH 7.6) for 3–5 min. After the enzyme reaction, the sections were washed in tap water, dehydrated in alcohol, cleared in xylene, and mounted in DPX. To demonstrate specificity of staining, the following controls were included:

(1) Preabsorption of diluted alpha antibodies of inhibin with ovine follicular fluid, a natural source of inhibin (dilution, 1:5) for 24 h at 4°C.

(2) Omission of the primary antisera, the secondary antibody or avidin–biotin complex. These control experiments did not showed positive staining for any antibody tested.

Results and Discussion

The BCS of the female camel was 3 at admission, and all clinical parameters were within normal limits (temperature=36.7°C, heart rate=45 beats/min, respiratory rate=9 breaths/min, rumen contractions=4 every 2 min). Trans-rectal palpation determined that the right ovary was abnormally enlarged. The left ovary was smaller in size with no structures. Ultrasound examination revealed that this mass at

the right ovary was generally homogenous, but with some hypoechoic areas within its substance (Fig 1). Grossly, the right ovary had a nearly-round smooth mass (~approximately 9 cm in diameter) attached to its lateral surface. On cross-section, this mass was smooth, greasy and shiny, resembling the testicular stroma with multiple cavities (Fig 2). Microscopically, this mass composed of tubules of immature Sertoli cells with clear cytoplasm intermingled with large interstitial Leydig cells in between with pink cytoplasm. Some cells acquire spindle cell appearance and some other cells acquire epithelial cells filled with mucous were also observed (Fig 3).

Examination of the immunuohistochemical staining with inhibin-α was expressed uniformly
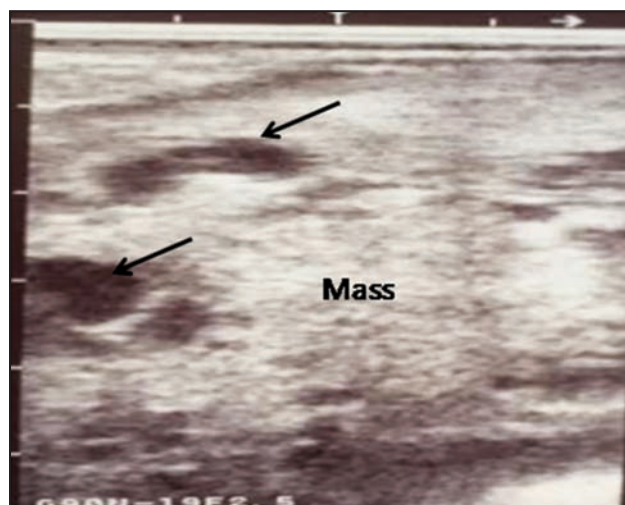
Fig 1. Sonogram revealed a large homogenous echogenic mass with some non-echogenic areas (arrows) attached to the right ovary.
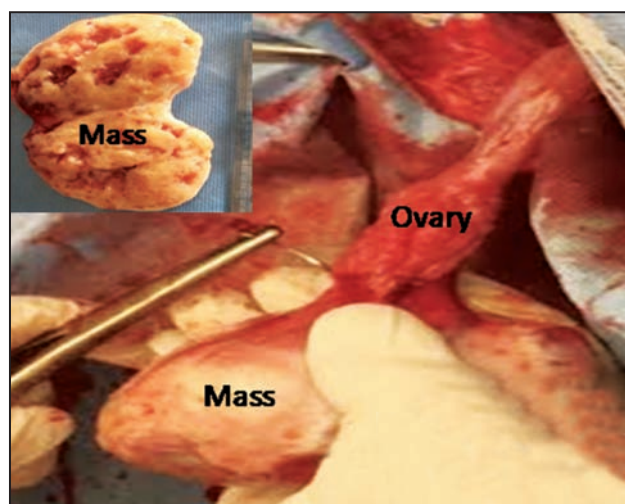
Fig 2. Morphology of the Sertoli-Leydig cell tumour, the mass is approximately round, smooth and pedunculated from the surface of the right ovary. The cut-surface was glistening with some cavities filled with serous fluid.
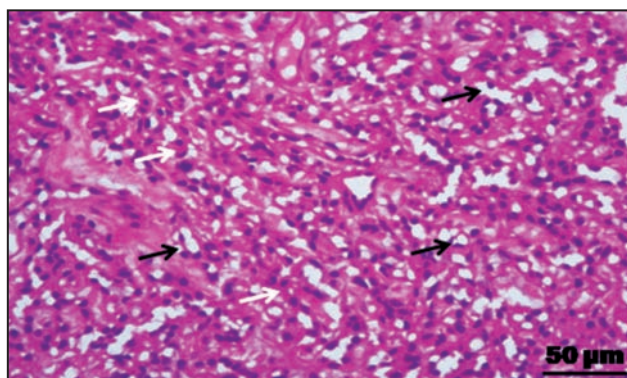
Fig 3. Histopathological sections of the ovarian tumour showing tubules of immature Sertoli cells with clear cytoplasm (black arrows), and large Leydig cells with pink cytoplasm (white arrow). H&E.
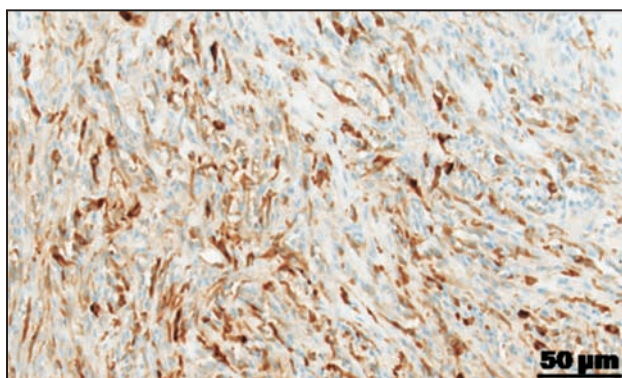

Fig 4. Immuno-histochemisty of Alpha-inhibin strongly expressed in the cytoplasm of the cells lining the tubules.

within the cytoplasm of the majority of cells lining tubules (Fig 4), providing a strong evidence that the found lesion is a Sertoli-Leydig cell tumour (intermediate differentiated, Meyer type II).

The tumour described has morphological and immunohistochemical characteristics consistent with both human (Durdík *et al,* 2012) and canine Sertoli-Leydig cell tumours (Banco *et al,* 2010).

Alpha-inhibin, a gonadal glycopeptide known to be a feedback inhibitor of pituitary secretion of follicle-stimulating hormone, is a useful marker of canine (Marino *et al,* 2003) and human sex cordestromal tumours (Mooney *et al,* 2002; Oliva *et al,* 2005; Young, 2005). Alpha-inhibin is not expressed by other types of canine ovarian tumour such as epithelial- or germ-cell tumours (Marino *et al,* 2003).

The exact cause of this tumour is not known. However, some studies have revealed that many cases are caused by germline mutations in the DICER1 gene (Frio *et al,* 2011; Slade *et al,* 2011). The current case was unilaterally affected and was in the beginning of her reproductive life. In women, most registered cases were unilateral (Young and Scully, 1985; Tandon *et al,* 2007). In contrast, in bitches the majority of reported cases were bilateral (Patnaik and Greenlee, 1987; Go´mez-Laguna *et al,* 2008). This type of ovarian tumour has been mostly seen in young ages women (Young and Scully, 1985; Tandon *et al,* 2007), conversely, in bitches, utmost observed cases were more than 10 years old (Patnaik and Greenlee, 1987).

Acknowledgement

References

Ali A, Al-Sobayil FA, Tharwat M, Mehana EE and Al-Hawas A (2013). Granulosa cell tumour in a female dromedary camel. Comparative Clinical Pathology 22:1251-1254.

Banco B, Giudice C, Veronesi MC, Gerosa E and Grieco V (2010). An immunohistochemical study of normal and neoplastic canine sertoli cells. Journal of Comparative Pathology 143:239-247.

Bancroft JD and Stevens A (2008). Theory and Practice of Histological Techniques, 6th edn. Churchill Livingstone, London.

Durdík Š, Danihel L and Galbavý Š (2012). Sertoli-Leydig cell tumour of the ovary-morphological and immunohistochemical analysis. Neuro Endocrinology Letters 33:257-259.

El-Khouly BA, El-Nasr A and Ontabli A (1990). Some pathologic affections of camel ovaries in U.A.E. Zagazig Veterinary Journal 18:210-217.

Elwishy AB (1990). Genital abnormalities in camels (*Camelus dromedarius*). In: Proceedings of the workshop "Is it possible to improve the reproductive performance of the Camel?", Paris. pp 163-174.

Frio TR; Bahubeshi A, Kanellopoulou C, Hamel N, Niedziela M, SabbaghianN, Pouchet C, Gilbert L and O'Brien PK *et al* (2011). Mutations in familial multinodular goiter with and without ovarian sertoli-leydig cell tumours. Journal of the American Medical Association 305:68-77.

Go´mez-Laguna J, Milla´n Y, Reymundo C, Domingo V, Martı´n de las and Mulas J (2008). Bilateral retiform sertolie-leydig cell tumour in a bitch. Alpha-inhibin and epithelial membrane antigen as useful tools for differential diagnosis. Journal of Comparative Pathology 139:137-140.

Marino G, Nicotina PA, Catone G, Bontempo RA and Zanghi A (2003). Alpha-inhibin expression in canine ovarian neoplasms: preliminary results. Veterinary Research Communications 27(Suppl. 1):237-240.

Mooney EE, Nogales FF, Bergeron C and Tavasoli FA (2002). Retiform Sertoli-Leydig cell tumours: clinical, morphological and immunohistochemical findings. Histopathology 41:110-117.

Mousa MA and Mousa SA (2003). Immunohistochemical localisation of inhibin and activin-like proteins in the

brain, pituitary gland, and the ovary of thin-lipped grey mullet, *Liza ramada* (Risso). General and Comparative Endocrinology 132:434-443.

Oliva E, Alvarez T and Young RH (2005). Sertoli cell tumours of the ovary: a clinicopathologic and immunohistochemical study of 54 cases. American Journal of Surgical Pathology 29:143e156.

Patnaik AK and Greenlee PG (1987). Canine ovarian neoplasms: a clinicopathologic study of 71 cases, including histology of 12 granulosa cell tumours. Veterinary Pathology 24:509-14.

Patnaik AK, Saigo PE, Lieberman PH and Greenlee PG (1988). Morphology of canine ovarian Sertoli-Leydig cell neoplasms. A report of 12 cases. Cancer 62:577-584.

Sachdeva Poonam, Arora Raksha, Dubey Chandan, Sukhija Astha, Daga Mridula and Kumar Singh Deepak (2008). Sertoli–Leydig cell tumour: A rare ovarian neoplasm. Case report and review of literature. Gynaecological Endocrinology 24:230-234.

Sghiri A and Driancourt MA (1999). Seasonal effects on fertility and ovarian follicular growth and maturation in camels (*Camelus dromedarius*). Animal Reproduction Science 55:223-237.

Slade I, Bacchelli C, Davies H, Murray A, Abbaszadeh F, Hanks S, Barfoot R, Burke A and Chisholm J (2011). Clarifying the diagnosis, clinical features and management implications of a pleiotropic tumour predisposition syndrome". Journal of Medical Genetics 48:273-278.

Tibary A and Anouassi A (1997). Reproductive disorders of the female Camelidae. In: A. Tibary (ed.) Theriogenology in Camelidae: Anatomy, Physiology, BSE, Pathology and Artificial breeding. Actes Editions: Institut Agronomique et Vétérinaire Hassan II: 317-368.

Vissiennon T, Schmidt T, Schneider E and Hildebrand M (2010). Sertoli Leydig cell tumour in a bitch, 10 years after spaying. A case report. Tierarztliche Praxis Ausgabe K: Kleintiere - Heimtiere 38:399-402.

Young RH (1993). Sertoli-Leydig cell tumours of the ovary: review with emphasis on historical aspects and unusual variants. International Journal of Gynecological Pathology 12:141-147.

Young RH (2005). Sex cordestromal tumours of the ovary and testis: their similarities and differences with consideration of selected problems. Modern Pathology 18(Suppl. 2):S81eS98.

Young RH and Scully RE (1985). Ovarian Sertoli-Leydig cell tumours. A clinicopathological analysis of 207 cases. American Journal of Surgical Pathology 9:543-569.

AUTHOR INDEX

Mohammed Mohammed E.A. 179
Mohammed T.E.A. 237

N

Nagy P. 1
Narenbatu 63
Narnaware S.D. 87

O

Osman Salama A. 81
Oyun Gowa 57

P

Paily N M 121
Pandey R.P. 189, 195
Pannu Urmila 255
Patil N.V. 87, 157
Pawar V.D. 245
Prakash Ved 157
Premasuthan A. 1
Purohit S. 189, 195
Purva Mukul 41

R

Raghavan R 121
Raja S. 1
Rangsun P. 259
Ranjan Amita 225
Ranjan Rakesh 225

Riad F. 149

S

Sadan Madeh 99, 287
San Ren 261
Sara Shaaeldin A.H. 21
Sawal R.K. 87
Sawane M.P. 245
Schuberth Hans-Joachim 105
Schuster R.K. 125
Schuster Rolf K. 231
Sharku 219
Sharma N. 157
Shawaf T. 91
Shawaf Turke 105, 173
Shyma K.P. 129
Si Rendalai 207
Singh A.P. 87
Singh S. 195
Singh Veer 129
Sivakumar Saritha 231
Surlig 201, 219
Suthar Dhirendra 41
Syriac G 121

T

Tabite R. 149
Tahri EH. 149
Tharwat Mohamed 169, 273
Thomas Sh M 121

Tingari M.D. 21
Tuteja F.C. 87
Tuya 201, 19

U

Umrikar U.D. 245

V

Varcasia A. 125
Vyas Sumant 157

W

Wang Xiuzhen 57
Wenfang 63
Wernery U 1, 121, 259
Wernery Ulrich 231
Wibbelt Gudrun 231
Wilson R. Trevor 11
WM El-Deeb 29
Wurihan 115

X

Yamini 255
Yang Bin 57, 63, 201, 219
Yang Hui 63
Yi Li 71, 133, 163, 207
Yue Weidong 261

Z

Zhao Rigetu 207
Zhou Jun-wen 207

SUBJECT INDEX

INSTRUCTIONS TO CONTRIBUTORS

The Journal of Camel Practice and Research is published by half-yearly from the Camel Publishing House, 67, Gandhi Nagar West, Near Lalgarh Palace, Bikaner, 334 001 (India). It is in offset print size of 20.5x27.5 cm in two columns with a print area of 17x22 cm. It will be known as **Journal of Camel Practice and Research** with **Volume** number on yearly basis and **Number** on issues per volume basis (in exceptional cases there can be more than two issues in a volume).

Nature of coverage: This journal is dedicated to disseminate scientific information about new and old world camelids in form of: **Original research** articles in camel health, husbandry, pastoralism, sports, specific behaviour, history and socio-economics. **Reports** on unusual clinical case(s) or unreported management of clinical case(s). Review articles will be accepted on invitation only. **Book review** directly or indirectly related to camels will be reviewed by subject-matter specialists and included if sent to the journal for this purpose. **Masters or Doctorate thesis/dissertation abstracts** will be published only if sent by the candidate with due certification from advisor/supervisor and head of the department where the research was carried out. All thesis/dissertation abstracts should be accompanied by attested or photocopy of their mandatory certificates only for official records. The Journal of Camel Practice and Research will occasionally contain an **invited editorial** commenting on the papers in the issue.

Each issue of the Journal of Camel Practice and Research will contain some titbits like My Camel Memories, Clinical Camelids, `**from the old literature', `cartoons' and interesting news** items'. Readers are welcome to contribute for these and due credit lines will suitably be included. However, all these are subject to scrutiny by members of the editorial board.

News of any International Association of Camel or Camelids will be included as and when necessary. `**Research in progress'**, is a special feature we intend to incorporate in the Journal of Camel Practice and Research. In this column researchers can report initial findings of their work in advance, so that others engaged in similar pursuit can exchange views about it. However, such short communications will be entertained on understanding that full article will also appear in this journal.

Submission of manuscript: Mail two hard copies of the manuscript and two complete sets of figures along with a CD or a soft copy in word files to **Dr.T.K. Gahlot**, Editor, Journal of Camel Practice and Research, Department of Surgery & Radiology, College of Veterinary & Animal Science, **Bikaner**, Rajasthan, 334 001 India. Send soft copy to Editor at tkcamelvet@yahoo.com.

The manuscript should be sent in a heavy paper envelope and photographs or illustrations should be enclosed in a cardboard to avoid damage during mail handling. The manuscript should be accompanied by a covering letter from the author responsible for correspondence. It should also contain a statement that manuscript has been seen and approved by all co-authors. Editor and members of the editorial board are not responsible for the opinions expressed by authors and reserves the right to reject any material or introduce editorial changes. Material will be accepted for publication on the understanding that it has not been published in any other form and is not being considered elsewhere. Any material once accepted for publication may not be republished in any form without prior permission of the author.

Manuscripts can also be accepted on 3.5" or 5.25" floppies, computers, PM5 or PM6 Microsoft-Word-5 or compatibles, Microsoft-Excel-4 or compatibles. It would be in the interest of authors to accompany a hard copy.

Preparation of the manuscript: Manuscript should be typed on white bond paper (A4 or 5 size) with a margin of 4 cm on right side, 3 cm on left side, top and bottom. British English, spellings and generic names of drugs should be used. International Code of Zoological Nomenclature, *Nomina Anatomica Veterinaria*, International Code of Nomenclature of Bacteria, International Code of Botanical Nomenclature and International Standards should be strictly followed. All terms should be identified by their scientific names and for easy comprehension common terms/names can be used. Population data and geographical distribution of camelids should invariably be avoided in introduction, unless it is warranted.

Each of the following sections should be types on separate pages:

Title page: This page should contain title of the article, name of the department/institution where work has been done, present postal address of each author and name of author with email to whom reprint request should be addressed. Following is the example:

Example: CLINICAL EVALUATION OF INTERDENTAL WIRING TECHNIQUE FOR MANDIBULAR FRACTURE REPAIR IN CAMELS

T.K. Gahlot[1], S.K. Chawla[2], R.J. Choudhary[3], D. Krishnamurthy[4] and D.S. Chouhan[5]

Department of Surgery & Radiology,[1,3 and 5] College of Veterinary and Animal Science,[2 and 4], College of Veterinary Sciences, CCS-Haryana Agricultural University, Hisar, 125004 INDIA.

SEND REPRINT REQUEST TO DR. T.K. GAHLOT email: tkcamelvet@yahoo.com.

Abstract and Key words: The abstract should begin with title of the article (in upper case), and have brief procedures, salient results and conclusions not more than 225 words, in one paragraph on second page. Proprietary names and abbreviations should be avoided. Provide four to six key words below the abstract for indexing services. Abstract is not necessary for short communications, case reports, news items etc.

Text: The proper text of the paper should start from third page and should again begin with title of the article (in upper case). The text should be divided into sections with headings, introduction, materials and methods, results, discussion, tables/illustrations and references.

Introduction: The logic of the introduction is to introduce the specificity and relevance of the topic to the readers. It should include the objective of the work in brief and most important related reference(s).

Materials and Methods: Should contain details regarding materials and brief account of procedures used.

However, sufficient details must be included to reproduce the results. For established or routine methods only related reference(s) can be cited. Any deviation from routine procedures should be specifically mentioned. Only generic names of the drugs and chemicals should be used in the running text. The trade names, source or other necessary related information should be mentioned in parenthesis there in.

In case reports, the case record sheet should also be included in materials and methods.

Statistical methods if used should be briefly described alongwith reference. If any analysis is done with the help of a computer programme, its complete name and source should be mentioned, however, it does not mean to exclude the mention of methods, level of significance and other relevant information.

Results and Discussion should be presented in logical sequence with implications of findings about other relevant studies. The data or information easily attainable from the tables or graphics need not be repeated in the results. Only important observations need to be summarised. Undue repetition of the text from results to discussion has to be avoided. To preclude it, depending on article, results and discussion can be combined. In discussion only significant results should be discussed. One should not always stick to the term `statistically significant' data rather biological importance or significance of any variation should be given due importance in discussion. Discussion should always end in conclusions linked with objectives of the study mentioned in the introduction and unqualified statements should be avoided.

Tables: Each tables should be typed on separate sheet. Large tables should be avoided and should not exceed one page. Each table should be numbered in Indo-Arabic numerals according to their sequence in the text that refers to it. In the text it should be referred as proper noun e.g., Table 1. The title of the table should be brief and self-explanatory. Footnotes can be included to enhance understanding ability of the contents of the table.

Illustrations and Legends: All illustrations should be submitted in duplicate and about twice the size desired for reproduction that is 17 cm for double column or 8.3 cm for single column. Photographs and photomicrographs should be printed on glossy paper with excellent details and contrast. Drawings and diagrams should be in India ink (Black) on smooth white paper. All illustrations should be referred as figures in the text and should also be numbered in Indo-Arabic numerals e.g., Fig 1. Legends of all these figures should be typed on a separate sheet. Each legend should be clear, concise and informative. A statement of magnifications or reductions should be given where it is applicable. Nothing should be written with pen or typed on the back of any illustration except it bears running title of the paper, figure number and arrow indicating top edge with light pencil. All graphs should be supported with data on a separate sheet to redo them (in certain special cases) according to format of the journal.

References: References to the work should be cited in the text with author's surname and year of publication in the parenthesis e.g., Gahlot (1995) or Gahlot *et al* (1995) or (Gahlot *et al*, 1995), depending upon construction of the sentence. In case there are two authors the conjunction `and' or its symbol `&' should be used according to construction of the sentence e.g.,

Gahlot and Chouhan (1995) or (Gahlot & Chouhan, 1995). When there are more than two authors the surname of first author will be followed by *et al*. When name of any author bears only first and second name, latter will be considered as surname for the text. However, in papers submitted to this journal both names should be used in the title page. Chronological order should be followed in citing several references together in the text.

References should be arranged in alphabetical order. Authors should not modify the title of the references. Mention full name of the journal. Examples of correct forms of references are given below:

Periodicals: Sharma SD, Gahlot TK, Purohit NR, Sharma CK, Chouhan DS and Choudhary RJ (1994). Haematological and biochemical alterations following epidural administration of xylazine in camels (*Camelus dromedarius*). Journal of Camel Practice and Research 1(1):26-29.

For edited symposium/congress/proceedings: Abdalla HS (1992). Camel trypanosomiasis in the Sudan. Proceedings First International Camel Conference, Dubai (UAE), February 2-6, pp 401-403.

Books (Personal authors): Gahlot TK and Chouhan DS (1992). Camel Surgery, Ist Edn. Gyan Prakashan Mandir, Gauri Niwas, 2b5, Pawanpuri, Bikaner, India. pp 37-50.

Chapter from multiauthored books: Chawla SK, Panchbhai VS and Gahlot TK (1993). The special sense organs-Eye. In: Ruminant Surgery, Eds., Tyagi RPS and Singh J. Ist Edn., CBS Publishers and Distributors, Delhi, India. pp 392-407.

Thesis: Rathod Avni (2006).Therapeutic studies on sarcopticosis in camels (*Camelus dromedarius*). Unpublished Masters Thesis (MVSc), Rajasthan Agricultural University, Bikaner, Rajasthan, India.

Commercial booklets: Anonymous/Name (1967). Conray-Contrast Media. IIIrd Edn., 12-15, May and Baker Ltd., Dagenham, Essex, England.

Magazine articles: Taylor D (1985). The Constipated Camel. Reader's Digest. Indian Edn. RDI Print & Publishing (P) Ltd., Mehra House, 250-C, New Cross Road, Worli, Bombay, India. 126:60-64

News paper articles: Anonymous or name of correspondent (1985). Bright Sunlight causes Cataract. Times of India, New Delhi, City-1, India October-9 pp 3, Col 3-5.

Personal communication: Hall LW (1995). Reader in Comparative Anaesthesia, Department of Clinical Veterinary Medicine, Madingley Road, University of Cambridge, Cambridge, CB3 0ES, England.

Reprints: There is no provision for free reprints. Author or person in correspondence has to pay INR 4500/- (for Indian Citizens only) or US $ 450, in advance for 10 reprints for the year 2020. Additional reprints in multiples of 10 may be requested and will be charged at the same rate but with minimum order of 30 reprints and every request for extra reprints should be made, if required, before 30th March, July or November every year.

Charges for colour and black and white pictures: Author(s) has to pay for production of colour plates in his/her manuscript. More than 4 black and white picture will be charged from the author(s) towards printing charges.

Copyright: The copyright of the article will remain with the owner, Dr. T.K. Gahlot and will be governed by the Indian Copyright Act.